Molecular mechanism of concentration-regulated methanol induction and its signaling pathway in methylotrophic yeasts

Koichi Inoue

2023

Contents

Introduction

Methylotrophic yeasts, such as *Komagataella phaffii* (synonym *Pichia pastoris*), *Ogataea polymorpha* (synonym *Hansenula polymorpha*), and *Candida boidinii,* can utilize methanol as the sole source of carbon and energy. During growth on methanol, these yeasts develop large peroxisomes containing considerable amounts of methanol metabolizing enzymes such as alcohol oxidase (AOX) and dihydroxyacetone synthase (DAS), whose gene expression is strongly induced by methanol. Owing to their strong methanol-induced gene promoters, methylotrophic yeasts have been used as hosts for recombinant protein production (Cregg *et al.*, 2000; Gellissen, 2000; Yurimoto, 2009). Their unique one-carbon (C1) metabolism and the molecular mechanism for methanol-induced gene expression have been extensively studied for more than 50 years (De *et al.*, 2021; Hartner *et al.*, 2006; Kalender *et al.*, 2020; Ogata *et al.*, 1969; van der Klei *et al.*, 2006; Yurimoto *et al.*, 2011; Yurimoto *et al.*, 2019). The advantages of methylotrophic yeasts for recombinant protein production are (1) easy and established methods of genetic modification, (2) low culture cost compared to mammalian systems, (3) efficient secretion of heterologous eukaryotic proteins because the yeasts are also eukaryotic organisms. In addition, methanol is synthesized from methane, the main component of natural gas, and has some advantages of being inexpensive, non-competitive with food, and easy to handle because it is liquid at room temperature. Methylotrophic yeasts have been also studied as a model to understand peroxisomal dynamics because it is easy to observe the synthesis and degradation of peroxisomes in response to different environmental conditions (Sakai *et al.*, 1998).

The methanol-utilizing pathway of methylotrophic yeasts has been revealed (Figure 0A) (Yurimoto *et al.*, 2005). Methanol is firstly oxidized by alcohol oxidase (AOX or AOD) to generate formaldehyde and H_2O_2 (Ozimek *et al.*, 2005). Formaldehyde, a central intermediate of the methanol metabolism pathway, is positioned at the branch point of the assimilatory and dissimilatory pathways. In the assimilatory pathway, formaldehyde is fixed by dihydroxyacetone synthase (DAS) to xylulose 5-phosphate (Xu5P) to produce dihydroxyacetone (DHA) and glyceraldehyde 3-phosphate (GAP), which are then consumed to synthesize cell components. AOD and DAS are both localized in peroxisomes. In the dissimilatory pathway, formaldehyde is further oxidized by formaldehyde dehydrogenase (FLD), *S*-formylglutathione hydrolase (FGH), and formaldehyde dehydrogenase (FDH), generating CO_2 and NADH via the oxidation of formate (Lee *et al.*, 2002; Sakai *et al.*, 1997; Yurimoto *et al.*, 2003).

In methylotrophic yeasts, methanol-induced gene expression is strictly regulated depending on the carbon source (Yurimoto *et al.*, 2011; Yurimoto *et al.*, 2019). The activation of methanol-induced genes undergoes two regulatory steps: the expression is strongly repressed in the presence of glucose but is activated to a certain level in the absence of glucose (derepression), and it is substantially induced in the

presence of methanol depending on the methanol concentration (methanol induction). A series of transcription factors involved in methanol-induced gene expression have been identified and characterized using *K. phaffii*, *C. boidinii* and *O. polymorpha* in previous studies (Figure 0B). Some of these transcription factors, such as KpMxr1 and CbTrm2 which are homologs of *Saccharomyces cerevisiae* Adr1, are involved in derepression (Lin-Cereghino *et al.*, 2006; Sasano *et al.*, 2010). Three kinds of transcription factors are involved in methanol induction; i) Mpp1 (HpMpp1 and KpMit1) (Leão-Helder *et al.*, 2003; Wang *et al.*, 2016b), ii) Trm1 (CbTrm1 and KpTrm1) (Sahu *et al.*, 2014; Sasano *et al.*, 2008), and iii) the CbHap complex (Oda *et al.*, 2015; Oda *et al.*, 2016). The expression of *KpMIT1/CbMPP1* is induced by methanol, which requires transcription factors KpMxr1/CbTrm2, Trm1 and Hap complex. These transcription factors then interact with the methanol-induced gene promoters (*AOX1*, *DAS1*, *FLD1*, etc.) (Yurimoto *et al.*, 2019).

Although the molecular characteristics of these transcription factors have been studied extensively, details on the molecular mechanism of how methylotrophic yeasts sense methanol concentration and transmit the methanol signal through intracellular signaling pathways to transcription factors were not clear. A previous study has revealed that Wsc family proteins in *K. phaffii* (KpWsc1 and KpWsc3) play a role in sensing methanol, and that KpWsc1 and KpWsc3 sense a wide range of methanol concentrations and regulate methanol-induced gene expression (Ohsawa *et al.*, 2017). Wsc family proteins are plasma membrane-spanning sensor proteins that have been well characterized in *S. cerevisiae* and are known to activate the cell wall integrity (CWI) pathway in response to cell surface stresses (Levin, 2005). In the CWI pathway, Wsc family proteins interact with ScRom2 and transmit the signal to ScRho1 and the mitogen-activated protein kinase (MAPK) cascade such as ScPkc1, ScBck1, ScMkk1/ScMkk2 and ScMpk1 (Levin, 2005). In *K. phaffii*, there is a clear indication of the involvement of KpRom2 in the methanol signaling pathway (Ohsawa *et al.*, 2017).

One of the main habitats of methylotrophic yeasts in nature is the phyllosphere, the aerial portions of plants. They utilize methanol that is generated from the methyl ester group of the cell wall component pectin on plant leaves (Kawaguchi *et al.*, 2011). Methanol concentration in the phyllosphere exhibits a daily periodicity from 0% to 0.2% (ca. 0-60 mM) (Kawaguchi *et al.*, 2011), and methylotrophic yeasts are considered to sense the presence and concentration of methanol. According to the previous study, the transcript levels of AOX- and DAS-encoding genes increased in the presence of 0.001-0.1% methanol but decreased in the presence of more than 0.1% methanol (Ohsawa *et al.*, 2017). I focused on such regulation of gene expression and defined it as "concentration-regulated methanol induction (CRMI)". Elucidating the molecular mechanism of CRMI will be important not only for understanding the adaptation mechanism of the yeasts to the phyllosphere environment where methanol concentration changes periodically, but also to improve the productivity of heterologous proteins.

Autophagy, a conserved mechanism of eukaryotes from yeasts to humans, is the major machinery for degrading the intracellular compartments. During this process, the target cargo is sequestered into a double-membrane organelle called autophagosome and then transferred to the vacuole/lysosome (Suzuki *et al.*, 2001; Suzuki *et al.*, 2007). More than 40 autophagy-related (ATG) genes have been identified in the budding yeast *Saccharomyces cerevisiae* since 1992, and their molecular mechanism has been clarified at the molecular level (Nakatogawa *et al.*, 2015; Oku *et al.*, 2016; Reggiori *et al.*, 2013; Wen *et al.*, 2016). However, physiological functions of ATG genes in yeasts have not been studied very well. Pexophagy, the selective autophagy of peroxisomes, contributes to the regulation of organelle abundance. Since peroxisome is a main compartment of methanol metabolism in methylotrophic yeast cells, peroxisomes are rapidly targeted to autophagic degradation by methanol depletion or the change of carbon source from methanol to glucose or ethanol (Sakai *et al.*, 2006). Autophagy, including pexophagy, is required for the proliferation and survival of methylotrophic yeast on the plant leaf surface (Kawaguchi *et al.*, 2011). And it is estimated that pexophagy is strictly controlled depending on methanol concentration in the phyllosphere.

In chapter I, the transcription factor KpMxr1 is described to be responsible for CRMI in *K. phaffii*. I studied its phosphorylation dynamics, show that the phosphoregulation of transcription factor KpMxr1 is involved in CRMI and propose the CRMI pathway from Wsc family proteins to KpMxr1 branching out from KpPkc1.

In chapter II, I focus on the physiological significance of *CbMPP1* whose expression is intensely induced by methanol in *Candida boidinii*. I hypothesize that methanol-induced expression of *CbMPP1* is responsible for balancing the expression level of multiple methanol-induced genes including methanol-metabolizing enzymes and avoiding the accumulation of formaldehyde. And I also determined Upstream Activating Sequences (UAS) involved in methanol-induced *CbMPP1* expression.

In chapter III, I describe the molecular mechanism and signaling pathway of negative regulation of pexophagy in the presence of methanol. I identified phosphatases for suppressing the phosphorylation of KpAtg30 depending on KpRlm1.
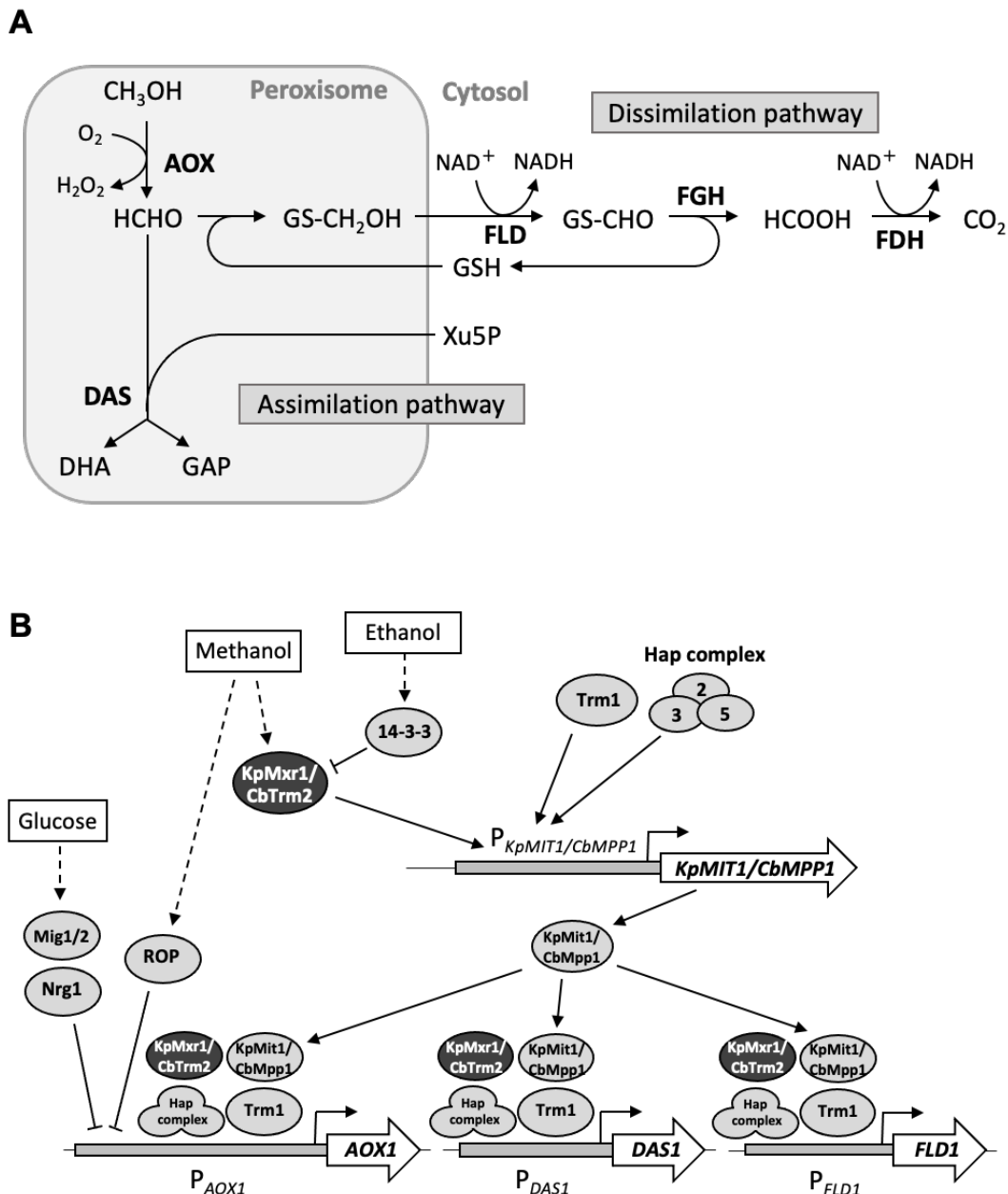
Figure 0. Enzymes associated with methanol metabolism and transcription factors involved in methanol-induced gene expression.

(A) The pathway of methanol metabolism. Methanol is first oxidized by alcohol oxidase (AOX) to generate formaldehyde and H_2O_2. Formaldehyde, a central intermediate of the methanol metabolism pathway, is positioned at the branch point of the assimilatory and dissimilatory pathways. In the assimilatory pathway, formaldehyde is fixed by dihydroxyacetone synthase (DAS) to xylulose 5-phosphate (Xu5P) to produce dihydroxyacetone (DHA) and glyceraldehyde 3-phosphate (GAP), which are then consumed to synthesize cell components. AOX and DAS are both localized in peroxisomes. In the dissimilatory pathway, formaldehyde is further oxidized to CO_2 by glutathione (GSH)-dependent formaldehyde oxidation pathway including formaldehyde dehydrogenase (FLD), *S*-formylglutathione hydrolase (FGH) and formate dehydrogenase (FDH). (B) Transcription factors involved in methanol-induced gene expression. The expression of *KpMIT1/CbMPP1* is induced by methanol, which requires transcription factors KpMxr1/CbTrm2, Trm1 and Hap complex (Hap2, Hap3 and Hap5). These transcription factors then interact with the methanol-induced gene promoters (*AOX1*, *DAS1*, *FLD1*, etc.) (Yurimoto *et al.*, 2019). KpROP and KpMxr1 function competitively but exhibit the same DNA binding specificity (Kumar *et al.*, 2012). KpMig1, KpMig2 and KpNrg1 repress the expression of methanol-induced genes under glucose-culture condition (Shi *et al.*, 2018; Wang *et al.*, 2016a). Under the ethanol-culture condition, 14-3-3 protein binds to KpMxr1 via S215 phosphorylation to inactivate KpMxr1 (Parua *et al.*, 2012). CbMig1 is involved in the glucose repression of methanol-induced genes (Zhai *et al.*, 2012).

Chapter I

Phosphoregulation of the transcription factor Mxr1 plays a crucial role in the concentration-regulated methanol induction in *Komagataella phaffii*

Introduction

KpMxr1 is the C_2H_2-type transcription factor that is necessary for the activation of many genes, including those involved in peroxisome biogenesis (Lin-Cereghino *et al.*, 2006). KpMxr1 regulates the gene expression of not only methanol but acetate and amino acid metabolism as well and thus functions as a global regulator of central carbon metabolism (Sahu *et al.*, 2016a; Sahu *et al.*, 2016b). KpMxr1 exists in the cytosol in the cells during metabolizing glucose and localizes to the nucleus when the cells are cultured in media containing non-fermentable carbon sources (Lin-Cereghino *et al.*, 2006; Sahu *et al.*, 2016b). In *S. cerevisiae*, the activity of ScAdr1 is regulated through its indirect phosphorylation and dephosphorylation by the ScSnf1/AMPK protein kinase (Ratnakumar *et al.*, 2009). In *K. phaffii*, serine 215 residue of KpMxr1 is phosphorylated under ethanol-culture conditions and this phosphoserine residue interacts with the 14-3-3 protein, resulting in loss of function for methanol induction of the genes as a transcription factor (Parua *et al.*, 2012). The involvement of S215 phosphorylation of KpMxr1 has also been shown in ethanol repression of methanol-induced genes (Ohsawa *et al.*, 2018).

Methanol concentration in the phyllosphere exhibits a daily periodicity with a dynamic range of 0-0.2% (ca. 0-60 mM) (Kawaguchi *et al.*, 2011). Thus, methylotrophic yeasts must sense the presence and concentration of methanol and regulate the expression of methanol-induced genes and the metabolism of methanol based on that information. Since formaldehyde is toxic to cells and unbalanced methanol metabolism results in the accumulation of formaldehyde, expression levels of the formaldehyde-generating enzyme, AOX, and formaldehyde-consuming enzymes, DAS and formaldehyde dehydrogenase (FLD), should be properly controlled according to environmental methanol concentrations.

In this chapter, I hypothesized that the transcription factor KpMxr1 is responsible for the CRMI in *K. phaffii* and studied its functional and phosphorylation dynamics. I revealed that the phosphorylation state of KpMxr1 is controlled depending on methanol concentration. Moreover, I discovered that KpMxr1 receives the methanol signal from Wsc family proteins via KpPkc1 and this process is independent of the MAPK cascade. The analysis of C-terminal truncated KpMxr1 and LC-MS/MS gave me an insight that phosphoregulation of KpMxr1 plays a crucial role in CRMI in *K. phaffii*.

Materials & Methods

Strains, media and culture conditions

The yeast strains used in this study are listed in Table 1-1. *K. phaffii* cells were grown at 28 °C on YPD (1% yeast extract, 2% peptone, 2% glucose) or YNB medium (0.67% yeast nitrogen base without amino acids, pH 6.0). 2% (w/v) glucose (synthetic dextrose medium; SD medium), 0.5% (v/v) ethanol (SE medium) or several concentrations of methanol (SM medium) were used as carbon sources in YNB medium. All the components other than the carbon sources used in these media were purchased from Difco Becton Dickinson (Franklin Lakes, NJ). The growth of the yeast was monitored by the optical density (OD) at 610 nm.

K. phaffii strain GS115 or PPY12 was used as the host of transformants. Gene disruption was performed by homologous recombination with the Blasticidin-S resistance gene (Bsd^R) as a selective marker. The transformation protocol of *K. phaffii* was based on the improved lithium acetate method (Cregg *et al.*, 1985; Wu *et al.*, 2004).

Escherichia coli HST08 Premium (Takara Bio, Otsu, Japan) was used as a host strain for plasmid DNA preparation. *E. coli* cells were grown in LB medium (1% tryptone, 0.5% yeast extract, 0.5% NaCl) at 37°C.

Plasmid construction

The plasmids used in this study are listed in Table 1-2. The oligonucleotide primers in this study are listed in Table 1-3. A gene deletion cassette for *KpTRM1* was constructed as follows: Primer pairs GeneD-trm1-A-Fw/GeneD-trm1-A-Rv and GeneD-trm1-B-Fw/GeneD-trm1-B-Rv were used to amplify 1.0 kbp of DNA from the genome (namely fragment A, B). The primer pair (trm1)-Bsd-Fw/(trm1)-Bsd-Rv was used to amplify the blasticidin S resistance gene using plasmid pPIC6A (Thermo Fisher Scientific, Waltham, MA) as a template (fragment C). These three fragments were combined by overlap PCR with the primer pair GeneD-trm1-A-Fw/GeneD-trm1-B-Rv, and a 3.1 kbp fragment (A-C-B) was obtained. This fragment was cloned (TA cloning) into the TOPO vector pCR2.1 (Takara Bio, Otsu, Japan), yielding the *KpTRM1* disruption vector pKI001. pKI001 was digested with EcoRI to disrupt the *KpTRM1* gene. These digested DNA fragments were used to transform *K. phaffii* by electroporation. Proper gene disruptions were confirmed by colony PCR. Gene deletion of *KpHAP3*, *KpMIT1, KpMIG1* or *KpROP1* was performed in the same way using the primer pairs listed in Table 1-3.

For copper-inducible expression of *KpMXR1*, the region from -235 to -1 of the *ScCUP1* promoter was amplified by PCR from *S. cerevisiae* genomic DNA as a template using the primer pair Infusion-Pcup1-pIB1arg-Fw/Infusion-Pcup1-pIB1arg-Rv. This fragment was cloned into the KpnI and BamHI

sites of pSN303 by In-Fusion cloning (Takara Bio, Otsu, Japan), resulting in pKI006.

The *KpMXR1* promoter and the DNA region of KpMxr1 1-525 a.a., 1-368 a.a., 1-230 a.a. and 1-211a.a. were amplified by PCR using primer pairs Inverse-Mxr1-5xFLAG-Fw/ Infusion-Mxr1(525)-Rv, Infusion-Mxr1-5xFLAG-Fw/Infusion-Mxr1(368)-Rv, Inverse-Mxr1-5xFLAG-Fw/Infusion-Mxr1(230)-Rv and Inverse-Mxr1-5xFLAG-Fw/Infusion-Mxr1(211)-Rv for pKI007, pKI008, pKI009 and pKI010, respectively. They were cloned into the KpnI and BamHI sites of pSN303 by In-Fusion cloning.

The *KpMXR1* promoter and the DNA region of KpMxr1 1-1155 a.a., 1-525 a.a. and 1-230 a.a. were amplified by PCR using primer pairs Infusion-Pmxr1-Mxr1-Fw/Infusion-Mxr1YFP-Rv, Infusion-Pmxr1-Mxr1-Fw/Infusion-Mxr1(525)YFP-Rv and Inverse-Mxr1-5xFLAG-Fw/Infusion-Mxr1(230)-Rv for pKI011, pKI012 and pKI013 respectively. They were cloned into the KpnI and BamHI sites of pNT205 by In-Fusion cloning.

pSN303 was subjected to site-directed mutagenesis by using the primer pairs Mutation-Mxr1-S(2)A-Fw/Mutation-Mxr1-S(2)A-Rv and Mutation-Mxr1-T(5)A-Fw/Mutation-Mxr1-T(5)A-Rv, resulting in pKI014 and pKI015, respectively. The *KpMXR1* promoter and the DNA region of KpMxr1 1-230 a.a. were amplified by PCR from pKI014 and pKI015 using primer pair Inverse-Mxr1-5xFLAG-Fw/Infusion-Mxr1(230)-Rv, resulting in pKI016 and pKI017, respectively.

The region from -235 to -1 of the *ScCUP1* promoter was amplified by PCR from *S. cerevisiae* genomic DNA as a template using the primer pair EcoRI-CUP1promoter-Fw/EcoRI-CUP1promoter-Rv. The DNA fragment and pIB1 were digested by EcoRI and ligated to obtain the plasmid Pc(EcoRI)-pIB1. The gene *KpRHO1* N-terminal tagged with myc was amplified by PCR from *K. phaffii* genomic DNA as a template using the primer pair KpnI-Myc-Rho1-Fw/HindIII-Rho1-Rv. The DNA fragment and Pc(EcoRI)-pIB1 were digested by HindIII and KpnI and ligated to obtain pKI018. The region from -235 to -1 of the *ScCUP1* promoter was amplified by PCR from *S. cerevisiae* genomic DNA as a template using the primer pair KpnI-CUP1promoter-Fw/KpnI-CUP1promoter-Rv. The DNA fragment and pSY006 were digested by KpnI and ligated to obtain the plasmid Pc(KpnI)-pSY006. The genes *KpPKC1* and *KpMkk1* were amplified by PCR from *K. phaffii* genomic DNA as a template using the primer pairs BamHI-Pkc1-Fw/ Xho1-Pkc1-Rv and XmaI-Mkk1-Fw/PstI-Mkk1-Rv, respectively. The DNA fragments and Pc(KpnI)-pSY006 were digested by BamHI/XhoI and XmaI/PstI, and then ligated to obtain pKI019 and pKI020, respectively. pKI018, pK019 and pKI020 were subjected to site-directed mutagenesis by using the primer pairs Rho1-Q68H-Fw/Rho1-Q68H-Rv, Pkc1-R390P-Fw/Pkc1-R390P-Rv and Mkk1-S313P-Fw/Mkk1-S313P-Rv, resulting in pKI021, pKI022 and pKI023, respectively.

Table 1-1. *K. phaffii* strains used in this study.

Designation	Genotype	Reference
PPY12	*arg4, his4*	Sakai *et al.*, 1998
GS115	*his4*	Cregg *et al.*, 1985
GS-mxr1	GS115, *mxr1Δ*::Bsd^R, *his4::HIS4*	This study
GS-trm1	GS115, *trm1Δ*::Bsd^R, *his4::HIS4*	This study
GS-hap3	GS115, *hap3Δ*::Bsd^R, *his4::HIS4*	This study
PPY12H-mxr1	PPY12, *mxr1Δ*::Bsd^R, *his4::HIS4*	This study
FL1155	PPY12H-mxr1, *arg4::(P$_{MXR1}$-MXR1-5xFLAG, ARG4)*	Ohsawa *et al.*, 2018
C-FL1155	PPY12, *arg::(P$_{CUP1}$-MXR1-5xFLAG, ARG4), his4::HIS4*	This study
TM525	PPY12H-mxr1, *arg4::(P$_{MXR1}$-MXR1(1-525a.a.)-5xFLAG, ARG4)*	This study
TM368	PPY12H-mxr1, *arg4::(P$_{MXR1}$-MXR1(1-368a.a.)-5xFLAG, ARG4)*	This study
TM230	PPY12H-mxr1, *arg4::(P$_{MXR1}$-MXR1(1-230a.a.)-5xFLAG, ARG4)*	This study
TM211	PPY12H-mxr1, *arg4::(P$_{MXR1}$-MXR1(1-211a.a.)-5xFLAG, ARG4)*	This study
FL1155YFP	PPY12H-mxr1, *arg4::(P$_{MXR1}$-MXR1-EYFP, ARG4)*	This study
TM525YFP	PPY12H-mxr1, *arg4::(P$_{MXR1}$-MXR1(1-525a.a.)-EYFP, ARG4)*	This study
TM230YFP	PPY12H-mxr1, *arg4::(P$_{MXR1}$-MXR1(1-230a.a.)-EYFP, ARG4)*	This study
MSA	PPY12H-mxr1, *arg4::(P$_{MXR1}$-MXR1(S110A,S111A)-5xFLAG, ARG4)*	This study
MTA	PPY12H-mxr1, *arg4::(P$_{MXR1}$-MXR1(T121A,T124A,T125A,T128A,T131A)-5xFLAG, ARG4)*	This study
TM230SA	PPY12H-mxr1, *arg4::(P$_{MXR1}$-MXR1(1-230a.a. S110A,S111A)-5xFLAG, ARG4)*	This study
TM230TA	PPY12H-mxr1, *arg4::(P$_{MXR1}$-MXR1(1-230a.a. T121A,T124A,T125A,T128A,T131A)-5xFLAG, ARG4)*	This study
MS215A	PPY12H-mxr1, *arg4::(P$_{MXR1}$-MXR1(S215A)-5xFLAG, ARG4)*	Ohsawa *et al.*, 2018
GS-RHO	GS115, *his4::(P$_{CUP1}$-Myc-RHO1, HIS4)*	This study
GS-RHO^M	GS115, *his4::(P$_{CUP1}$-Myc-RHO1(Q68H), HIS4)*	This study
GS-PKC	GS115, *his4::(P$_{CUP1}$-PKC1-3xHA, HIS4)*	This study
GS-PKC^M	GS115, *his4::(P$_{CUP1}$-PKC1(R390P)-3xHA, HIS4)*	This study
GS-MKK	GS115, *his4::(P$_{CUP1}$-MKK1-3xHA, HIS4)*	This study
GS-MKK^M	GS115, *his4::(P$_{CUP1}$-MKK1(S313P)-3xHA, HIS4)*	This study
RHO^M-mxr1	GS115, *mxr1Δ*::Bsd^R, *his4::(P$_{CUP1}$-Myc-RHO1(Q68H), HIS4)*	This study
RHO^M-mit1	GS115, *mit1Δ*::Bsd^R, *his4::(P$_{CUP1}$-Myc-RHO1(Q68H), HIS4)*	This study
RHO^M-trm1	GS115, *trm1Δ*::Bsd^R, *his4::(P$_{CUP1}$-Myc-RHO1(Q68H), HIS4)*	This study
RHO^M-hap3	GS115, *hap3Δ*::Bsd^R, *his4::(P$_{CUP1}$-Myc-RHO1(Q68H), HIS4)*	This study
RHO^M-mig1	GS115, *mig1Δ*::Bsd^R, *his4::(P$_{CUP1}$-Myc-RHO1(Q68H), HIS4)*	This study
RHO^M-rop1	GS115, *rop1Δ*::Bsd^R, *his4::(P$_{CUP1}$-Myc-RHO1(Q68H), HIS4)*	This study
PKC^M-TM230	PPY12, *mxr1Δ*::Bsd^R, *arg4:: (P$_{MXR1}$-MXR1(1-230a.a.)-5xFLAG, ARG4), his4::(P$_{CUP1}$-PKC1 (R390P)-3xHA, HIS4)*	This study

Table 1-2. Plasmids used in this study.

Designation	Description	Reference
pIB1	*KpHIS4*	Sears *et al.*, 1998
pNT204	*KpARG4*	Tamura *et al.*, 2010
pNT205	EYFP *ARG4*	Tamura *et al.*, 2010
pSY006	*3xHA/pIB1*	Ohsawa *et al.*, 2017
pSN102	*Kpmxr1Δ*::Bsd^R	Ohsawa *et al.*, 2018
pKI001	*Kptrm1Δ*::Bsd^R	This study
pKI002	*Kphap3Δ*::Bsd^R	This study
pKI003	*Kpmit1Δ*::Bsd^R	This study
pKI004	*Kpmig1Δ*::Bsd^R	This study
pKI005	*Kprop1Δ*::Bsd^R	This study
pSN303	P$_{MXR1}$-*MXR1*-5xFLAG/pNT204	Ohsawa *et al.*, 2018
pSN304	P$_{MXR1}$-*MXR1*(S215A)-5xFLAG/pNT204	Ohsawa *et al.*, 2018
pKI006	P$_{CUP1}$-*MXR1*-5xFLAG/pNT204	This study
pKI007	P$_{MXR1}$-*MXR1*(1-525 a.a.)-5xFLAG/pNT204	This study
pKI008	P$_{MXR1}$-*MXR1*(1-368 a.a.)-5xFLAG/pNT204	This study
pKI009	P$_{MXR1}$-*MXR1*(1-230 a.a.)-5xFLAG/pNT204	This study
pKI010	P$_{MXR1}$-*MXR1*(1-211 a.a.)-5xFLAG/pNT204	This study
pKI011	P$_{MXR1}$-*MXR1*-EYFP/pNT205	This study
pKI012	P$_{MXR1}$-*MXR1*(1-525 a.a.)-EYFP/pNT205	This study
pKI013	P$_{MXR1}$-*MXR1*(1-230 a.a.)-EYFP/pNT205	This study
pKI014	P$_{MXR1}$-*MXR1*(S110A, S111A)-5xFLAG/pNT204	This study
pKI015	P$_{MXR1}$-*MXR1*(T121A, T124A, T125A, T128A, T131A)-5xFLAG/pNT204	This study
pKI016	P$_{MXR1}$-*MXR1*(1-230 a.a. S110A, S111A)-5xFLAG/pNT204	This study
pKI017	P$_{MXR1}$-*MXR1*(1-230 a.a. T121A, T124A, T125A, T128A, T131A)-5xFLAG /pNT204	This study
Pc(EcoRI)-pIB1	P$_{ScCUP1}$/pIB1	This study
pKI018	P$_{CUP1}$-Myc-*RHO1*/pIB1	This study
Pc(KpnI)-pSY006	P$_{ScCUP1}$/pSY006	This study
pKI019	P$_{CUP1}$-*PKC1*-3xHA/pSY006	This study
pKI020	P$_{CUP1}$-*MKK1*-3xHA/pSY006	This study
pKI021	P$_{CUP1}$-Myc-*RHO1*(Q68H)/pIB1	This study
pKI022	P$_{CUP1}$-*PKC1*(R390P)-3xHA/pSY006	This study
pKI023	P$_{CUP1}$-*MKK1*(S313P)-3xHA/pSY006	This study

Table 1-3. Oligonucleotide primers used in this study.

Designation	DNA Sequence
GeneD-trm1-A-Fw	5'-CACAAGGTTGTTCACTATGTCCTC-3'
GeneD-trm1-A-Rv	5'-GAAGCTATGGTGTGTGGGCTCAGGGCAAAGATGATTGTGA-3'
GeneD-trm1-B-Fw	5'-CGAAGGCTTTAATTTGCAAGCTCGTGAATGTGACATAAGACTCCA-3'
GeneD-trm1-B-Rv	5'-CAGCAGAATCGTTCAACCAA-3'
(trm1)-Bsd-Fw	5'-TCACAATCATCTTTGCCCTGAGCCCACACACCATAGCTTC-3'
(trm1)-Bsd-Rw	5'-TGGAGTCTTATGTCACATTCACGAGCTTGCAAATTAAAGCCTTCG-3'
GeneD-hap3-A-Fw	5'-AGCAAGGTCCACCTCTTCTG-3'
GeneD-hap3-A-Rv	5'-TTTGAAGCTATGGTGTGTGGGTGAGGCTTCTGGAAACGAGT-3'
GeneD-hap3-B-Fw	5'-CGAAGGCTTTAATTTGCAAGCTTTCCTCGACAAAGAGGACAGA-3'
GeneD-hap3-B-Rv	5'-TGGATGAAGAGGACTTGATGG-3'
(hap3)-Bsd-Fw	5'-ACTCGTTTCCAGAAGCCTCACCCACACACCATAGCTTCAAA-3'
(hap3)-Bsd-Rw	5'-TCTGTCCTCTTTGTCGAGGAAAGCTTGCAAATTAAAGCCTTCG-3'
GeneD-mit1-A-Fw	5'-TTTGATCGAAGCGAGCTACA-3'
GeneD-mit1-A-Rv	5'-GAAGCTATGGTGTGTGGGCTGGAAGAAGAGGGAAGCCAAC-3'
GeneD-mit1-B-Fw	5'-CGAAGGCTTTAATTTGCAAGCTATCCAACCAACCAAACCAAA-3'
GeneD-mit1-B-Rv	5'-ACTCCTTCATCCTCCGGTCT-3'
(mit1)-Bsd-Fw	5'-GTTGGCTTCCCTCTTCTTCCAGCCCACACACCATAGCTTC-3'
(mit1)-Bsd-Rw	5'-TTTGGTTTGGTTGGTTGGATAGCTTGCAAATTAAAGCCTTCG-3'
GeneD-mig1-A-Fw	5'-AGGGTGAGGGTGATCAAGG-3'
GeneD-mig1-A-Rv	5'-GAAGCTATGGTGTGTGGGCTCCAGGGGAGAAACAGAAAAA-3'
GeneD-mig1-B-Fw	5'-CGAAGGCTTTAATTTGCAAGCTTCACTTCCTCCTTTCTTTTTCTG-3'
GeneD-mig1-B-Rv	5'-GTCAGACGCCGTTCAAAACT-3'
(mig1)-Bsd-Fw	5'-TTTTTCTGTTTCTCCCCTGGAGCCCACACACCATAGCTTC-3'
(mig1)-Bsd-Rw	5'-CAGAAAAAGAAAGGAGGAAGTGAAGCTTGCAAATTAAAGCCTTCG-3'
GeneD-rop1-A-Fw	5'-GTTTGAGCCCACTGACACCT-3'
GeneD-rop1-A-Rv	5'-GAAGCTATGGTGTGTGGGCTATTGTAAAGGCCAGGTGGTG-3'
GeneD-rop1-B-Fw	5'-CGAAGGCTTTAATTTGCAAGCTGAACGAAGTTCAGTCGCATTT-3'
GeneD-rop1-B-Rv	5'-GCTAATTTCGCACCTTGGAA-3'
(rop1)-Bsd-Fw	5'-CACCACCTGGCCTTTACAATAGCCCACACACCATAGCTTC-3'
(rop1)-Bsd-Rw	5'-AAATGCGACTGAACTTCGTTCAGCTTGCAAATTAAAGCCTTCG-3'
Infusion-Pcup1-pIB1arg-Fw	5'-GGCGAATTGGGTACCAGCCGATCCCATTACCGA-3'
Infusion-Pcup1-pIB1arg-Rv	5'-GGGTAGATTGCTCATGGATCCAGTTTGTTTTTCTTA-3'
Infusion-Mxr1-5xFLAG-Fw	5'-GGATCCACTAGTCTCGAGATCC-3'
Infusion-Mxr1(525)-Rv	5'-CGAGACTAGTGGATCCCTCATTCTCATCTAAAATTGCC-3'
Infusion-Mxr1(368)-Rv	5'-CGAGACTAGTGGATCCCTCAAGTTCTTGAATGGTATTAGC-3'

Table1-3. Continued.

Designation	DNA Sequence
Infusion-Mxr1(230)-Rv	5'-CGAGACTAGTGGATCCATTATTCACATAATGGGCATAATTATTTC-3'
Infusion-Mxr1(211)-Rv	5'-CGAGACTAGTGGATCCTAGTCCAAGATCAAACAAATTG-3'
Infusion-Pmxr1-Mxr1-Fw	5'-TATAGGGCGAATTGGGTACCGGTGTCATCAAGTGGCGT-3'
Infusion-Mxr1-YFP-Rv	5'-GAGACTAGTGGATCCGACACCACCATCTAG-3'
Infusion-Mxr1(525)YFP-Rv	5'-ATGCCTGCAGCTCGAGCTCATTCTCATCTAAAATTGC-3'
Infusion-Mxr1(230)YFP-Rv	5'-ATGCCTGCAGCTCGAGATTATTCACATAATGGGCATAATTATTTCC-3'
Mutation-Mxr1-S(2)A-Fw	5'-AAGGCAACTCGTCGGGCTGCTAATGCCGCGGGTTC-3'
Mutation-Mxr1-S(2)A-Rv	5'-GAACCCGCGGCATTAGCAGCCCGACGAGTTGCCTT-3'
Mutation-Mxr1-T(5)A-Fw	5'-TTCTGCTCCGGTGGCAGCGCCAAATGCTATGGGTGCGC-3'
Mutation-Mxr1-T(5)A-Rv	5'-GCGCACCCATAGCATTTGGCGCTGCCACCGGAGCAGAA-3'
EcoRI-CUP1promoter-Fw	5'-GGAATTCTCCCATTACCGACATTTGGGC-3'
EcoRI-CUP1promoter-Rv	5'-GGAATTCACAGTTTGTTTTTCTTAATATCTATTTCG-3'
KpnI-Myc-Rho1-Fw	5'-GGGGTACCATGGAACAAAAACTCATCTCAG AAGAGGATCTGGCTGTTAATAATCCGTCTGAATTTAG-3'
HindIII-Rho1-Rv	5'-CCCAAGCTTTTAAACAATGTTACACTTCTTCTTACG-3'
Rho1-Q68H-Fw	5'-GCCGGACACGAAGATTATGATAGACTG-3'
Rho1-Q68H-Rv	5'-ATCTTCGTGTCCGGCAGTATCCCATAG-3'
KpnI-CUP1promoter-Fw	5'-GGGGTACCTCCCATTACCGACATTTGGGC-3'
KpnI-CUP1promoter-Rv	5'-GGGGTACCACAGTTTGTTTTTCTTAATATCTATTTCG-3'
BamHI-Pkc1-Fw	5'-CGGGATCCATGTCAGACACAAGCAATGATGA-3'
XhoI-Pkc1-Rv	5'-CCGCTCGAGAGTGTGATCATCGTTCACATACG-3'
Pkc1-R390P-Fw	5'-TTGGGTCCTCATGGAGCTATTCGTCAG-3'
Pkc1-R390P-Rv	5'-TCCATGAGGACCCAAACCACCCATGAA-3'
XmaI-Mkk1-Fw	5'-CCCGGGATGATTCATAAAATGTCAAGATCCAG-3'
PstI-Mkk1-Rv	5'-CTGCAGCTCTTCCCAGCACTGTCTGAC-3'
Mkk1-S313P-Fw	5'-GGAACGCCCTATTATATGGCGCCAGAA-3'
Mkk1-S313P-Rv	5'-ATAATAGGGCGTTCCTGTGAATGTTGT-3'
RT-AOX1-Fw	5'-TTTCGAAGGTCCAATCAAGG-3'
RT-AOX1-Rv	5'-GTTCAGCACCGTGAGCAGTA-3'
RT-DAS1-Fw	5'-GGTGACGAGTTAGTAAAGAAC-3'
RT-DAS1-Rv	5'-CCTCTAACACGAGAAAGGAAC-3'
RT-MXR1-Fw	5'-CCACCGTAAGGACAATCCAC-3'
RT-MXR1-Rv	5'-GCCAAAGTGTTGTGGGAACT-3'
RT-MIT1-Fw	5'-GACTAATGACGATGAACTAAG-3'
RT-MIT1-Rv	5'-TGCTGTTGTTGGTAGAAT-3'
RT-GAP-Fw	5'-CCACCGGTGTTTTCACCACT-3'
RT-GAP-Rv	5'-CACCGACAACGAACATTGGA-3'

Extraction of genomic DNA from *K. phaffii* cells

A single colony of the yeast was inoculated in YPD medium and grown overnight at 28°C. Cells equivalent to 10 OD_{610} units were harvested by centrifugation at 5,000 g for 3 min at 4°C and resuspended in 1 mL of SZB solution (10 mM sodium citrate, 100 mM sorbitol, 50 mM EDTA, 50 mg/L Zymolyase 100T and 1% v/v β-mercaptoethanol, pH 7.5) after the supernatant was removed. The solution was incubated at 37°C for 1 h and mixed with 150 µL of SDS-TE solution (10 mM Tris-HCl, 2% SDS and 1 mM EDTA, pH 7.5). Subsequently, the solution was incubated at 65°C for 30 min and 150 µL of 5M potassium acetate was added to the solution and incubated at 4°C for 30 min. The sample was centrifuged (20,000 g, 10 min, 4°C) and the supernatant was added to the same volume of isopropanol including 650 mM ammonium acetate. Then, the sample was incubated at -20°C for 10 min and centrifuged (20,000 g, 10 min, 4°C). The supernatant was removed and the precipitation was washed with 1 mL of 70% ethanol. The supernatant was removed again, and the precipitation was dried. The precipitation was dissolved in 300 µL of RNase solution (10 mM Tris-HCl, 1 mM EDTA, 100 mg/L RNaseA, 200 mg/L Proteinase K and 110 mM sodium chloride, pH 7.5) and incubated at 37°C for 30 min. The solution was mixed with phenol/ chloroform/ isoamyl alcohol (25: 24: 1) and an aqueous layer was corrected. Subsequently, the solution was added to the same volume of isopropanol including 300 mM sodium acetate and incubated at -20°C for 10min. The sample was centrifuged (20,000 g, 20 min, 4°C), and washed with 70% ethanol as described above. The precipitation was dissolved in 300 µL of TE buffer (10 mM Tris-HCl and 1 mM EDTA, pH 7.5), and used as a genomic DNA solution.

RNA isolation and quantitative reverse transcription-PCR (qRT-PCR)

A single colony was inoculated in YPD medium and grown overnight at 28°C. Yeast cells were transferred into SD medium and cultivated to the early exponential phase. The cells were shifted to SM medium and cultured for 2 h. Cells equivalent to 5 OD_{610} units were harvested at the indicated time point by centrifugation at 10,000 g for 1 min at 4°C. Total RNA was extracted from cells using an RNeasy Mini Kit and RNase-Free DNase Set (QIAGEN, Hilden, Germany). Cells were suspended in RLT buffer including 10% β-mercaptoethanol and then lysed using Multi-Beads Shocker (2,500 rpm, 30 sec of ON, 30 sec of OFF, 20 cycles). Subsequently, RNA concentration in the obtained samples was measured by NanoDrop Lite Spectrometer (Thermo Fisher Scientific, Waltham, MA) and cDNA was synthesized from 800 ng of total RNA using ReverTra Ace qPCR RT Kit (Toyobo, Tokyo, Japan). After amplifying cDNA, qRT-PCR was performed by a Light Cycler (Roche Diagnostics) using TB Green Premix Ex Taq II Tli RNaseH Plus (Takara Bio, Otsu, Japan) and corresponding primers for *AOX1, DAS1, KpMIT1, KpMXR1, GAP* (show in Table 1-3). The transcript level of all genes in methanol culture was first quantified using *GAP* as the control, and then, indicated as the relative value to that in glucose culture. The PCR procedure

was shown below: 10 sec of denaturation at 95°C in the first cycle, 40 repetitions in the second cycle (95°C for 5 sec, 60°C for 20 sec, all temperature transitions, 20°C s^{-1}). The number of copies of each sample was determined with the Light Cycler software Version 4.1.

Preparation of protein extracts from yeast cells

Yeast cells were grown in YPD and SD as described above, and the cells were shifted from SD to SM medium at 28°C for 30 min to 2 h. The cells equivalent to about 2 OD_{610} units (for immunoblot analysis), 100 OD_{610} units (for immunoprecipitation and immunoblot analysis) or 2,000 OD units (for immunoprecipitation and LC-MS/MS analysis) were cultured and collected for protein extraction. They were suspended in 0.2 N NaOH solution containing 0.5% β-mercaptoethanol for 15 min on ice and trichloroacetic acid (Fujifilm, Osaka, Japan) was added to a final concentration of 10% v/v for cell lysis. The samples were centrifuged (20,000 g, 5 min, 4°C) and protein pellets were washed three times with 100% acetone by brief sonication. Subsequently, protein pellets were re-suspended in the sample buffer (62.5 mM Tris-HCl, 2% SDS, 10% Glycerol, 5% β-mercaptoethanol, 0.005% BPB, pH 6.8) or the buffer for immunoprecipitation (62.5 mM Tris-HCl, 2% SDS, pH 6.8). The samples were incubated at 65°C for 10 min.

Immunoprecipitation

To the obtained protein extract solution, 20 times the amount of the buffer without SDS (62.5 mM Tris-HCl, protease inhibitor cocktail (Roche Diagnostics, Basel, Switzerland), and phosphatase inhibitor cocktail (Nakalai tesque, Kyoto, Japan), pH 6.8) were added. The solution was pre-cleared with mouse IgG-Agarose beads (Merck KGaA, Darmstadt, Germany) for 2 h at 4°C to remove nonspecific binding proteins. Mouse IgG-agarose beads and protein debris were removed by centrifugation in a swing rotor at 1,500 g for 10 min. Anti-FLAG-M2 affinity agarose beads (Merck KGaA, Darmstadt, Germany) were added and incubated for 2 h at 4°C. The beads were collected by centrifugation in a swing rotor at 1,500 g for 5 min and washed with 62.5 mM Tris-HCl buffer (pH 6.8). For LC-MS/MS analysis, the target protein was eluted with the sample buffer for 20 min at 80°C, and the eluted protein sample was condensed by ultra-filtration with amicon ultra-4 centrifugal filter 50K (Merck KGaA, Darmstadt, Germany). For phos-tag SDS-PAGE, anti-FLAG-M2 affinity agarose beads harboring the target protein were washed and treated with or without λ-phosphatase (New England Biolabs, Ipswich, MA, USA) at 30°C for 1 h. Then, the target protein was eluted with the sample buffer for 20 min at 80°C.

Immunoblot analysis

The samples were first centrifuged at 20,000 g for 1 min. 10 μL of the supernatant was electrophoresed

13

on a 6-10% SDS-PAGE gel. Precision Plus Protein Dual Color Standard (Bio-Rad, Hercules, USA) was used as a protein-loading marker. The proteins were transferred to an Immobilon-P PVDF membrane (0.2 µm, Merck KGaA, Darmstadt, Germany) by semidry blotting (Bio-Rad, Hercules, USA). The membranes were incubated in Blocking One (Nakalai tesque, Kyoto, Japan) and then in the solution containing anti-DYKDDDDK antibody (called anti-FLAG antibody in this study, 1E6; Fujifilm, Tokyo, Japan), anti-beta actin (Abcam, Cambridge, UK), anti-phosphoserine antibody (Abcam, Cambridge, UK), anti-phosphothreonine antibody (Abcam, Cambridge, UK) or anti-phosphotyrosine antibody (Abcam, Cambridge, UK) at dilutions recommended in the protocol with TBS-T buffer. The membranes were washed 3 times with TBS-T buffer and incubated with anti-mouse-HRP (Merck Millipore, Darmstadt, Germany) or anti-rabbit-HRP (#7074, goat polyclonal, Abcam, Cambridge, UK) at a 1:5,000 dilution for 1 h. Finally, bound secondary antibodies were detected using Western Lightning (Perkin-Elmer Life Science, Waltham, MA) and the signals were detected using Lummino-Graph II (ATTO, Tokyo, Japan). The band intensity was quantified with ImageJ (National Institutes of Health, USA).

In the phos-tag analysis, SuperSep Ace gels with or without 50 µM phos-tag (7.5%, 13 wells; Fujifilm, Tokyo, Japan) were mainly used. Hand-made gels containing Zn^{2+} were also used with or without 20 µM of phos-tag (8.5% Wako, Osaka, Japan) according to the instruction manual of Wako.

LC-MS/MS analysis

The protein samples purified by immunoprecipitation were loaded in 12.5% SDS-PAGE gels (SuperSep Ace, Wako). The electrophoresed gels were stained with CBB Stain One Super (Nakalai tesque, Kyoto, Japan), and a part of the gel of the target protein band was cut out. According to the manufacturer's instructions, the gels were digested using an in-gel tryptic digestion kit (Thermo Fisher Scientific). The recovered tryptic digests were separated using nano-flow liquid chromatography (Nano-LC-Ultra 2D-plus equipped with cHiPLC Nanoflex, Eksigent, Dublin, CA, USA) in a trap and elute mode, with a trap column (200 µm x 0.5 mm ChromXP C18-CL 3 µm 120 Å (Eksigent)) and an analytical column (75 µm x 15 cm ChromXP C18-CL 3 µm 120 Å (Eksigent)). The gradient program used for the separation was as follows; A98%/B2% to A66.8%/B33.2% in 125 min, A66.8%/B33.2% to A2%/B98% in 2 min, A2%/B98% for 5 min, A2%/B98% to A98%/B2% in 0.1 min, and A98%/B2% for 17.9 min, in which 0.1% formic acid/water and 0.1% formic acid/acetonitrile were utilized as mobile phases A and B, respectively. The flow rate was 300 nL/min. The analytical column temperature was 40ºC. The eluate was directly infused into a mass spectrometer (TripleTOF 5600+ System coupled with a NanoSpray III source and heated interface, SCIEX, Framingham, MA, USA), and ionized in the electrospray ionization-positive mode. Data acquisition was performed using an information-dependent acquisition method. The acquired datasets were analyzed using ProteinPilot software, version 5.0.1 (SCIEX), with the NCBI

protein library for *K. phaffii* (April 2020) appended with the amino acid sequence of KpMxr1[1-525]-FLAG and known contaminants database (SCIEX). Various protein modifications were detected in KpMxr1, such as phosphorylation, oxidation, methylation, acetylation, etc., Identifications with at least 95% confidence were considered significant.

Fluorescence microscopy observation

Yeast cells were grown in YPD and SD as described above and shifted from SD to SM medium containing 0, 0.01, 0.1 or 1 % methanol at 28°C for 3 h. The cells were treated with 5% formaldehyde (using 35% formaldehyde solution containing 7% methanol, Nakalai chemicals, Japan) for 1 h, and subsequently incubated in DAPI solution (100 μg/L, Nakalai tesque, Kyoto, Japan) for 30 min. Observations were carried out with an IX81 fluorescence microscope (Olympus, Tokyo, Japan). Fluorescent images were captured with a charged coupled device (CCD) camera (SenSys; PhotoMetrics, Tucson, AZ) at the fixed exposure time of 200 msec in DIC field, 1000 msec in YFP field and 50 msec in DAPI field using MetaMorph software (Universal Imaging, West Chester, PA).

Statistical analysis

All data were obtained from three independent biological replicates and presented as mean ± S.E. Student's t-test was performed to determine the differences among grouped data. Statistical significance was assessed at $p < 0.05$. For comparison between some groups, a parametric one-way analysis of variance (one-way ANOVA) based on Turkey-Kramer test was performed.

Results

1.1 Methanol-induced gene expression and the phosphorylation of KpMxr1 are regulated by the methanol concentration

To identify the transcription factor related to the CRMI, I studied the transcript level of the methanol-induced genes, *AOX1* and *DAS1*, using the transcription factor gene-disrupted strains under various methanol concentrations. As reported previously, I confirmed that the transcript levels of *AOX1* and *DAS1* in the wild-type strain showed the peak expression with 0.1 % methanol concentration (Figure 1-1A) (Ohsawa *et al.*, 2017). The transcript level of *KpMXR1* was not affected by methanol concentration (Figure 1-1A). Cells of *Kpmxr1Δ, Kpmit1Δ, Kptrm1Δ* and *Kphap3Δ* (which is a subunit of KpHap complex) strains grown on glucose media were shifted to YNB medium containing 0.01%, 0.1% or 1% methanol or no methanol (0%) and were incubated for 2 h (Figure 1-1B). In the *Kptrm1Δ* and *Kphap3Δ* strains, the transcript levels of *AOX1* and *DAS1* peaked with 0.1% methanol and exhibited a pattern similar to the wild-type strain, although the level itself was significantly low (Figure 1-1B). Notably, the *Kpmxr1Δ* and *Kpmit1Δ* strains completely lost the methanol-induced gene expression seen in the other strains. The expression of *KpMIT1* is induced by methanol and requires transcription factors, KpMxr1, KpTrm1 and a KpHap complex (Figure 0B). Since the transcript level of *KpMIT1* itself exhibited methanol concentration dependence and was found to be under the control of CRMI (Figure 1-1A), I focused on KpMxr1 for further analysis.

Next, I examined the protein level of KpMxr1 in relation to the methanol concentration. Immunoblot analysis was performed using the strain expressing KpMxr1-FLAG under the control of the *KpMXR1* promoter. Although the protein level of KpMxr1 was remarkably decreased by the medium shift from glucose to methanol, there was no significant difference related to the methanol concentrations tested (Figure 1-2A).

Subsequently, I analyzed the phosphorylation state of KpMxr1-FLAG under various methanol concentrations by immunoblot analysis with antibodies against phosphor-serine, phosphor-threonine and phosphor-tyrosine residues. Due to the low expression level of KpMxr1-FLAG protein in methanol culture, the protein was produced under the control of the *ScCUP1* promoter to enable detection in the immunoprecipitated fraction (IP). As shown in Figure 1-2B, KpMxr1-FLAG was strongly induced by the addition of Cu^{2+} into the medium. Cells grown in glucose media containing Cu^{2+} were shifted to YNB media containing 0%, 0.01%, 0.1% or 1% methanol for 30 min, and KpMxr1-FLAG protein was immunoprecipitated with anti-FLAG antibody. When anti-phosphoserine antibody was used, a strong band corresponding to phosphorylated serine was observed under glucose-culture condition, but the band intensity decreased with the medium shift from glucose to methanol, regardless of methanol concentration

(Figure 1-2C). When anti-phosphothreonine antibody was used, I observed a faint phosphorylated threonine band in the glucose-cultured sample, but more intense bands were detected in the methanol-cultured sample with the strongest band at 0.1% methanol (Figure 1-2C). The phosphorylated tyrosine residue was not detected (Figure 1-2C). These bands were not detected with the samples from *Kpmxr1Δ* strain (Figure 1-10C), which confirms the specificity of the antibodies. These results indicate that the total phosphorylation level of serine residues in KpMxr1 was higher under the glucose-culture condition and lower under the methanol-culture conditions. In contrast, the threonine residues are phosphorylated under the methanol-culture condition in a methanol concentration-dependent manner. It was also suggested that the threonine residues in KpMxr1 may play a key role in the control of CRMI.
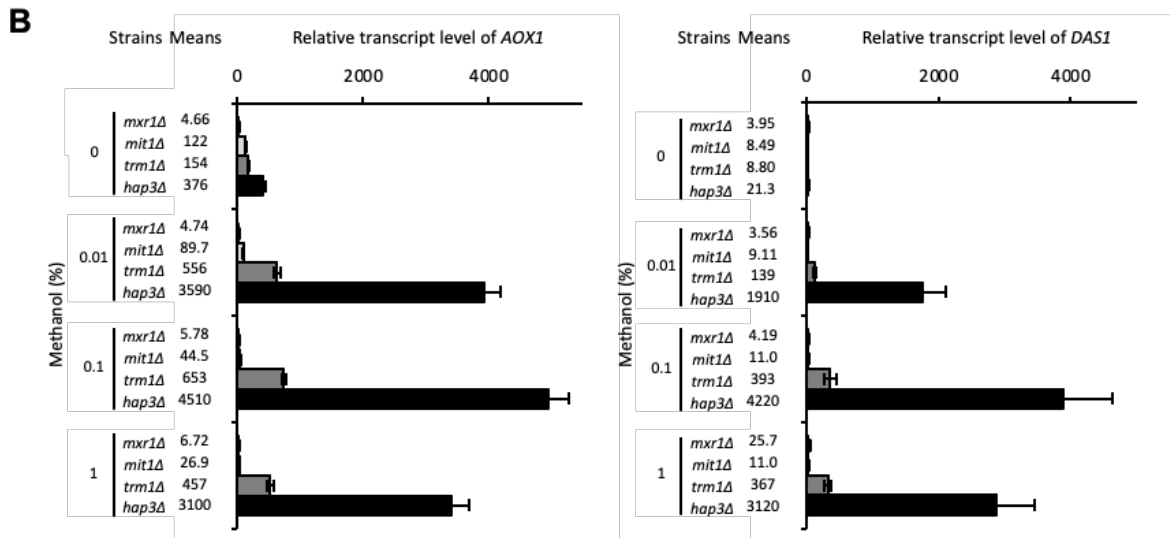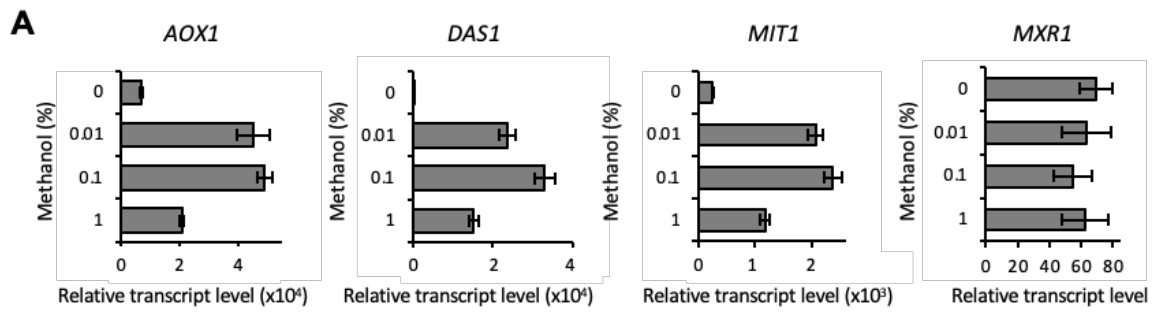
Figure 1-1. CRMI of the methanol-induced genes and related transcription factors.

(A) Transcript levels of methanol-induced genes, *AOX1* and *DAS1,* and transcription factor genes, *KpMIT1* and *KpMXR1*. Total mRNA was prepared from wild-type cells cultured on various methanol concentrations (0, 0.01, 0.1, 1%) for 2 h. The transcript levels were normalized using *GAP* gene as the standard. Relative transcript levels compared to that of the glucose pre-cultured sample are indicated. Error bars represent standard error values from three independent experiments. (B) Transcript levels of *AOX1* and *DAS1* in *Kpmxr1Δ* (white bars), *Kpmit1Δ* (light grey bars)*, Kptrm1Δ* (dark grey bars) and *Kphap3Δ* (black bars) strains. Total mRNA was prepared from cells of each strain cultured under various methanol concentrations (0, 0.01, 0.1, 1%) for 2 h. The transcript levels were normalized using *GAP* gene as the standard. The strains used in this experiment and the mean value of relative transcript levels are indicated on left side of the graphs. Relative transcript levels compared to that of the glucose pre-cultured sample are also presented. Error bars represent standard error values from three independent experiments.
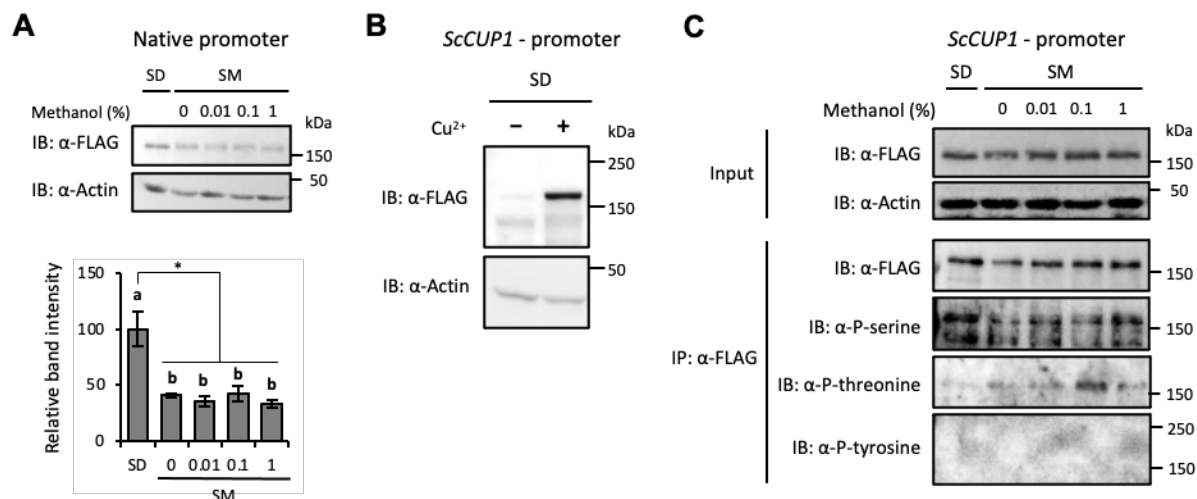
Figure 1-2. Involvement of KpMxr1 in the CRMI and phosphorylation of KpMxr1.

(A) Immunoblot analysis of KpMxr1-FLAG protein level in response to varying methanol concentrations (α-FLAG). Actin was blotted as a loading control (α-Actin). Cells were shifted from glucose media (SD) to media with indicated methanol concentration (SM) for 30 min. The samples were loaded on 8% acrylamide SDS-PAGE gel. Molecular weights of each band calculated from the protein size marker are indicated. Error bars represent standard error values from three independent experiments. The groups indicated with different symbol means significant difference (between **a** and **b**, *: $p < 0.05$) by the statistical analysis (One-way ANOVA) (B) Immunoblot analysis of KpMxr1-FLAG protein (α-FLAG) expressed under the control of *ScCUP1* promoter. Actin was blotted as a loading control (α-Actin). Cells were cultured in glucose medium (SD) with or without $CuSO_4$ (50 μM) for 30 min. Molecular weights of the protein size marker were indicated. The samples were loaded on 8% acrylamide SDS-PAGE gel. The strain used in this experiment is indicated at the top of the figure. (C) Phosphorylation levels of KpMxr1-FLAG in response to varying methanol concentrations. SD, 2% glucose medium; SM, 0, 0.01, 0.1, or 1% methanol media. KpMxr1-FLAG in whole cell extracts was detected in an input sample with anti-FLAG antibody (α-FLAG), and actin was blotted as a loading control (α-Actin). KpMxr1-FLAG was immunoprecipitated with anti-FLAG antibody (IP), and phosphorylation of KpMxr1-FLAG was detected with anti-phosphoserine (α-P-serine), anti-phosphothreonine (α-P-threonine) or anti-phosphotyrosine (α-P-tyrosine) antibodies (IB). Cells were shifted from glucose medium (SD) containing $CuSO_4$ (50 μM) to medium with indicated methanol concentrations (SM) containing $CuSO_4$ (50 μM) for 30 minutes. The input and immunoprecipitated samples were loaded on 8% acrylamide SDS-PAGE gel. Molecular weights of the protein size marker are indicated.

1.2 Identification of the functional region of KpMxr1 responsible for the regulation of the CRMI and analysis of the phosphorylation state

To survey the possible functional region in KpMxr1 responsible for regulating CRMI, KpMxr1 C-terminal truncated mutant proteins were constructed based on the amino acid sequence alignments of KpMxr1 homologs in methylotrophic yeasts viz. *K. phaffii* Mxr1 (KpMxr1), *C. boidinii* Trm2 (CbTrm2), and *O. polymorpha* Adr1 (OpAdr1) (Figure 1-3). I speculated that the region crucial for methanol-induced gene expression is well-conserved in the methylotrophic yeasts. Amino acid sequence alignment showed that the DNA binding region and 14-3-3 protein interacting region were conserved in these yeasts, and that 13 other conserved regions were also present in three methylotrophic yeast strains.
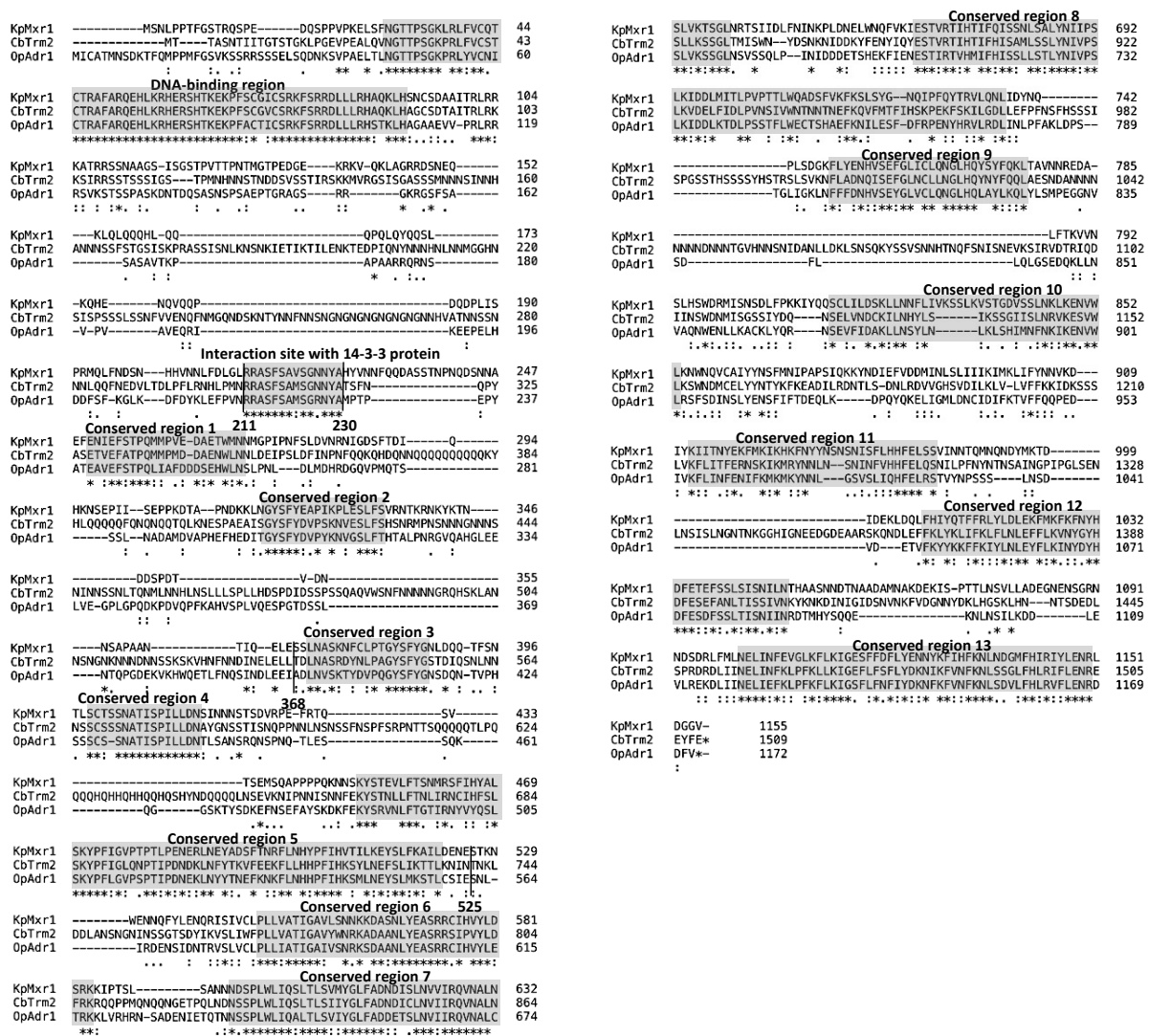
Figure 1-3. Amino acid sequence alignment of KpMxr1, CbTrm2 and OpAdr1.

Sequence alignment of KpMxr1, CbTrm2 and OpAdr1 was created using CLUSTALW. Conserved regions in all methylotrophic yeasts are highlighted with grey boxes. The symbols represent sequence conservation as described below. "*": identical or conserved in all sequences in the alignment, ":": conserved substitutions, ".": semi-conserved substitutions.

Next, I designed the C-terminal truncated KpMxr1 proteins, KpMxr1$^{1-525}$, KpMxr1$^{1-368}$, KpMxr1$^{1-230}$ and KpMxr1$^{1-211}$ (Figure 1-4A). The strains expressing these KpMxr1-truncated mutant proteins tagged with FLAG were constructed using PPY12 *Kpmxr1Δ* strain as a host of transformation, and the resulting strains were named TM525, TM368, TM230 and TM211, respectively. *KpMXR1* gene disruption of each strain was checked by colony PCR (Figure 1-4B) and the expression of KpMxr1-truncated mutant protein was confirmed by immunoblot analysis (Figure 1-4C).
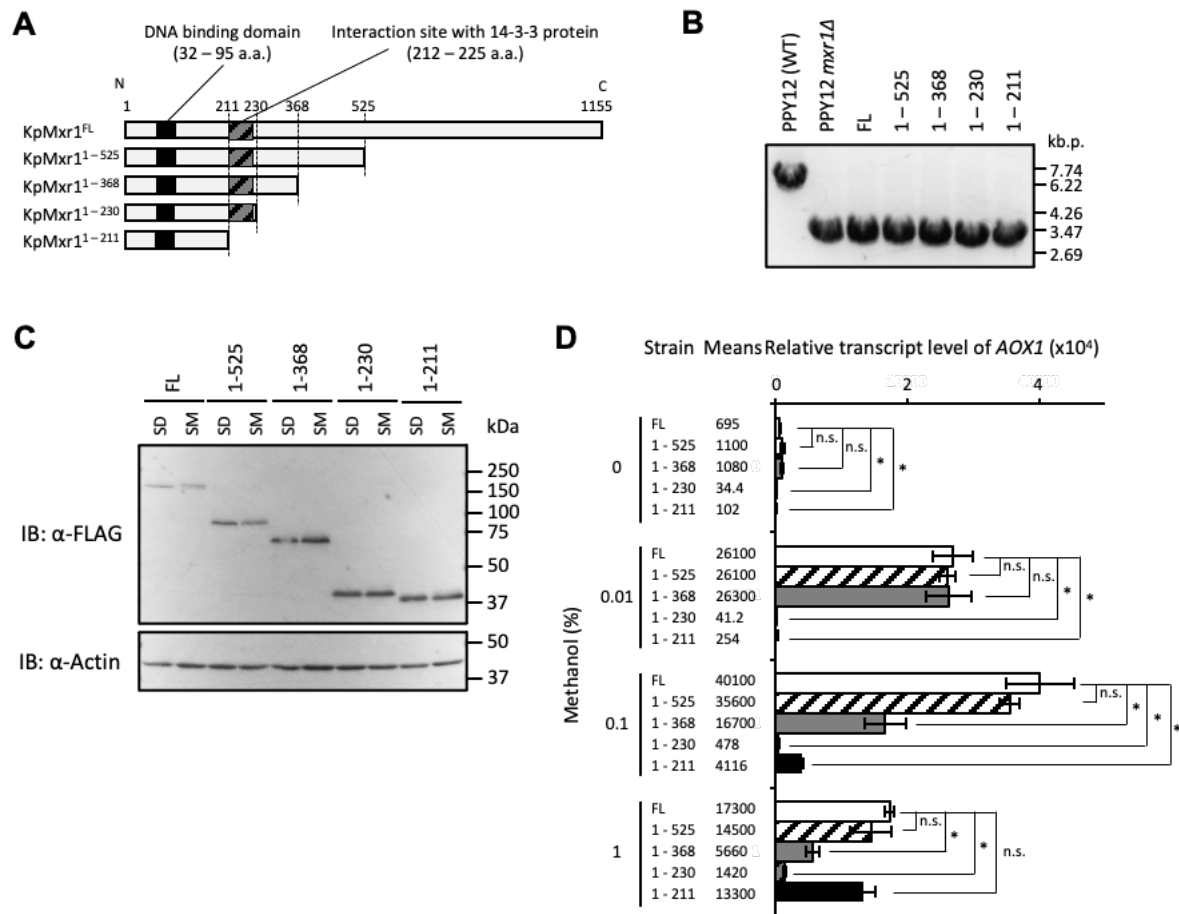
Figure 1-4. Functional analyses of C-terminal truncated KpMxr1 proteins for methanol metabolism.

(A) Construction of C-terminal truncated KpMxr1 mutant proteins. (B) Confirmation of *mxr1* gene deletion in each strain by colony PCR. *K. phaffii* cells of each strain were used as a template in the PCR using the primer pairs ColoP-mxr1d-Fw/ColoP-mxr1d-Rv. DNA size marker (OneSTEP marker 6, NIPPON GENE, Tokyo, Japan) was indicated in the right side. (C) Immunoblot analysis of truncated KpMxr1-FLAG protein (α-FLAG). Actin was blotted as a loading control (α-Actin). Cells of FL1155, TM525, TM368, TM230 and TM211 strains were shifted from glucose medium (SD) to YNB medium with 0.1% methanol (SM) for 2 h. The samples were loaded on 8% acrylamide SDS-PAGE gel. Molecular weights of the protein size marker were indicated. The strain used in this experiment is indicated at the top of the figure. (D) Transcript levels of *AOX1* in strains expressing the full-length KpMxr1^{FL} protein (FL1155) (white bars), KpMxr1$^{1-525}$ (TM525) (white bars with diagonal line), KpMxr1$^{1-368}$ (TM368) (grey bars), KpMxr1$^{1-230}$ (TM230) (grey bars with diagonal line) and KpMxr1$^{1-211}$ (TM211) (black bars). Total mRNA was prepared from cells of each strain cultured on various concentrations of methanol (0, 0.01, 0.1, 1%) for 2 h. The transcript levels were normalized using *GAP* gene as the standard. Relative transcript levels compared to that of the glucose pre-cultured sample are also presented. Error bars represent standard error values from three independent experiments. *: p < 0.05, n.s.: not significant.

A previous report showed that the 1-400 a.a. region of KpMxr1 is sufficient for its function in methanol-induced gene expression (Parua *et al.*, 2012). The *AOX1* transcript level of the control strain FL1155 expressing full-length KpMxr1 (KpMxr1^{FL})-FLAG and the TM525 strain showed a similar pattern (Figure 1-4D). However, the transcript level of the TM368 strain decreased by 0.1% and 1% of methanol compared to the control strain, and that of the TM230 strain decreased in all methanol concentrations (Figures 1-4D). Interestingly, the *AOX1* transcript level in the TM211 strain under 0.1% and 1% conditions was higher than that in the TM230 strain (Figure 1-4D), which supports the assumption that the region from 212 to 230 a.a., which includes the interaction site with 14-3-3 protein, plays a role in repressing the *AOX1* gene expression under high (> 0.1%) methanol conditions.

Regarding the effect of KpMxr1 truncation on methanol growth, a previous study reported that the strain expressing KpMxr1$^{1-400}$ under the control of the glyceraldehyde-3-phosphate dehydrogenase (*GAP*) gene promoter was incapable of growth on 1% methanol medium (Gupta *et al.*, 2021). In this study, I used the original *KpMXR1* promoter, and the strains TM525 and TM368 exhibited similar growth on methanol as the control strain FL1155 (Figure 1-5A). Overexpressed truncated KpMxr1$^{1-400}$ expressed by the strong *GAP* promoter may cause growth defects on methanol. I observed a significant growth delay in the strains TM230 and TM211 (Figure 1-5A). From these results, it is clear that the region from 230 to 368 has an indispensable function in cell growth on methanol. Growth on glucose and ethanol was not affected by KpMxr1 truncation except that the TM211 strain exhibited a slight growth defect on ethanol (Figures 1-5B and 1-5C).
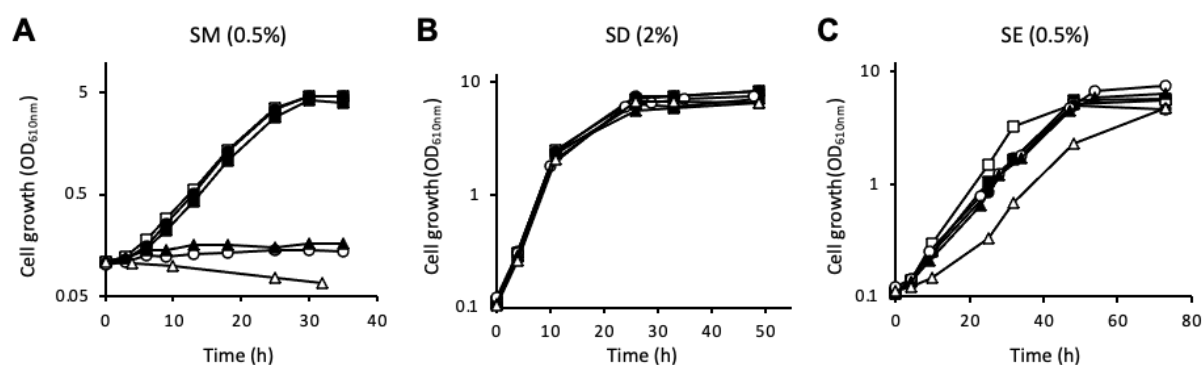

Figure 1-5. Cell growth of the strains expressing truncated KpMxr1 mutant proteins.

Growth of strains expressing truncated KpMxr1 mutant proteins on methanol (A), glucose (B) and ethanol (C). Strains expressing KpMxr1^{FL} (filled squares), KpMxr1$^{1-525}$ (open squares), KpMxr1$^{1-368}$ (filled circles), KpMxr1$^{1-230}$ (open circles) and KpMxr1$^{1-211}$ (filled triangles) and the *Kpmxr1Δ* strain (open triangles) were grown on SD media and cells of exponential phase were shifted to 0.5% methanol medium (SM) or 2% glucose medium (SD) or 0.5% ethanol medium (SE), respectively.

KpMxr1 has been reported to be distributed in the cytosol under glucose-culture condition and localized to the nucleus by the medium shift from glucose to methanol (Lin-Cereghino *et al.*, 2006). Truncated KpMxr1[1-400] localizes to the nucleus under both glucose- and methanol-culture conditions (Gupta *et al.*, 2021). While KpMxr1[FL]-YFP localized to the nucleus in all concentrations of methanol, there was no difference in KpMxr1[FL]-YFP localization based on the methanol concentrations in the medium (Figure 1-6A). Truncated KpMxr1[1-525]-YFP and KpMxr1[1-230]-YFP localized in the nucleus under glucose or methanol condition (Figure 1-6B). These results suggested that the truncated KpMxr1 proteins contain the nuclear localization signal (NLS) but lacked a nuclear export signal (NES) and the decrease in *AOX1* transcript level in strains possessing truncated KpMxr1 proteins (Figure 1-4D) is not a result of the deficiency in nuclear localization.
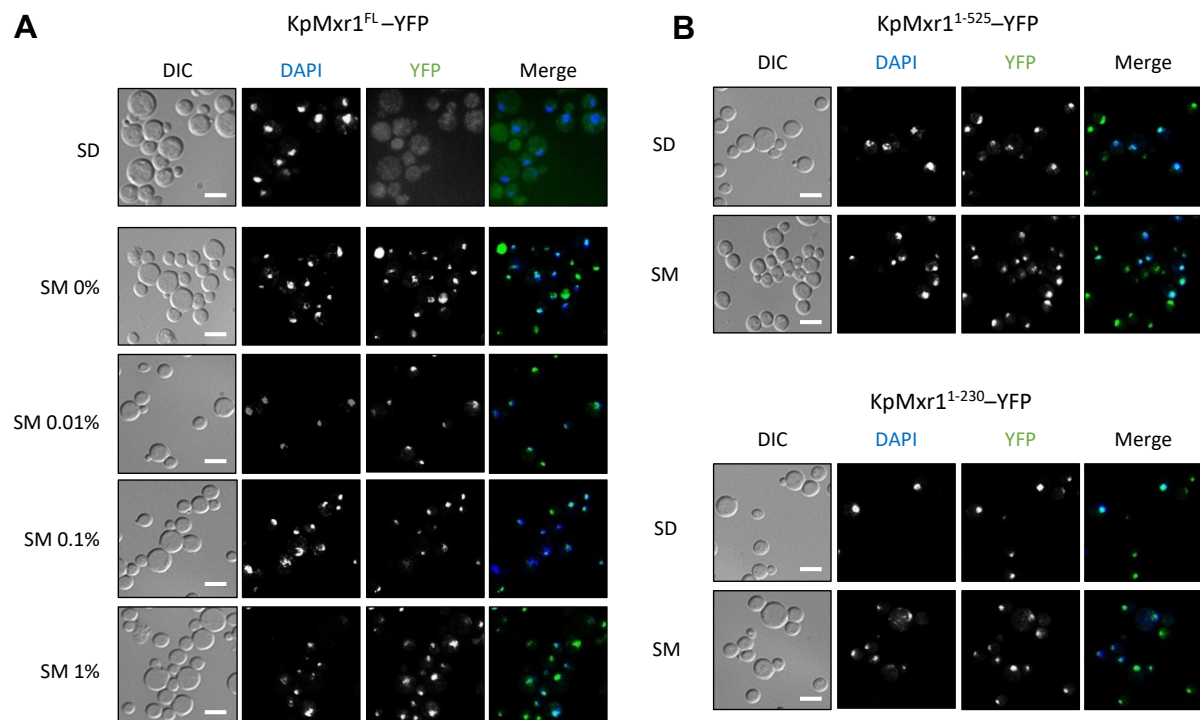

Figure 1-6. Intracellular localization of KpMxr1 and the truncated mutants.

(A) Fluorescence microscopy of KpMxr1-YFP expressed under the control of the *KpMXR1* promoter. Cells were shifted from SD to SM medium containing 0, 0.01, 0.1 or 1% methanol at 28℃ for 3h. Subsequently, they were treated with 5% formaldehyde for 1 h and stained with 100 µg/L DAPI. (B) Fluorescence microscopy of KpMxr1[1-525] and KpMxr1[1-230] tagged with YFP at the C-terminus expressed under the control of the *KpMXR1* promoter. Cells were shifted from SD to SM medium containing 0.1% methanol at 28℃ for 3 h. Subsequently, they were treated with 5% formaldehyde for 1 h and stained with 100 ng/mL DAPI. DAPI was used to stain the cell nucleus. DIC, differential interference contrast. The scale bars in (A) and (B) correspond to 5.0 µm.
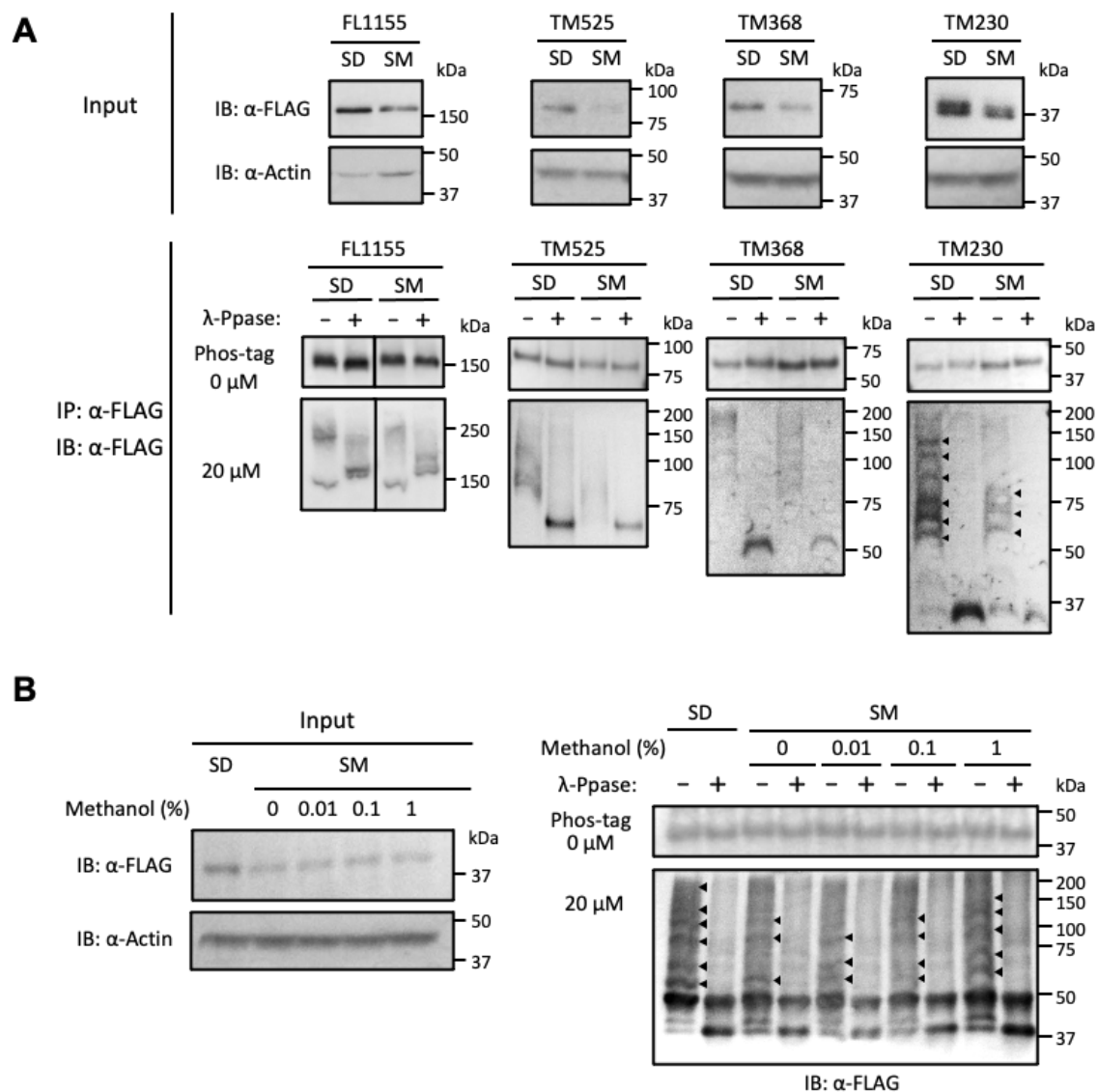
Figure 1-7. Phosphorylation analysis of C-terminal truncated KpMxr1 under methanol culture condition.

(A) Phosphorylation levels of truncated KpMxr1-FLAG proteins were evaluated by phos-tag SDS-PAGE. Cells of FL1155, TM525, TM368 and TM230 were grown on glucose (SD) and shifted to 0.1% methanol (SM) medium for 30 min. C-terminal FLAG-tagged KpMxr1^{FL}, KpMxr1$^{1-525}$, KpMxr1$^{1-368}$ and KpMxr1$^{1-230}$ were immunoprecipitated with FLAG antibody and treated with or without λ-phosphatase (λ-Ppase). The input samples were loaded on 8% acrylamide SDS-PAGE gel. Actin was blotted as a loading control (α-Actin). IP samples were loaded on an 8.5% acrylamide SDS-PAGE gel with or without 20 μM phos-tag (containing 40μM Zn^{2+}), transferred to a PVDF membrane and the truncated KpMxr1-FLAG proteins were detected with an anti-FLAG antibody. Molecular weights of the protein size marker are indicated. Black arrowheads correspond to the bands of phosphorylated KpMxr1 protein. (B) The phosphorylation level of KpMxr1$^{1-230}$-FLAG protein based on methanol concentration. Cells of TM230 were shifted from glucose medium (SD) to medium with indicated methanol concentration (SM) for 30 min. KpMxr1$^{1-230}$-FLAG was immunoprecipitated with FLAG antibody and subjected to phos-tag analyses as described in (A). Molecular weights of the protein size marker are indicated. Black arrowheads correspond to the detected bands of phosphorylated KpMxr1 protein.

KpMxr1 protein has a large molecular mass (1155 amino acids, 141 kDa) and it is expected to have multiple phosphorylation sites. Indeed, KpMxr1-FLAG protein was detected in gels with or without phos-tag, but the phosphorylated KpMxr1 bands were unclear and their differences could not be evaluated. To improve the resolution of the phosphorylation state of KpMxr1 by phos-tag SDS-PAGE, strains expressing truncated KpMxr1 mutants were used in the following analyses instead of the full-length strain. As shown in Figure 1-7A, the intensity of the phosphorylated bands decreased due to the medium shift from glucose to methanol in strains FL1155, TM525, TM368 and TM230. Especially in the TM230 strain, at least 6 phosphorylated bands were detected in glucose-cultured cells and some upper bands were not detected in methanol-cultured cells (Figure 1-7A). These results suggest that KpMxr1 has multiple phosphorylation sites, and some of them are dephosphorylated by the medium shift from glucose to methanol.

Subsequently, the phosphorylation state of KpMxr1$^{1-230}$ under various methanol concentrations was analyzed. FLAG-tagged KpMxr1$^{1-230}$ was immunoprecipitated and subjected to phos-tag SDS-PAGE analysis (Figure 1-7B). KpMxr1$^{1-230}$ was highly phosphorylated in 1% methanol-cultured cells, and it was comparable to the level of glucose-cultured cells. This indicates that highly phosphorylated KpMxr1 is involved in the repression of *AOX1* gene expression at 1% methanol condition.

1.3 Analysis of phosphorylated residues in KpMxr1 by LC-MS/MS

LC-MS/MS analysis of FLAG-tagged KpMxr1 was performed to survey the phosphorylation sites in KpMxr1 under glucose- or methanol-culture condition. The analysis of KpMxr1^{FL} phosphorylation failed to detect the peptides probably because of a larger molecular mass as I mentioned above. Thus, in this experiment, KpMxr1$^{1-525}$-FLAG protein extracted from TM525 was subjected to LC-MS/MS. The samples were purified by immunoprecipitation, confirmed by immunoblot analysis and using a CBB-stained gel (Figure 1-8A). Then the band corresponding to KpMxr1$^{1-525}$-FLAG in CBB stained gel was cut out and digested with trypsin, and then analyzed by LC-MS/MS. Peptides derived from KpMxr1$^{1-525}$-FLAG was successfully detected in the glucose-cultured and the methanol-cultured samples (Tables 1-4 and 1-5). Detected peptides satisfied the requirements of "phosphorylated" and "at least 95% confidence" were extracted from the data and the sum values of detected peak intensity were indicated (Figure 1-8B). Amino acid residues S110 and S111 were significantly phosphorylated both in the glucose-cultured and methanol-cultured samples and the phosphorylation levels were higher in the glucose-cultured sample. Similar phosphorylation states were observed for other serine residues, e.g., S116, S149, S190, S215 and S217. On the other hand, the phosphorylation level of T121, T124, T125 T128 and T131 were higher in the methanol-cultured samples. These results show that KpMxr1 harbor multiple phosphorylation sites in addition to S215 which was reported previously (Parua *et al.*, 2012), and indicate that these threonine- and serine-residues were phosphoregulated in accordance with the medium shift from glucose to methanol. Interestingly, phosphorylated residues of KpMxr1$^{1-525}$ were mainly detected in N-terminal of the protein, which is consistent with multiple phosphorylation of KpMxr1$^{1-230}$ (Figure 1-7A right panel).

Table 1-4. Detected peptides from the glucose-cultured cell extract.

Number	Accession	Name	Species	Frequency
1	Mxr1-525-FLAG	KpMxr1_1-525_5xFLAG	*K. phaffii*	999
2	SOP79829.1	Dipeptidyl-peptidase III	*K. phaffii* CBS 7435	224
3	XP_002491367.1	Protein serine/threonine kinase	*K. phaffii* GS115	136
4	XP_002490239.1	Heat shock protein Hsp90	*K. phaffii* GS115	72
5	XP_002491046.1	Cobalamin-independent methionine synthase	*K. phaffii* GS115	98

Table 1-5. Detected peptides from the methanol-cultured cell extract.

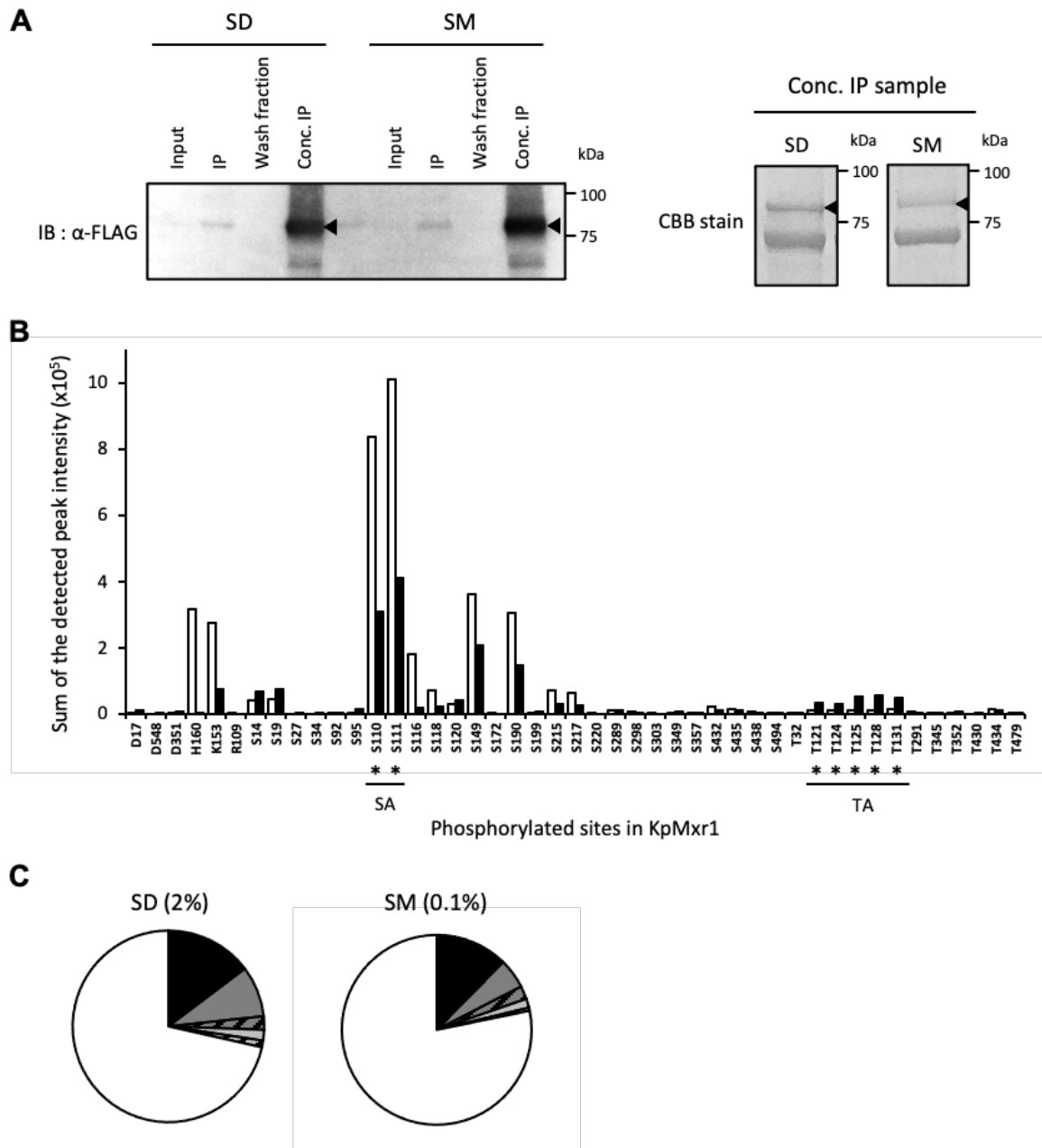| Number	Accession	Name	Species	Frequency
1	Mxr1-525-FLAG	KpMxr1_1-525_5xFLAG	*K. phaffii*	795
2	SOP79829.1	Dipeptidyl-peptidase III	*K. phaffii* CBS 7435	279
3	XP_002491367.1	Protein serine/threonine kinase	*K. phaffii* GS115	145
4	XP_002491046.1	Cobalamin-independent methionine synthase	*K. phaffii* GS115	105
5	XP_002490239.1	Heat shock protein Hsp90	*K. phaffii* GS115	74

Figure 1-8. Identification of KpMxr1 phosphorylation sites related to the regulation of the CRMI by LC-MS/MS analysis.

(A) Immunoblot analysis and CBB stained gel of KpMxr1[1-525]-FLAG protein injected into LC-MS/MS analysis. Cells of TM525 strain cultured in glucose (2%) or methanol (0.1%) media for 30 min were lysed and KpMxr1[1-525]-FLAG protein was immunoprecipitated with anti-FLAG antibody. The input sample, IP sample, wash fraction in the step of IP and concentrated IP sample by ultra-filtration were loaded on 12.5% acrylamide SDS-PAGE gel (SuperSep Ace, Wako). The samples were stained by CBB or transferred to a PVDF membrane, and the truncated KpMxr1-FLAG proteins were detected with an anti-FLAG antibody (α-FLAG). Molecular weights of the protein size marker are indicated. Black arrowheads correspond to the bands of KpMxr1[1-525]-FLAG subjected to LC-MS/MS. The target band was cut out and treated with Trypsin. (B) LC-MS/MS analysis of KpMxr1 phosphorylation. The sum values of detected peak intensity obtained from glucose-cultured samples (white bars) and methanol-cultured samples (black bars) are indicated. Asterisks mean mutated serine and threonine residues in the SA and TA strains. (C) The protein modification of detected peptides derived from KpMxr1[1-525]-FLAG. Phosphorylation (black areas), oxidation (dark grey areas), methylation and di-methylation (dark grey areas with diagonal line), acetylation (light grey areas), sulfonylation (light grey areas with diagonal line) and others including no modification (white areas) were indicated.

Not only phosphorylation but various protein modifications were identified from KpMxr1[1-525]-FLAG by LC-MS/MS (Fig. 1-8C). The phosphorylation of KpMxr1 was the most caused under both glucose- and methanol-culture conditions. Oxidation (of arginine, proline and methionine), methylation (of serine, leucine and lysine), acetylation (of serine and threonine) and sulfonylation (of serine, threonine and tyrosine) were observed, which implies the possibility of KpMxr1 regulation by the protein modification in addition to phosphorylation.

A previous study has reported that S215 in KpMxr1 is phosphorylated under ethanol culture condition and this phosphorylation is crucial for its interaction with 14-3-3 protein (Parua *et al.*, 2012). It has been demonstrated that the phosphorylation of S215 is responsible for ethanol repression of methanol-induced genes (Ohsawa *et al.*, 2018). But in this study, I found that the S215A mutation of KpMxr1 did not affect the peak pattern of the CRMI (Figure 1-9A). I also found that there was no difference in the cell growth on methanol between the strains expressing KpMxr1-FLAG and KpMxr1(S215A)-FLAG (Figure 1-9B).
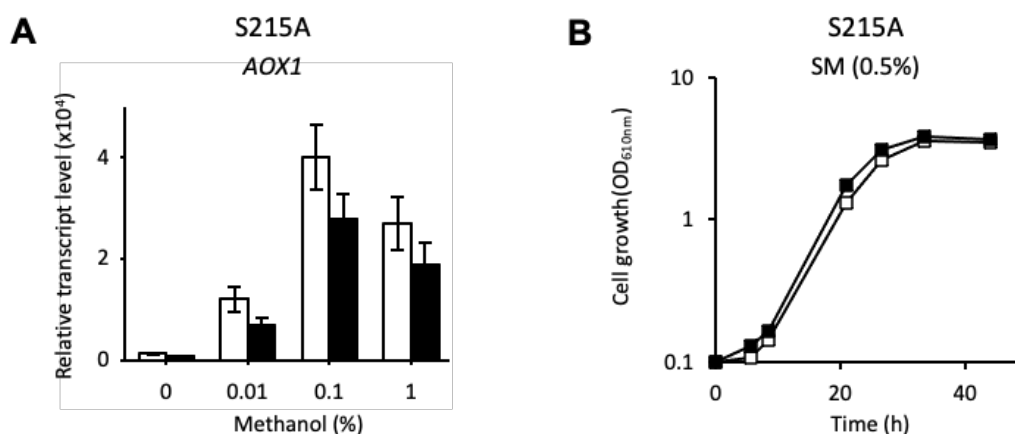

Figure 1-9. Functional analysis of KpMxr1[S215A] mutant protein.

(A) Transcript levels of *AOX1* in the control strain (white bars) or the strain expressing KpMxr1[S215A]-FLAG (black bars). Total mRNA was prepared from cells of each strain cultured on various concentrations of methanol (0, 0.01, 0.1, 1%) for 2 h. The transcript levels were normalized using *GAP* gene as the standard. Relative transcript levels compared to that of the glucose pre-cultured sample are indicated. Error bars represent standard error values from three independent experiments. (B) Growth of strains expressing KpMxr1[FL]-FLAG (open squares) and KpMxr1[FL](S215A)-FLAG (filled squares) on 0.5% methanol medium (SM).

Based on the results from LC-MS/MS, I constructed strains containing mutations in putative phosphorylation sites of KpMxr1, i.e., KpMxr1$^{T121A, T124A, T125A, T128A, T131A}$ (TA mutant) and KpMxr1$^{S110A, S111A}$ (SA mutant) (Figure 1-8B). CRMI was analyzed with strains expressing KpMxr1^{FL}-TA-FLAG and KpMxr1^{FL}-SA-FLAG (MTA and MSA strains) under the control of the *KpMXR1* promoter to evaluate the effect of TA and SA mutations on the CRMI. The *AOX1* transcript level was determined at various methanol concentrations with strains MTA and MSA compared with the control strain expressing KpMxr1^{FL}-FLAG (Figure 1-10A). The TA mutant strain MTA showed decrease in the *AOX1* transcript level at 0% and 0.01% methanol-culture conditions. Moreover, the peak of *AOX1* transcript level in strain MTA was detected at 0.1% methanol, while the peak of the control strain was at 0.03%. Therefore, the expression peak of *AOX1* shifted to a higher methanol concentration in strain MTA, which seemed to be due to an impairment in methanol-sensing at low methanol concentrations (less than 0.03%). Considering that phosphoregulation of threonine residues depends on methanol concentration (Figure 1-2C), these results indicate that phosphorylation of threonine residues in KpMxr1 (T121/T124/T125/T128/T131) plays a critical role in CRMI. On the other hand, the SA mutant strain MSA showed decrease in the *AOX1* transcript level at low methanol concentrations (0% and 0.01%) and increase in the expression level at 1% methanol. Although the peak of the *AOX1* expression did not change in strain MSA, phosphorylation of serine residues (S110/S111) may also be involved in CRMI at lower methanol concentration (Figure 1-10A).

I investigated the effect of SA and TA mutations on the phosphorylation state of KpMxr1 using the TM230SA and TM230TA strains (Figure 1-10B). Consistent with the result of Figures 1-7A and 1-7B, the strain expressing KpMxr1$^{1-230}$-FLAG exhibited multiple bands and the intensity of the phosphorylated bands decreased by medium shift from glucose to methanol (Figure 1-10B). The band indicated by the black arrowhead observed in the sample from the glucose-grown cells expressing KpMxr1$^{1-230}$-FLAG was not detected in the sample from the TM230SA strain (Figure 1-10B). Moreover, this band was lost in the samples from all strains under methanol-culture condition. From these results, the residues S110 and/or S111 in KpMxr1 are suggested to be phosphoregulated during CRMI. The phosphorylation of threonine and serine residues of KpMxr1 in MTA and MSA strains was analyzed using anti-phosphothreonine and anti-phosphoserine antibodies (Figure 1-10C). In the immunoprecipitated samples of all strains, threonine residues were phosphorylated by the medium shift from glucose to methanol, and serine residues were dephosphorylated in total by the medium shift. This result was consistent with the phosphorylation level of threonine and serine residues (Figure 1-2C). The phosphorylated bands were not lost by TA and SA mutations, suggesting that KpMxr1 has phosphorylation sites other than the mutated threonine and serine residues (T121/T124/T125/T128/T131 and S110/ S111).
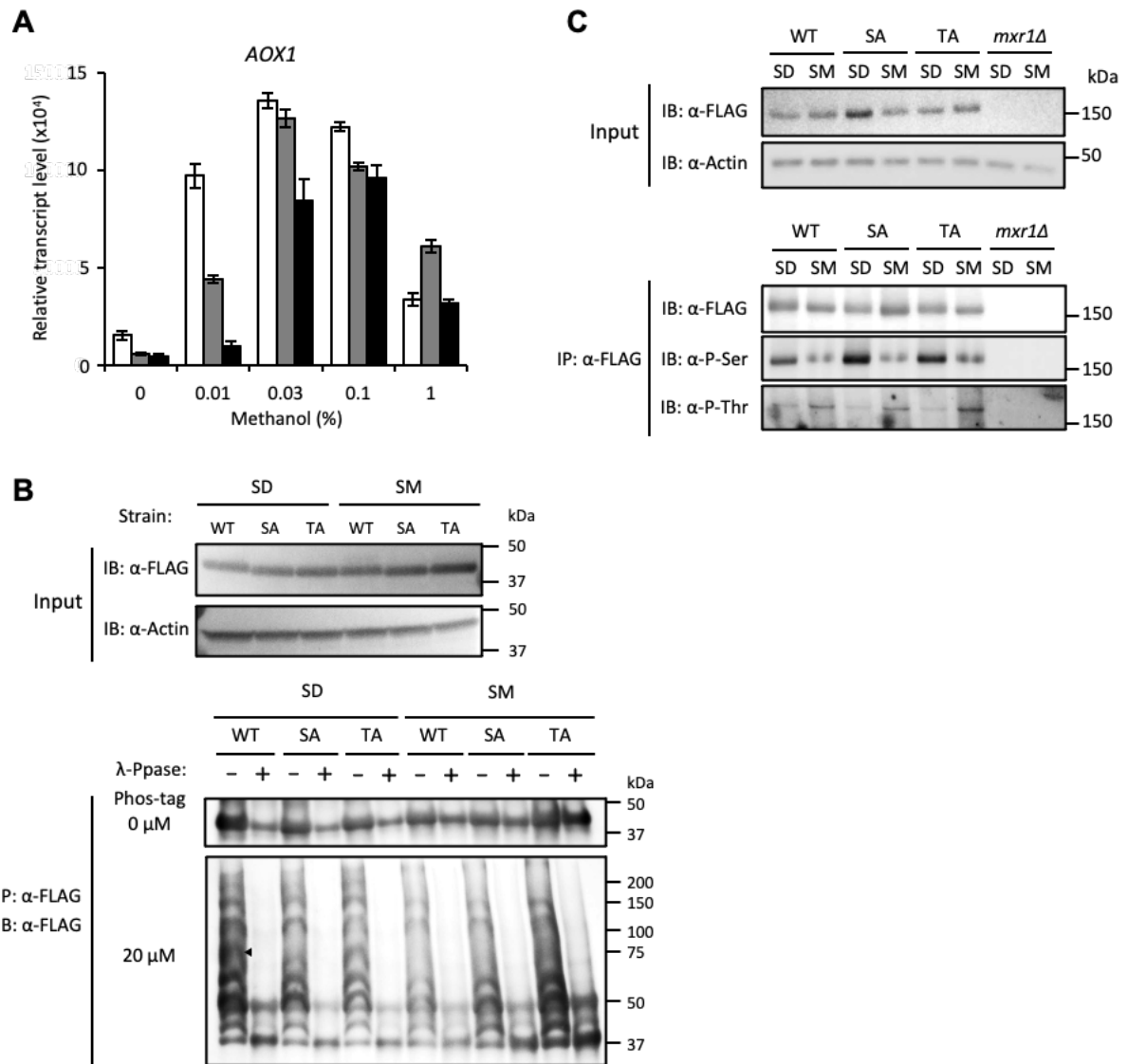
Figure 1-10. SA and TA mutation in KpMxr1 influences on the transcript level of *AOX1*.

(A) Transcript levels of *AOX1* in the control strain expressing KpMxr1^{FL}-FLAG (white bars), strain MSA expressing KpMxr1^{FL}-SA-FLAG (grey bars) and strain MTA expressing KpMxr1^{FL}-TA-FLAG (black bars). Total mRNAs were prepared from cells of each strain cultured on various concentrations of methanol (0, 0.01, 0.03, 0.1, 1%) for 2 h. The transcript levels were normalized using *GAP* gene as the standard. Relative transcript levels compared to that of the glucose pre-cultured sample are indicated. Error bars represent standard error values from three independent experiments. (B) Phosphorylation levels of KpMxr1$^{1-230}$-FLAG (WT), KpMxr1$^{1-230}$SA-FLAG (SA) and KpMxr1$^{1-230}$TA-FLAG (TA) proteins. Cells were grown on glucose (SD) and shifted to 0.1% methanol (SM) medium for 30 min. C-terminal FLAG-tagged KpMxr1$^{1-230}$, KpMxr1$^{1-230}$ SA and KpMxr1$^{1-230}$ TA were immunoprecipitated with FLAG antibody, and treated with or without l-phosphatase (λ-Ppase). The samples were loaded on an 8.5% acrylamide SDS-PAGE gel with or without 20 μM phos-tag, and transferred to a PVDF membrane, and truncated KpMxr1-FLAG proteins were detected with anti-FLAG antibody. The black arrowhead indicates the band which is lost in the SA samples from glucose-grown cells. Molecular weights of the protein size marker are indicated. (C) Immunoblot analysis of KpMxr1-FLAG phosphorylation using strains expressing KpMxr1^{FL}-FLAG (WT), KpMxr1^{FL}-SA-FLAG (SA) and KpMxr1^{FL}-TA-FLAG (TA) and the *Kpmxr1Δ* strain. Cells were shifted from glucose medium (SD) to medium with indicated methanol concentration (SM) for 30 min. KpMxr1-FLAG in whole cell extracts was detected in an input sample with anti-FLAG antibody (α-FLAG), and actin was blotted as a loading control (α-Actin). KpMxr1-FLAG was immunoprecipitated with anti-FLAG antibody (IP), and phosphorylation of KpMxr1-FLAG was detected with anti-phosphoserine (α-P-Ser) or anti-phosphothreonine (α-P-Thr) antibodies. Molecular weights of the protein size marker are indicated.
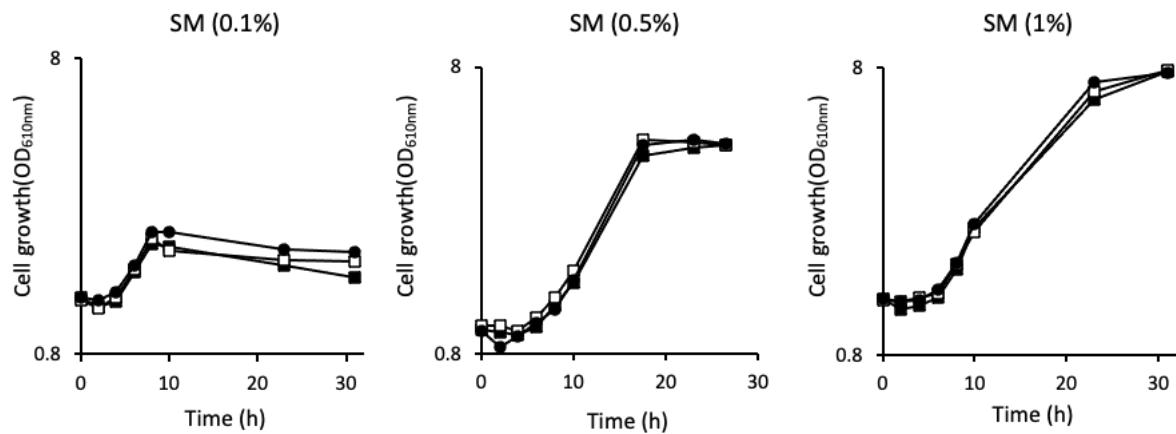
Figure 1-11. Cell growth of the strains expressing KpMxr1 SA and TA mutant proteins.

Growth of strains expressing mutated KpMxr1 proteins on methanol. The control strain expressing KpMxr1[FL]-FLAG (filled squares), strain MSA (open squares) and strain MTA (filled circles) were grown on SD media, and the cells of exponential phase were shifted to 0.1%, 0.5% or 1% methanol medium (SM) at 28°C.

The effect of SA or TA mutations in KpMxr1 for the growth on methanol was also investigated (Figure 1-11). However, there were no obvious differences in the growth on 0.1, 0.5 or 1% methanol among the control, MSA and MTA strains. Therefore, SA or TA mutations impair the CRMI of methanol-induced genes in the early stage of methanol culture, but they do not influence on the cell growth.

1.4 KpMxr1 receives the methanol signal from KpPkc1 but not from the MAPK cascade

I then focused on the signal transduction pathway with respect to CRMI. Previously, it has been reported that KpWsc1 and KpWsc3 contribute toward sensing the environmental methanol concentration and that KpWsc1 responds to a lower range of methanol concentrations than KpWsc3 (Ohsawa *et al.*, 2017). In *S. cerevisiae*, Wsc family proteins are known to be a cell surface stress sensor that transmits the signal to the CWI pathway through the MAPK cascade (Levin, 2005). The downstream regulators of Wsc family proteins are GTP-binding protein ScRho1, protein kinase C (ScPkc1) and MAPKK protein (ScMkk1), and their dominant active mutants ScRho1^{Q68H} (GTP-locked mutant), ScPkc1^{R398P} and ScMkk1^{S386P} are known (Madaule *et al.*, 1987; Nonaka *et al.*, 1995; Yashar *et al.*, 1995). To investigate the involvement of downstream regulators of KpWsc1 and KpWsc3 in the CRMI, *K. phaffii* strains corresponding to each hyperactive mutant, i.e., KpRho1^{Q68H}, KpPkc1^{R390P} and KpMkk1^{S313P}, together with their wild type proteins, were constructed under the *ScCUP1* promoter. I confirmed that the levels of expressed proteins increased with the added Cu^{2+} concentration to the medium, and also confirmed the activation of MAPK cascade using immunoblot analysis with anti-phospho-Mpk1 antibody in the hyperactive mutant proteins, but not in control proteins (Figure 1-12 upper panels).

The transcript level of *AOX1* decreased with the induction of hyperactive mutant proteins KpRho1^{Q68H} (Figures 1-12A lower panel) and KpPkc1^{R390P} (Figure 1-12B lower panel). On the other hand, the expression of KpMkk1^{S313P} did not affect the *AOX1* transcript level (Figure 1-12C lower panel). These results indicate that the methanol signal from Wsc family proteins is transmitted to KpRho1 and then to KpPkc1, but not to KpMkk1, indicating that the CRMI pathway is not downstream of the MAPK cascade.

To discern which transcription factor receives the methanol signal, the *AOX1* transcript levels in the transcription factor-deleted *K. phaffii* strains, i.e., *Kpmxr1Δ, Kpmit1Δ, Kptrm1Δ, Kphap3Δ, Kpmig1Δ* and *Kprop1Δ*, were investigated under the expression of KpRho1^{Q68H}. As shown in Figure 1-12D, the *AOX1* transcript level in the *Kpmxr1Δ* strain was not affected by the induction of KpRho1^{Q68H}, but it was reduced in all the other strains. These results imply that KpMxr1 receives the methanol signal from Wsc family proteins via KpRho1.
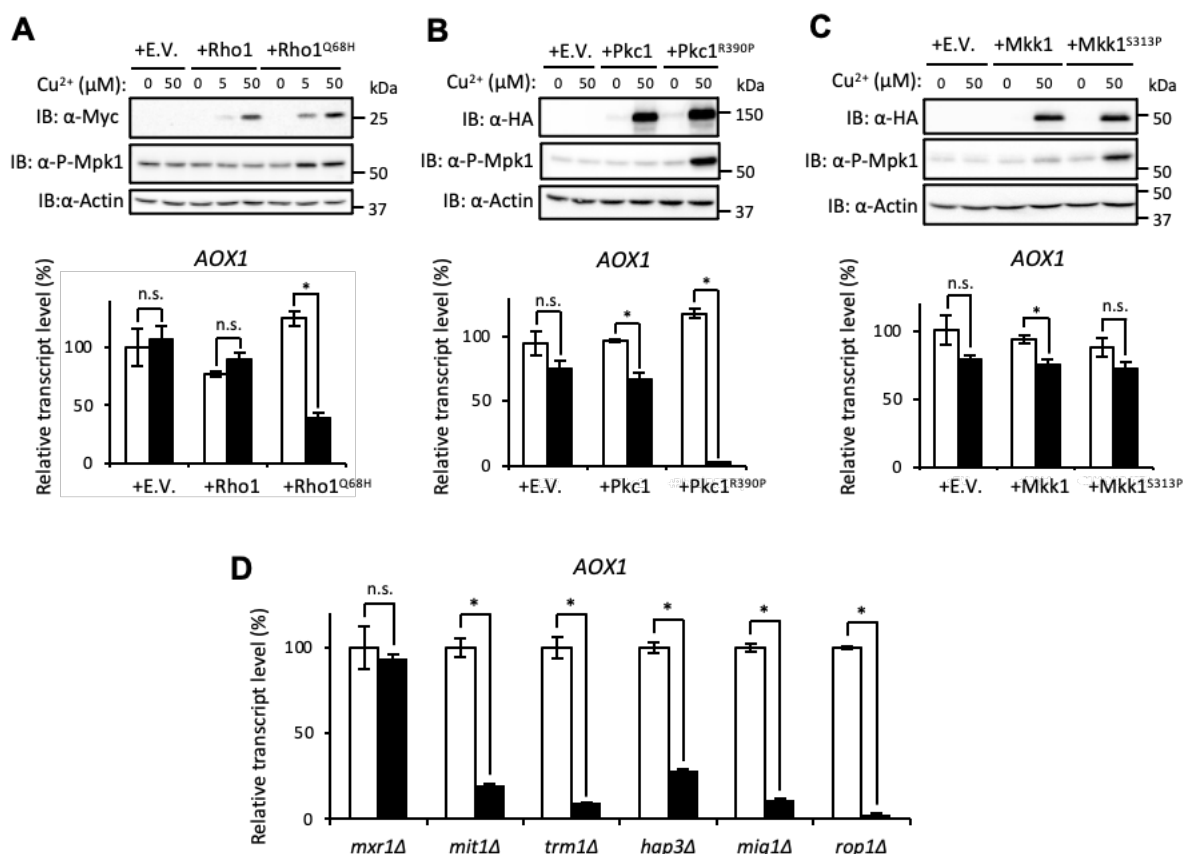
Figure 1-12. The induction of wild-type or hyperactive mutants of KpRho1-Myc, KpPkc1-HA and KpMkk1-HA effects on KpMpk1 phosphorylation and *AOX1* transcript level.

(A-C) Upper panels, immunoblot analysis of expressed proteins detected with anti-Myc antibody or anti-HA antibody, and phosphorylated KpMpk1 (P-Mpk1) detected with anti-phospho-Mpk1 antibody. Molecular weights of the protein size marker are indicated. Lower panels, transcript levels of *AOX1*. Total mRNA was prepared from the cells of each strain cultured in 0.01% methanol media without (white bars) or with 50 μM $CuSO_4$ (black bars) for 2 h. The transcript levels were normalized using *GAP* gene as the standard. Relative transcript levels compared to that of the control strain without $CuSO_4$ are indicated. Error bars represent standard error values from three independent experiments. (A) The strain expressing KpRho1-Myc and the strain expressing KpRho1^{Q68H}-Myc;(B) the strain expressing KpPkc1-HA and the strain expressing KpPkc1^{R390P}-HA; (C) the strain expressing KpMkk1-HA and the strain KpMkk1^{S313P}-HA under the control of the *ScCUP1* promoter. (D) Transcript levels of *AOX1* in the *Kpmxr1Δ, Kpmit1Δ, Kptrm1Δ, Kphap3Δ, Kpmig1Δ* and *Kprop1Δ* strains expressing KpRho1^{Q68H} under the control of the *ScCUP1* promoter. Total mRNA was prepared from the cells of each strain cultured in 0.01% methanol media without (white bars) or with 50 μM $CuSO_4$ (black bars) for 2 h. The transcript levels were normalized using *GAP* gene as the standard. Relative transcript levels compared to that of the control strain without $CuSO_4$ are indicated. Error bars represent standard error values from three independent experiments.

To understand how the activated signal transduction affects the phosphorylation state of KpMxr1, hyperactive KpPkc1^{R390P}-HA was expressed under the control of the *ScCUP1* promoter. The protein level of hyperactive KpPkc1^{R390P}-HA was confirmed to be induced by the addition of 50 μM Cu^{2+} to the SM medium (Figure 1-13A left panel). The amount of KpMxr1$^{1-230}$-FLAG slightly decreased by inducing KpPkc1^{R390P} under methanol-culture condition (Figure 1-13A left panel).

My earlier observation showed that the phosphorylation level of KpMxr1$^{1-230}$-FLAG was reduced with the medium shift from glucose to methanol (Figure 1-7A). But I observed that the phosphorylation level increased with the expression of hyperactive KpPkc1^{R390P}-HA and the addition of 50 μM Cu^{2+} in the medium after the medium shift to methanol medium for 30 min (Figure 1-13A right panel). Both the protein level of KpPkc1^{R390P}-HA and the phosphorylation level of KpMpk1 increased with increase in Cu^{2+} concentration (Figure 1-13B). The protein level of KpMxr1-FLAG decreased with the increase of Cu^{2+} concentration (Figure 1-13B), while there were no significant differences in the KpMxr1 protein level related to the methanol concentration (Figure 1-2A). Next, I examined the *AOX1* transcript level after the medium shift for 30 min with the addition of various concentrations of Cu^{2+}. The *AOX1* transcript level showed the peak pattern (maximum. at 1 μM) with the increase of KpPkc1^{R390P}-HA protein, which was similar to the response observed for the increase in methanol concentration (Figure 1-13C). These results imply that KpPkc1 receives the methanol signal, which then leads to the CRMI. The phosphorylation level of KpMxr1$^{1-230}$-FLAG according to the induction level of KpPkc1^{R390P}-HA by increasing Cu^{2+} concentration was also observed under 0.1% methanol-culture condition (Figure 1-13D). From these results, I concluded that KpMxr1 receives the methanol signal from Wsc family proteins via KpPkc1 in the regulation of the CRMI.
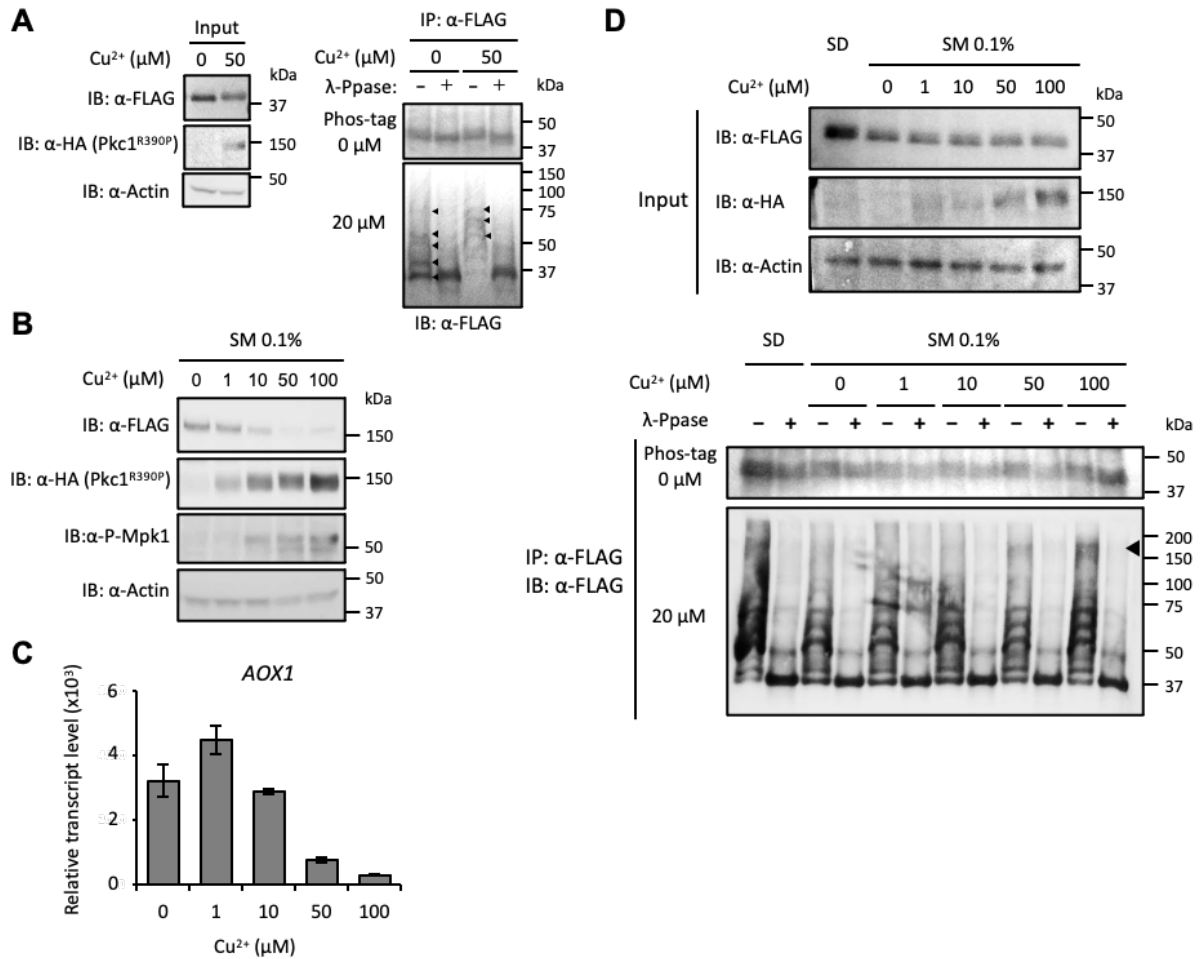
Figure 1-13. Hyperactive mutation KpPkc1^{R390P} facilitates KpMxr1-phosphorylation and changes *AOX1* transcript level.

(A) Phosphorylation level of KpMxr1$^{1-230}$-FLAG detected with phos-tag immunoblot analysis using the strain co-expressing KpPkc1^{R390P}-HA under the control of the *ScCUP1* promoter. Protein samples were prepared from the cells cultured in 0.1% methanol media with (50 μM) or without (0 μM) CuSO$_4$ for 30 min. (Left panel) KpMxr1$^{1-230}$-FLAG expression under the original promoter and KpPkc1^{R390P}-HA under the *ScCUP1* promoter in whole cell extracts was detected in input samples with anti-FLAG antibody and anti-HA antibody, respectively. (Right panel) KpMxr1$^{1-230}$-FLAG was immunoprecipitated with FLAG antibody. The samples were treated with or without λ-phosphatase (λ-Ppase), loaded on an 8.5% acrylamide SDS-PAGE gel with 20 μM or without phos-tag, and transferred to a PVDF membrane, and detected with an anti-FLAG antibody. Molecular weights of the protein size marker are indicated. Black arrowheads correspond to the detected bands of phosphorylated KpMxr1 protein. (B) Immunoblot analysis of KpMxr1-FLAG, Pkc1^{R390P}-HA, phosphorylated KpMpk1 and β-actin in the strain expressing KpPkc1^{R390P} under the control of the *ScCUP1* promoter. Cells were grown on glucose and shifted to methanol (SM) medium for 2 h at various concentrations of Cu^{2+}. The lysed samples were subjected to immunoblot analysis. Phosphorylation of KpMpk1 was detected with anti-phopho-Mpk1 antibody (α-P-Mpk1). Molecular weights of the protein size marker are indicated. (C) Transcript levels of *AOX1* in the strain expressing KpPkc1^{R390P} under the control of the *ScCUP1* promoter. Total mRNA was prepared from cells cultured on methanol containing various concentrations of CuSO$_4$ (0, 1, 10, 50 and 100 μM) for 2 h. The transcript levels were normalized using *GAP* gene as the standard. Relative transcript levels compared to that of the glucose pre-cultured sample are indicated. Error bars represent standard error values from three independent experiments. (D) Phosphorylation level of KpMxr1$^{1-230}$-FLAG detected with phos-tag immunoblot analysis using the strain expressing KpPkc1^{R390P}-HA under the control of the *ScCUP1* promoter. Protein samples were prepared from the cells cultured in 0.1% methanol media containing indicated concentration of CuSO$_4$ (0, 1, 10, 50, 100 μM) for 30 min. KpMxr1$^{1-230}$-FLAG expressed under the original promoter was immunoprecipitated with anti-FLAG antibody. The samples were treated with or without λ-phosphatase (λ-Ppase), loaded on an 8.5% acrylamide SDS-PAGE gel with 20 μM or without phos-tag, and transferred to a PVDF membrane, and detected with an anti-FLAG antibody. Molecular weights of the protein size marker are indicated. An arrowhead indicates the position of the phosphorylated bands in the sample induced by higher concentrations of CuSO$_4$.

35

Discussion

In nature and in the fermenter, methylotrophic yeasts sense environmental methanol concentration and regulate the expression level of their methanol-induced genes to avoid unbalanced methanol metabolism that may result in the accumulation of formaldehyde, a toxic metabolite. In addition to the transcription factors involved in methanol-induced gene expression, it has been previously reported that the Wsc family proteins are involved in methanol sensing (Ohsawa *et al.*, 2017; Yurimoto *et al.*, 2019). However, it is unclear how methylotrophic yeasts transmit the methanol signal to transcription factors. Results of the present study revealed that KpMxr1 is involved in the regulation of the CRMI and that its phosphorylation is regulated through the novel methanol signaling pathway from Wsc family proteins via KpPkc1 to KpMxr1 (CRMI pathway), which is independent of the MAPK cascade (Figure 1-14).

The phosphorylation state of KpMxr1 is dependent on the carbon sources and methanol concentration (Figures 1-2C, 1-7A and 1-7B). The serine residues in KpMxr1 were highly phosphorylated under glucose-culture condition and partly dephosphorylated under methanol-culture condition (Figure 1-7A). On the other hand, the threonine residues were phosphorylated in the methanol culture in a concentration-dependent manner with a peak at 0.1% methanol concentration (Figure 1-7A); this pattern correlated with the regulatory profile of methanol-induced gene expression (Figure 1-1A). The total phosphorylation level of KpMxr1$^{1-230}$-FLAG was decreased by the medium shift from glucose to methanol medium (Figures 1-7A and 1-7B) and changed depending on the methanol concentration (Figure 1-7B).

The results from truncated KpMxr1 mutant analyses (Figure 1-4D) suggest that the 231-368 a.a. region of KpMxr1 is responsible for response to lower methanol concentrations (0.01-0.1%) and the 369-525 a.a. region for response to higher methanol concentration (0.1-1.0%). These regions contained conserved regions 1-5 in KpMxr1 homologs in methylotrophic yeasts (Figure 1-3) indicating the conserved function of KpMxr1 in the CRMI among the methylotrophic yeasts. Interestingly, the *AOX1* transcript level increased in TM211 with increasing methanol concentration (0.1 to 1.0%) (Figure 1-4D). The amino acid region from 212 to 230 containing three serine residues S215/S217/S220 may be involved in CRMI through phosphoregulation.

The regulation of KpMxr1 subcellular localization is also an interesting issue. The KpMxr1^{FL}-YFP was distributed in the cytosol under glucose-culture condition and localized to the nucleus under methanol-culture condition (Figure 1-6A). However, truncated KpMxr1 proteins remained in the nucleus under both glucose- and methanol-culture conditions (Figure 1-6B), which may be due to the lack of NES region. Further analyses will be needed to elucidate where KpMxr1 is phosphor regulated and how its subcellular localization is affected by phosphoregulation.

In *S. cerevisiae*, ScAdr1, a homolog of KpMxr1, has been reported as a transcription factor that

activates genes involved in the utilization of nonfermentable carbon sources (Young *et al.*, 2003), and its activity is controlled by the AMP-activated protein kinase ScSnf1 via the dephosphorylation of the serine residue S230 (Ratnakumar *et al.*, 2009). The serine residue S215 in KpMxr1, which corresponds to S230 in ScAdr1, has been reported to be phosphorylated under glucose- or ethanol-culture condition, and the phosphorylated S215 interacts with 14-3-3 protein to inactivate KpMxr1(Parua *et al.*, 2012). In this study, LC-MS/MS analysis revealed that multiple serine and threonine residues in KpMxr1 are phosphorylated (Figure 1-8B). Mutation of some of these residues resulted in a decrease of the *AOX1* transcript level under lower methanol concentration conditions (< 0.03%) (Figure 1-10A). On the other hand, SA and TA mutations of KpMxr1 did not influence the growth on methanol medium (Figure 1-11). As S215A mutation did not influence the *AOX1* transcript level and the growth on methanol (Figure 1-9), non-phosphorylatable mutation of serine or threonine residues may not be sufficient to cause a deficiency in the cell growth.

In *K. phaffii*, methanol-sensing Wsc family proteins play a role not only in regulating methanol-induced gene expression but also in negatively regulating pexophagy, the degradation process of peroxisomes (Ohsawa *et al.*, 2021) (described in chapter III). The CRMI pathway I demonstrate here does not involve the MAPK cascade and the methanol signal is transmitted to KpMxr1 through the pathway that is branched out from KpPkc1 (Figures 1-12, 1-13 and 1-14). In the strains overexpressing hyperactive mutants KpRho1^{Q68H} or KpPkc1^{R390P}, the *AOX1* transcript level decreased (Figure 1-12), which may be caused by the strong methanol signal. In other words, overexpression of KpRho1^{Q68H} or KpPkc1^{R390P} mimics the condition of high methanol concentration.

In general, gene expression is regulated simply in an on/off manner, and the strength of the expression is usually dependent on the dose of the inducer and the expression level eventually reaches a plateau. However, in CRMI, methanol-induced gene expression essentially needs to be regulated more delicately to avoid unbalanced methanol metabolism resulting in the accumulation of formaldehyde. To achieve such a "delicate" regulation, *K. phaffii* seems to have developed a sophisticated mechanism as follows: after Wsc family proteins sense the environmental methanol concentration, the methanol signal is transmitted to KpRom2, KpRho1, and then to KpPkc1. The KpPkc1 activity determined by the methanol-signal strength presumably determines the signal strength to the CRMI pathway regulating the phosphorylation state of KpMxr1. Various phosphorylation patterns of KpMxr1 at multiple phosphorylation sites then determine the molecular structure of KpMxr1 depending on the methanol signal, which regulates the level of downstream methanol-induced gene expression (Figure 1-14).

In the future, I want to identify the kinase or phosphatase that directly reacts with KpMxr1. Based on the screening analysis of the kinases in *K. phaffii*, 152 annotated kinases involved in cell growth and *AOX1* promoter regulation were identified, and they include one of the three β-subunits of the KpSnf1

complex, KpGal83 (Shen *et al.*, 2016). In *S. cerevisiae*, Snf1 complex controls the activity of ScAdr1, but Snf1 complex is not a direct kinase of ScAdr1. Therefore, there must be other yet unknown kinases and phosphatases downstream of KpPkc1 or KpSnf1 complex. Further research in this area would help unravel these downstream players and their specific roles in methanol-induced gene expression in *K. phaffii*.
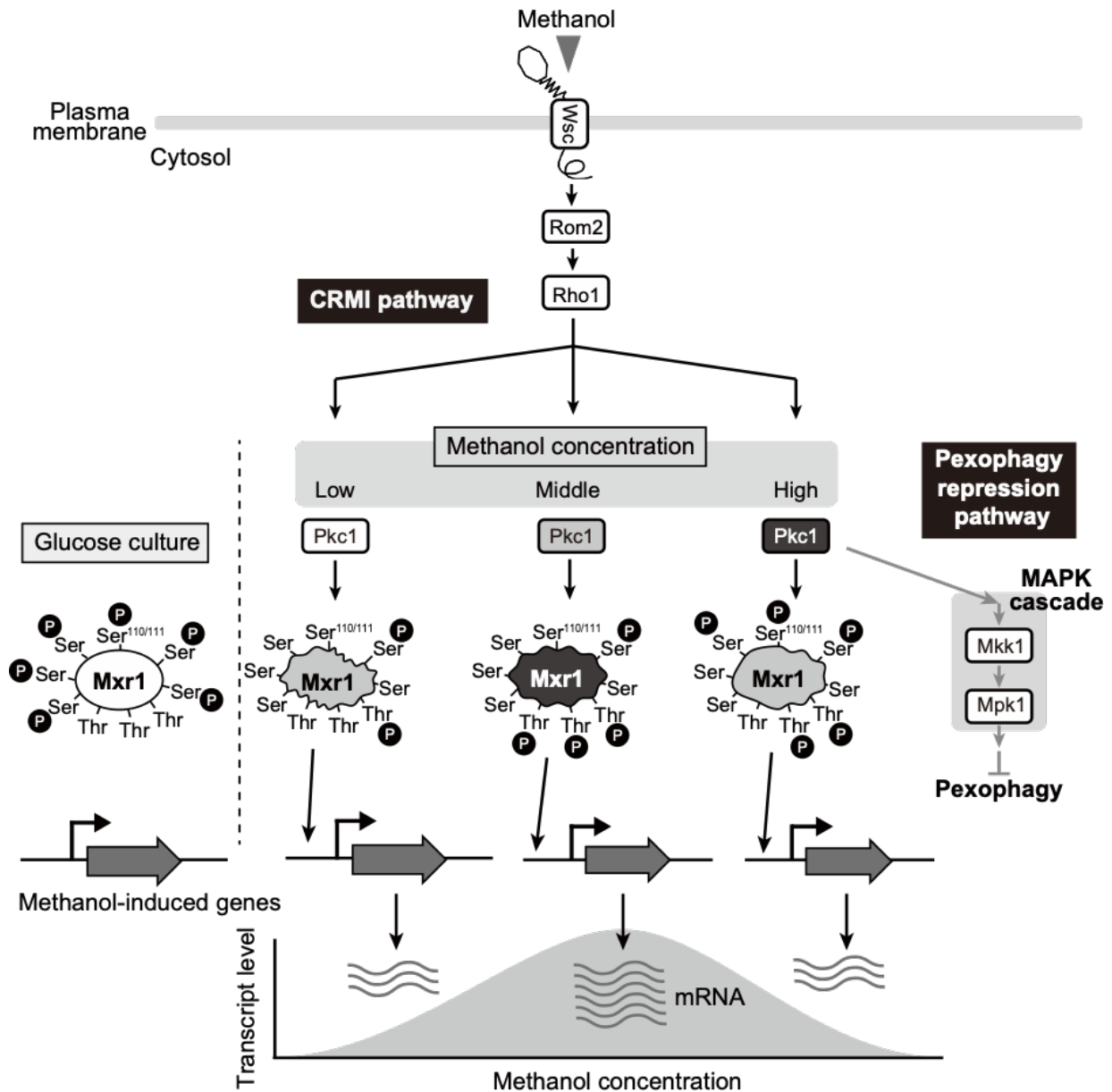
Figure 1-14. Regulatory model of CRMI via the control of KpMxr1 phosphorylation pattern.

The phosphorylation state of KpMxr1 is controlled by the CRMI pathway including KpWsc1/KpWsc3 (Wsc), KpRom2, KpRho1 and KpPkc1. The methanol signal according to methanol concentration is transmitted from this pathway to KpMxr1 independent of the MAPK cascade, which inhibits pexophagy under high methanol conditions (pexophagy-repression pathway). The serine residues (including S110/S111) in KpMxr1 are dephosphorylated by the medium shift from glucose to methanol, while the threonine residues are phosphorylated by the same medium shift. Multiple serine and threonine residues are phosphorylated in various patterns based on the methanol concentration. KpPkc1 regulates the phosphorylation status of KpMxr1 corresponding to methanol concentration. The active form of KpPkc1 increases depending on methanol concentration. The middle level of KpPkc1 activity (light gray) makes KpMxr1 the most active form (dark gray), but the high level of KpPkc1 activity (dark gray) phosphorylates serine residues (including S110/S111) and dephosphorylates threonine residues of KpMxr1 to repress methanol-induced gene expression. This phosphoregulation of KpMxr1 plays a critical role in maintaining the appropriate level of expression of methanol-induced genes.

Chapter II

Role of the transcription factor Mpp1 in the concentration-regulated methanol induction in *Candida boidinii*

Introduction

C. boidinii is a methylotrophic yeast that was isolated for the first time in the world from this laboratory in 1969 (Ogata *et al.*, 1969). Since then, other methanol-utilizing yeasts such as *K. phaffii* and *O. polymorpha* have been isolated and studied as a host for heterologous protein production (Yurimoto, 2009). Recently, heterologous protein production systems using *C. boidinii* have been established and focused on because of the low-cost method for high density cell culture and the established protocols for DNA modification. In addition, *C. boidinii* does not sporulate and is haploid, so it is easy to disrupt genes. On the other hand, the molecular mechanism of methanol-induced gene expression in this yeast remains to be elucidated.

C. boidinii has the almost same methanol-utilizing pathway as *K. phaffii* (Fig. 0A) (Yurimoto *et al.*, 2005) and enzymes for methanol metabolism. CbMpp1, a homolog of OpMpp1 in *O. polymorpha* and *KpMit1* in *K. phaffii*, is a $Zn(II)_2Cys_6$-type zinc finger protein and is responsible for methanol induction. In *O. polymorpha*, OpMpp1 regulates the level of peroxisomal matrix proteins and peroxins (Leão-Helder *et al.*, 2003). In *K. phaffii*, KpMit1 regulates the expression of many genes involved in methanol metabolism, including *AOX1*, but does not participate in peroxisome proliferation and transportation of peroxisomal proteins (Wang *et al.*, 2016b). KpMit1, KpMxr1, and KpTrm1 bind to P_{AOX1} at different sites and positively regulate the expression of P_{AOX1} in response to methanol (Wang *et al.*, 2016b).

In the previous studies, a series of transcriptional factors (CbTrm1, CbTrm2, CbMpp1 and CbHap complex) were identified involved in methanol-inducible gene expression in *C. boidinii* (Oda *et al.*, 2015; Sasano *et al.*, 2008; Sasano *et al.*, 2010; Zhai, 2012). These transcription factors bind to the promoter regions of methanol-induced genes and induce the expression of downstream genes. The function and dynamics of each transcription factor have been studied and a model diagram of their mechanism of action has been proposed based on these findings (Fig. 0B). Among the above four transcription factors, *CbTRM1*, *CbTRM2*, and *CbHAP* genes are constitutively expressed regardless of the carbon source. On the other hand, the expression of Cb*MPP1* is suppressed in the presence of carbon sources other than methanol, and its expression is strongly induced by the CbTrm1, CbTrm2, and CbHap complex in the presence of methanol as a sole carbon source (Zhai, 2012). Since only CbMpp1 showed methanol inducibility, it is considered to play a central role in the early stage of methanol induction. However, it

has been unclear about the physiological significance of methanol-induced *CbMPP1* and the interactions of CbTrm1, CbTrm2, CbMpp1 and CbHap complexes with the Cb*MPP1* promoter.

In this study, the physiological significance of methanol inducibility of CbMpp1 is investigated by analyzing the effects on the growth on methanol and methanol-induced gene expression by modifying the regulation and expression level of *CbMPP1*. CRMI of methanol-induced genes is also confirmed in *C. boidinii.* Since it was demonstrated in chapter I that KpMxr1 and KpMit1 are necessary for CRMI of *AOX1* and *DAS1* (Figure 1-1B), the role of CbMpp1 (a homolog of KpMit1) for CRMI is analyzed in this chapter. Moreover, the transcriptional activation regions on the *CbMPP1* promoter (P$_{MPP1}$) are investigated by promoter deletion analysis.

Materials & Methods

Strains, media and culture conditions

C. boidinii strains, plasmids and primers used in this study are shown in Tables 2-1, 2-2 and 2-3, respectively. *C. boidinii* cells were grown at 28 °C on YPD (1% yeast extract, 2% peptone, 2% glucose) or YNB medium (0.67% yeast nitrogen base without amino acids, pH 6.0) under aerobic conditions with gently shaking (120 rpm). 2% glucose (SD medium), 0.5% ethanol (SE medium) or several concentrations of methanol (SM medium) were used as carbon sources in YNB medium. All the components other than the carbon sources used in these media were purchased from Difco Becton Dickinson (Franklin Lakes, NJ). The growth of the yeast was monitored by the optical density (OD) at 610 nm.

 C. boidinii strain TK62 (*ura3*) was mainly used as the host of transformants. The transformation protocol of *C. boidinii* was performed using the Fast Yeast Transformation Kit (G-Biosciences, MO, USA) and the experimental manipulations followed the protocol.

 E. coli HST08 Premium (Takara Bio, Otsu, Japan) was used as a host strain for plasmid DNA preparation. *E. coli* cells were grown in LB medium (1% tryptone, 0.5% yeast extract, 0.5% NaCl) at 37°C.

Table 2-1. *C. boidinii* strains used in this study.

Designation	Genotype	Reference
TK62	*ura3*	Sakai *et al.*, 1991
TK62-*URA3*	*ura3::URA3*	Sakai *et al.*, 1991
TK62-*mpp1Δ*	*Cbmpp1Δ, ura3*	Zhai, 2012
TK62-*trm2Δ*	*Cbtrm2Δ, ura3*	Sasano *et al.*, 2010
M1	TK62-*mpp1Δ, ura3::(P$_{MPP1}$-CbMPP1-YFP, URA3)*	Zhai, 2012
M2	TK62*, ura3::(P$_{MPP1}$-CbMPP1-YFP URA3)*	This study
T1	TK62-*mpp1Δ, ura3::(P$_{TDH3}$-CbMPP1-YFP, URA3)*	This study
T3	TK62-*mpp1Δ, ura3::(P$_{TDH3}$-CbMPP1-YFP, URA3; 3 copies)*	This study
PHO-FL	TK62*, ura3::(P$_{MPP1}$-ScPHO5, URA3)*	This study
PHOΔ1000-800	TK62*, ura3::(P$_{MPP1}$ [from -1700 to -1000 and from -800 to -1]-ScPHO5, URA3)*	This study
PHOΔ1100-800	TK62*, ura3::(P$_{MPP1}$ [from -1700 to -1100 and from -800 to -1]-ScPHO5, URA3)*	This study
PHOΔ1200-800	TK62*, ura3::(P$_{MPP1}$ [from -1700 to -1200 and from -800 to -1]-ScPHO5, URA3)*	This study
PHOΔ1300-800	TK62*, ura3::(P$_{MPP1}$ [from -1700 to -1300 and from -800 to -1]-ScPHO5, URA3)*	This study
PHOΔ1400-800	TK62*, ura3::(P$_{MPP1}$ [from -1700 to -1400 and from -800 to -1]-ScPHO5, URA3)*	This study

Table 2-1. Continued.

Designation	Genotype	Reference
PHOΔ2Δ1000-800	TK62-*trm2Δ, ura3::(P$_{MPP1}$ [from -1700 to -1000 and from -800 to -1]-ScPHO5, URA3*)	This study
PHOΔ2Δ1100-800	TK62-*trm2Δ, ura3::(P$_{MPP1}$ [from -1700 to -1100 and from -800 to -1]-ScPHO5, URA3*)	This study
PHOΔ2Δ1200-800	TK62-*trm2Δ, ura3::(P$_{MPP1}$ [from -1700 to -1200 and from -800 to -1]-ScPHO5, URA3*)	This study
PHOΔ2Δ1300-800	TK62-*trm2Δ, ura3::(P$_{MPP1}$ [from -1700 to -1300 and from -800 to -1]-ScPHO5, URA3*)	This study
PHOΔ2Δ1400-800	TK62-*trm2Δ, ura3::(P$_{MPP1}$ [from -1700 to -1400 and from -800 to -1]-ScPHO5, URA3*)	This study
PHOΔ1700-1400	TK62, *ura3::(P$_{MPP1}$ [from -1400 to -1]-ScPHO5, URA3*)	This study
PHOΔ1700-1300	TK62, *ura3::(P$_{MPP1}$ [from -1300 to -1]-ScPHO5, URA3*)	This study
PHOΔ1700-1200	TK62, *ura3::(P$_{MPP1}$ [from -1200 to -1]-ScPHO5, URA3*)	This study
PHOΔ1700-1175	TK62, *ura3::(P$_{MPP1}$ [from -1175 to -1]-ScPHO5, URA3*)	This study
PHOΔ1700-1153	TK62, *ura3::(P$_{MPP1}$ [from -1153 to -1]-ScPHO5, URA3*)	This study
PHOΔ1700-1000	TK62, *ura3::(P$_{MPP1}$ [from -1000 to -1]-ScPHO5, URA3*)	This study
PHOΔ1700-950	TK62, *ura3::(P$_{MPP1}$ [from -950 to -1]-ScPHO5, URA3*)	This study
PHOΔ1700-900	TK62, *ura3::(P$_{MPP1}$ [from -900 to -1]-ScPHO5, URA3*)	This study
PHOΔ1700-650	TK62, *ura3::(P$_{MPP1}$ [from -650 to -1]-ScPHO5, URA3*)	This study
PHOΔ2Δ1700-1400	TK62-*trm2Δ, ura3::(P$_{MPP1}$ [from -1400 to -1]-ScPHO5, URA3*)	This study
PHOΔ2Δ1700-1300	TK62-*trm2Δ, ura3::(P$_{MPP1}$ [from -1300 to -1]-ScPHO5, URA3*)	This study
PHOΔ2Δ1700-1200	TK62-*trm2Δ, ura3::(P$_{MPP1}$ [from -1200 to -1]-ScPHO5, URA3*)	This study
PHOΔ2Δ1700-1175	TK62-*trm2Δ, ura3::(P$_{MPP1}$ [from -1175 to -1]-ScPHO5, URA3*)	This study
PHOΔ2Δ1700-1153	TK62-*trm2Δ, ura3::(P$_{MPP1}$ [from -1153 to -1]-ScPHO5, URA3*)	This study
PHOΔ2Δ1700-1000	TK62-*trm2Δ, ura3::(P$_{MPP1}$ [from -1000 to -1]-ScPHO5, URA3*)	This study
PHOΔ2Δ1700-950	TK62-*trm2Δ, ura3::(P$_{MPP1}$ [from -950 to -1]-ScPHO5, URA3*)	This study
PHOΔ2Δ1700-900	TK62-*trm2Δ, ura3::(P$_{MPP1}$ [from -900 to -1]-ScPHO5, URA3*)	This study
PHOΔ2Δ1700-650	TK62-*trm2Δ, ura3::(P$_{MPP1}$ [from -650 to -1]-ScPHO5, URA3*)	This study
PHOΔ1400-1350	TK62, *ura3::(P$_{MPP1}$ [from -1700 to -1400 and from -1350 to -1]-ScPHO5, URA3*)	This study
PHOΔ1400-1300	TK62, *ura3::(P$_{MPP1}$ [from -1700 to -1400 and from -1300 to -1]-ScPHO5, URA3*)	This study
PHOΔ1400-1250	TK62, *ura3::(P$_{MPP1}$ [from -1700 to -1400 and from -1250 to -1]-ScPHO5, URA3*)	This study
PHOΔ1200-1100	TK62, *ura3::(P$_{MPP1}$ [from -1700 to -1200 and from -1100 to -1]-ScPHO5, URA3*)	This study
PHOΔ1100-1000	TK62, *ura3::(P$_{MPP1}$ [from -1700 to -1100 and from -1000 to -1]-ScPHO5, URA3*)	This study
PHOΔ1000-900	TK62, *ura3::(P$_{MPP1}$ [from -1700 to -1000 and from -900 to -1]-ScPHO5, URA3*)	This study

Table 2-1. Continued.

Designation	Genotype	Reference
PHOΔ2Δ1400-1350	TK62-*trm2Δ*, *ura3*::(P*MPP1* [*from -1700 to -1400 and from -1350 to -1]-ScPHO5, URA3*)	This study
PHOΔ2Δ1400-1300	TK62-*trm2Δ*, *ura3*::(P*MPP1* [*from -1700 to -1400 and from -1300 to -1]-ScPHO5, URA3*)	This study
PHOΔ2Δ1400-1250	TK62-*trm2Δ*, *ura3*::(P*MPP1* [*from -1700 to -1400 and from -1250 to -1]-ScPHO5, URA3*)	This study
PHOΔ2Δ1200-1100	TK62-*trm2Δ*, *ura3*::(P*MPP1* [*from -1700 to -1200 and from -1100 to -1]-ScPHO5, URA3*)	This study
PHOΔ2Δ1100-1000	TK62-*trm2Δ*, *ura3*::(P*MPP1* [*from -1700 to -1100 and from -1000 to -1]-ScPHO5, URA3*)	This study
PHOΔ2Δ1000-900	TK62-*trm2Δ*, *ura3*::(P*MPP1* [*from -1700 to -1000 and from -900 to -1]-ScPHO5, URA3*)	This study
PHO-R1-A	TK62, *ura3*::(P*MPP1* [*from -1350 to -1250]-PACT1-ScPHO5, URA3*)	This study
PHO-R2-A	TK62, *ura3*::(P*MPP1* [*from -1200 to -1100]-PACT1-ScPHO5, URA3*)	This study
PHO-R3-A	TK62, *ura3*::(P*MPP1* [*from -1000 to -900]-PACT1-ScPHO5, URA3*)	This study
PHO2Δ-R1-A	TK62-*trm2Δ*, *ura3*::(P*MPP1* [*from -1350 to -1250]-PACT1-ScPHO5, URA3*)	This study
PHO2Δ-R2-A	TK62-*trm2Δ*, *ura3*::(P*MPP1* [*from -1200 to -1100]-PACT1-ScPHO5, URA3*)	This study
PHO2Δ-R3-A	TK62-*trm2Δ*, *ura3*::(P*MPP1* [*from -1000 to -900]-PACT1-ScPHO5, URA3*)	This study

Plasmid construction

The plasmids and primers used in this study are shown in Table 2-2 and Table 2-3, respectively. The empty plasmid pCBU1 possessing *URA3* marker gene was prepared from pAPU1 by In-Fusion cloning using the primer pair Inverse-tAOD1-Fw/ Infusion-pCBU1-Rv.

The promoter of *TDH3* was amplified by PCR from *C. boidinii* genomic DNA as a template using primer pairs EcoRI-Ptdh3-Fw/ NotI-Ptdh3-Rv. The fragment was ligated with pCBU1 vector digested by EcoRI and BamHI, resulting in pTDH3eI. *CbMPP1* gene and the DNA sequence of fluorescent protein YFP were amplified from pMMY1 using the primer pair NEB-Ptdh3-Mpp1YFP-Fw/ NEB-Ptdh3-Mpp1YFP-Rv. Subsequently, the fragment was ligated with vector DNA amplified from pTDH3eI using the primer pair Inverse-pTDH3eI-Fw/ Inverse-pTDH3eI-Rv by NEBuilder HiFi DNA Assembly (New England Biolabs, Ipswich, MA, USA), resulting in pTMY1.

The DNA region from -800 to -1 in *CbMPP1* promoter was amplified from pMPU1 using the primer pairs NEB-Pmpp1-800-Fw/ NEB-Pmpp1-1-Rv. And the region from -1700 to -1000, -1700 to -1100, -1700 to -1200, -1700 to -1300 and -1700 to -1400 were amplified using the primer pairs NEB-Pmpp1-

1700-Fw/ NEB-Pmpp1-1000-Rv, NEB-Pmpp1-1700-Fw/ NEB-Pmpp1-1100-Rv, NEB-Pmpp1-1700-Fw/ NEB-Pmpp1-1200-Rv, NEB-Pmpp1-1700-Fw/ NEB-Pmpp1-1300-Rv and NEB-Pmpp1-1700-Fw/ NEB-Pmpp1-1400-Rv, respectively. pMPU1 was digested by BamHI and SacI and used as a vector DNA. DNA fragments of -800 to -1, -1700 to -1000 and the vector were ligated to obtain pMPUΔ1000-800. pMPUΔ1100-800, pMPUΔ1200-800, pMPUΔ1300-800 and pMPUΔ1400-800 were prepared in the same method.

The DNA region from -1400 to -1 in *CbMPP1* promoter was amplified from pMPU1 using the primer pairs Infusion-Pmpp1-1400-Fw/ Infusion-Pmpp1-1-Rv. pMPU1 was digested by BamHI and SacI, and used as a vector DNA. These DNA fragments were ligated by In-Fusion cloning (Takara Bio, Otsu, Japan), resulting in pMPUΔ1700-1400. In the same way, pMPUΔ1700-1300, pMPUΔ1700-1200, pMPUΔ1700-1175, pMPUΔ1700-1153, pMPUΔ1700-1000, pMPUΔ1700-950, pMPUΔ1700-900 and pMPUΔ1700-650 were prepared using the primer pairs Infusion-Pmpp1-1300-Fw/ Infusion-Pmpp1-1-Rv, Infusion-Pmpp1-1200-Fw/ Infusion-Pmpp1-1-Rv, Infusion-Pmpp1-1175-Fw/ Infusion-Pmpp1-1-Rv, Infusion-Pmpp1-1153-Fw/ Infusion-Pmpp1-1-Rv, Infusion-Pmpp1-1000-Fw/ Infusion-Pmpp1-1-Rv, Infusion-Pmpp1-950-Fw/ Infusion-Pmpp1-1-Rv, Infusion-Pmpp1-900-Fw/ Infusion-Pmpp1-1-Rv and Infusion-Pmpp1-650-Fw/ Infusion-Pmpp1-1-Rv, respectively.

pMPUΔ1400-1350 was prepared from the fragment amplified by the primer pair NEB-d1400-1350-Fw/ NEB-d1400-1350-Rv. pMPUΔ1400-1300, pMPUΔ1400-1250, pMPUΔ1200-1100, pMPUΔ1100-1000 and pMPUΔ1000-900 were created in the same way using the primer pairs NEB-d1400-1250-Fw/ NEB-d1400-1250-Rv, NEB-d1200-1100-Fw/ NEB-d1200-1100-Rv, NEB-d1100-1000-Fw/ NEB-d1100-1000-Rv and NEB-d1000-900-Fw/ NEB-d1000-900-Rv, respectively.

The DNA region from -525 to -1 in *CbACT1* promoter was amplified from pACT1 using the primer pair NEB-Pact1-ScPHO5-Fw/ NEB-Pact1-ScPHO5-Rv. pMPU1 was digested by BamHI and SacI, and used as a vector DNA. These fragments were ligated by NEBuilder HiFi DNA Assembly (New England Biolabs, Ipswich, MA, USA) and then obtain pACTPU1. I defined the DNA region from -1350 to -1250, -1200 to -1100 and -1000 to -900 as "Region 1", "Region 2" and "Region 3", respectively. They were amplified from pMPU1 using the primer pairs NEB-1350-1250-ACT-Fw/ NEB-1350-1250-ACT-Rv, NEB-1200-1100-ACT-Fw/ NEB-1200-1100-ACT-Rv and NEB-1000-900-ACT-Fw/ NEB-1000-900-ACT-Rv. Subsequently, they were ligated with the vector DNA amplified from pACTPU1 using primer pairs Inverse-pACTPU1-Fw/ Inverse-pACTPU1-Rv, resulting in pR1-ACTPU1, pR2-ACTPU1 and pR3-ACTPU1, respectively.

Table 2-2. Plasmids in this study.

Designation	Description	Reference
pAPU1	P$_{AOD1}$-*ScPHO5, URA3*	Yurimoto *et al.*, 2000
pCBU1	*URA3* (designed from pAPU1, Empty vector for *C. boidinii*)	This study
pTDH3e1	P$_{TDH3}$, *URA3*	This study
pMMY1	pCBU1/ P$_{MPP1}$-*CbMPP1-YFP*	Zhai, 2012
pTMY1	pCBU1/ P$_{TDH3}$-*CbMPP1-YFP*	This study
pMPU1	P$_{MPP1}$-*ScPHO5, URA3*	Zhai, 2012
pMPUΔ1000-800	pMPU1/ P$_{MPP1}$ [from -1000 to -800]-*ScPHO5*	This study
pMPUΔ1100-800	pMPU1/ P$_{MPP1}$ [from -1100 to -800]-*ScPHO5*	This study
pMPUΔ1200-800	pMPU1/ P$_{MPP1}$ [from -1200 to -800]-*ScPHO5*	This study
pMPUΔ1300-800	pMPU1/ P$_{MPP1}$ [from -1300 to -800]-*ScPHO5*	This study
pMPUΔ1400-800	pMPU1/ P$_{MPP1}$ [from -1400 to -800]-*ScPHO5*	This study
pMPUΔ1700-1400	pMPU1/ P$_{MPP1}$ [from -1400 to -1]-*ScPHO5*	This study
pMPUΔ1700-1300	pMPU1/ P$_{MPP1}$ [from -1300 to -1]-*ScPHO5*	This study
pMPUΔ1700-1200	pMPU1/ P$_{MPP1}$ [from -1200 to -1]-*ScPHO5*	This study
pMPUΔ1700-1175	pMPU1/ P$_{MPP1}$ [from -1175 to -1]-*ScPHO5*	This study
pMPUΔ1700-1153	pMPU1/ P$_{MPP1}$ [from -1153 to -1]-*ScPHO5*	This study
pMPUΔ1700-1000	pMPU1/ P$_{MPP1}$ [from -1000 to -1]-*ScPHO5*	This study
pMPUΔ1700-950	pMPU1/ P$_{MPP1}$ [from -950 to -1]-*ScPHO5*	This study
pMPUΔ1700-900	pMPU1/ P$_{MPP1}$ [from -900 to -1]-*ScPHO5*	This study
pMPUΔ1700-650	pMPU1/ P$_{MPP1}$ [from -650 to -1]-*ScPHO5*	This study
pMPUΔ1400-1350	pMPU1/ P$_{MPP1}$ [from -1700 to -1400 and 1350 to -1]-*ScPHO5*	This study
pMPUΔ1400-1300	pMPU1/ P$_{MPP1}$ [from -1700 to -1400 and 1300 to -1]-*ScPHO5*	This study
pMPUΔ1400-1250	pMPU1/ P$_{MPP1}$ [from -1700 to -1400 and 1250 to -1]-*ScPHO5*	This study
pMPUΔ1200-1100	pMPU1/ P$_{MPP1}$ [from -1700 to -1200 and 1100 to -1]-*ScPHO5*	This study
pMPUΔ1100-1000	pMPU1/ P$_{MPP1}$ [from -1700 to -1100 and 1000 to -1]-*ScPHO5*	This study
pMPUΔ1000-900	pMPU1/ P$_{MPP1}$ [from -1700 to -1000 and 900 to -1]-*ScPHO5*	This study
pACT1	P$_{ACT1}$, *URA3*	Sakai *et al.*, 1998
pACTPU1	pMPU1/ P$_{ACT1}$-*ScPHO5*	This study
pR1-ACTPU1	pMPU1/ P$_{MPP1}$ [from -1350 to -1250]-P$_{ACT1}$-*ScPHO5*	This study
pR2-ACTPU1	pMPU1/ P$_{MPP1}$ [from -1200 to -1100]-P$_{ACT1}$-*ScPHO5*	This study
pR3-ACTPU1	pMPU1/ P$_{MPP1}$ [from -1000 to -900]-P$_{ACT1}$-*ScPHO5*	This study

Table 2-3. Oligonucleotide primers used in this study.

Designation	DNA sequence (5'-3')
Inverse-tAOD1-Fw	GCGGCCGCTAATTCAACAAG
Infusion-pCBU1-Rv	TGAATTAGCGGCCGCGAATTCGTAATCATGGTCATAGCTGTTTCC
EcoRI-Ptdh3-Fw	CCATGATTACGAATTCACACGTAACCGAAT
NotI-Ptdh3-Rv	GTTGAATTAGCGGCCGCTTTGTTTTATTTGAAGAAGTTTTT
NEB-Ptdh3-Mpp1YFP-Fw	CAAATAAAACAAAGCGGCCGCATGACAACAAC
NEB-Ptdh3-Mpp1YFP-Rv	ACTTGTTGAATTAGCGGCCGCTTATTTATATAATTCATCCATACCTAAAG
Inverse-pTDH3eI-Fw	GCTAATTCAACAAGTTGTATCTTTTTTTAC
Inverse-pTDH3eI-Rv	CGCTTTGTTTTATTTGAAGAAGTTTTTG
NEB-Pmpp1-800-Fw	TGATCATGTTCTTGTTTATATGTTTATGG
NEB-Pmpp1-1-Rv	AATCTCGAATTTGCGGATCCTATATGAAATAAATGAAGTAAGTAAGAAAGTAAG
NEB-Pmpp1-1700-Fw	ACAAAAGCTGGAGCTCCGCTTGTTACGTAATCTTGC
NEB-Pmpp1-1000-Rv	ACAAGAACATGATCAGCTTTCAATCAACTGAAAGTGAG
NEB-Pmpp1-1100-Rv	ACATATAAACAAGAACATGATCATATAGTAATATATTAACATTTTATAATGTACTGTC
NEB-Pmpp1-1200-Rv	ACAAGAACATGATCACACACAACTCAAATTTTTTTATAGTTTTAAA
NEB-Pmpp1-1300-Rv	ACAAGAACATGATCACGATTTATCCTATTCATATTAAGTATAAATAAC
NEB-Pmpp1-1400-Rv	ACAAGAACATGATCATTGTTATATTTTATTATATTGTACTGTATTGTATTGTATTGT
Infusion-Pmpp1-1400-Fw	GGGAACAAAAGCTGGAGCTCTGAATCAAAATAGTTTATGGTC
Infusion-Pmpp1-1-Rv	TCGAATTTGCGGATCCTATATGAAATAAATGAAGTAAGTA
Infusion-Pmpp1-1300-Fw	GGGAACAAAAGCTGGAGCTCGATTGTTTTTTAATTGGATT
Infusion-Pmpp1-1200-Fw	GGGAACAAAAGCTGGAGCTCGATTACGTAATGCACTATTTAAAGTTTCC
Infusion-Pmpp1-1175-Fw	ACAAAAGCTGGAGCTCTTCCGAATAATGCTTTCCCCACA
Infusion-Pmpp1-1153-Fw	GGGAACAAAAGCTGGATTTTTCACTTTATAAATGACAG
Infusion-Pmpp1-1000-Fw	GGGAACAAAAGCTGGAATTAGCAGGCAATTAGCATT
Infusion-Pmpp1-950-Fw	ACAAAAGCTGGAGCTCGATTTACTCCTATTAGATTCAATGGATTCC
Infusion-Pmpp1-900-Fw	ACAAAAGCTGGAGCTCGTTGAGTTCCTTCTTTGTTTGTTTC
Infusion-Pmpp1-650-Fw	GGGAACAAAAGCTGGAGCTCAGCTTAATTCAAGGCTCAAG
NEB-d1400-1350-Fw	TAATAAAATATAACATAGTATTATATAGTTATAGTTATTTATACTTAATATGAATAGG
NEB-d1400-1350-Rv	TGTTATATTTTATTATATTGTACTGTATTGTATTGTATTGTATTG
NEB-d1400-1300-Fw	TAATAAAATATAACAGGATTGTTTTTTAATTGGATTG
NEB-d1400-1300-Rv	TGTTATATTTTATTATATTGTACTGTATTGTATTGTATTGTATTG
NEB-d1400-1250-Fw	TAATAAAATATAACAACTGTATATTAAATTATATATTTAAAACTATAAAAAAATTTGAG
NEB-d1400-1250-Rv	TGTTATATTTTATTATATTGTACTGTATTGTATTGTATTGTATTG

Table 2-3. Continued.

Designation	DNA sequence (5'-3')
NEB-d1200-1100-Fw	AGTACATATTGATATATAGTAGTATATGGTAGGAATATTATATTG
NEB-d1200-1100-Rv	ATATCAATATGTACTACACAACTCAAATTTTTTTATAGTTTTAAAT
NEB-d1100-1000-Fw	CAATTAGCAGGCAATTAGCATTTAATTAGCATTTAATTAGC
NEB-d1100-1000-Rv	ATTGCCTGCTAATTGATAGTAATATATTAACATTTTATAATGTACTG
NEB-d1000-900-Fw	CGTTGAGTTCCTTCTTTGTTTGTTTCTGTTTC
NEB-d1000-900-Rv	AGAAGGAACTCAACGCTTTCAATCAACTG
NEB-Pact1-ScPHO5-Fw	ACAAAAGCTGGAGCTCTTAGCCACTTTAACCACTCTGC
NEB-Pact1-ScPHO5-Rv	AATCTCGAATTTGCGGATCCAATATATATTAAATTAAATTTATAAAATCTATCTAGGTTATAAATCTAG
NEB-1350-1250-ACT-Fw	ACAAAAGCTGGAGCTTAGTATTATATAGTTATAGTTATTTATACTTAATATGAATAGC
NEB-1350-1250-ACT-Rv	AAGTGGCTAAGAGCTAAATTAATAAATTAAATTAAAAATTTTTCAATCC
NEB-1200-1100-ACT-Fw	ACAAAAGCTGGAGCTGATTACGTAATGCACTATTTAAAG
NEB-1200-1100-ACT-Rv	AAGTGGCTAAGAGCTTATAGTAATATATTAACATTTTATAATGTACTGTC
NEB-1000-900-ACT-Fw	ACAAAAGCTGGAGCTAATTAGCAGGCAATTAGC
NEB-1000-900-ACT-Rv	AAGTGGCTAAGAGCTGGAACGGAACTGAACG
Inverse-pACTPU1-Fw	AGCTCTTAGCCACTTTAACCACTCTG
Inverse-pACTPU1-Rv	AGCTCCAGCTTTTGTTCCCTTTAG
RT-MPP1-Fw	TTCACCACCTTCACTTTCAGG
RT-MPP1-Rv	GCATGCCATATCTGTGATTTTG
RT-AOD1-Fw	TGCTGCTCCAGATTTCGATCC
RT-AOD1-Rv	GGTTCACCAGCAAAACATTCC
RT-DAS1-Fw	TGCAGCCCCAGCATTAAGAA
RT-DAS1-Rv	GCAATAGGTTGATGTGTTGGTCC
RT-FLD1-Fw	GACCGATGGTGGTTGTGATTTC
RT-FLD1-Rv	GCGGCAACACCAATGATAACAG
RT-ACT1-Fw	TTGTCCCAATTTACGCTGG
RT-ACT1-Rv	CAGCAGTGGTGGAGAAAGTG
Southern-URA3-Fw	TGTTGATCTCACCACAACCAA
Southern-URA3-Rv	GCATTCCAACCTGCTTTCAT

Extraction of genomic DNA from *C. boidinii* cells

A single colony of the yeast was inoculated in YPD medium and grown overnight at 28°C. Cells equivalent to 10 OD_{610} units were harvested by centrifugation at 5,000 g for 3 min at 4°C and resuspended in 600 μL of SCEM solution (100 mM Tris-HCl, 900 mM sorbitol, 100 mM EDTA, 100 mg/L Zymolyase 100T and 0.5%v/v β-mercaptoethanol, pH 7.5) after the supernatant was removed. The solution was incubated at 37°C for 1 h and mixed well with 75 μL of 10% SDS solution. Subsequently, the solution was incubated at 65°C for 30 min and 300 μL of Solution III (3 M potassium acetate and 2 M acetate) was added to the solution, and then incubated at 4°C for 1 h. The sample was centrifuged (20,000 g, 10 min, 4°C) and the supernatant was added to the same volume of isopropanol including 300 mM sodium acetate. Then, the sample was incubated at 4°C for 10 min and centrifuged (20,000 g, 10 min, 4°C). The supernatant was removed, and the precipitation was washed with 1 mL of 70% ethanol. The supernatant was removed again, and the precipitation was dried. The precipitation was dissolved in 300 μL of RNase solution (10 mM Tris-HCl, 1 mM EDTA and 50 mg/L RNaseA, pH 7.5) and incubated at 37°C for 30 min. The solution was mixed with phenol/ chloroform/ isoamyl alcohol (25: 24: 1) and an aqueous layer was corrected. Subsequently, the solution was added to the same volume of isopropanol including 300 mM sodium acetate and incubated at -20°C for 10min. The sample was centrifuged (20,000 g, 20 min, 4°C), and washed with 70% ethanol as described above. The precipitation was dissolved in 300 μL of TE buffer (10 mM Tris-HCl and 1 mM EDTA, pH 7.5), and then I obtained a genomic DNA solution. 200 ng of genomic DNA was used for quantitative PCR (qPCR). qPCR was performed in the same way as qRT-PCR described below.

RNA isolation and quantitative reverse transcription-PCR (qRT-PCR)

A single colony was inoculated in YPD medium and grown overnight at 28°C. Yeast cells were transferred into SD medium and cultivated to early exponential phase. The cells were shifted to SM medium. Cells equivalent to 5 OD_{610} units were harvested at the indicated time points by centrifugation at 10,000 g for 1 min at 4°C. Total RNA was extracted from the cells as described in chapter I. Primers for *CbMPP1, AOD1, DAS1, FLD1* and *ACT1* are shown in Table 2-3. Transcript levels of all genes in methanol culture were first quantified using *ACT1* as the control, and then, indicated as the relative value to that in glucose culture.

Preparation of protein extracts from yeast cells

Cells were grown in YPD and SD as described above, and the cells were shifted from SD to SM medium at 28°C for 20 h. The cells equivalent to about 2 OD_{610} units were collected for protein extraction. They were suspended in 0.2 N NaOH solution containing 0.5% β-mercaptoethanol for 15 min on ice and

trichloroacetic acid was added to a final concentration of 10% v/v for cell lysis. The samples were centrifuged (20,000 g, 5 min, 4°C) and protein pellets were washed three times with 100% acetone by brief sonication. Subsequently, protein pellets were re-suspended in the sample buffer (62.5 mM Tris-HCl, 2% SDS, 10% Glycerol, 5% β-mercaptoethanol, 0.005% BPB, pH 6.8) and incubated at 65°C for 10 min.

Immunoblot analysis

The samples were first centrifuged at 20,000 g for 1 min. 10 μL of the supernatant was electrophoresed on a 7.5% SDS-PAGE gel (SuperSep Ace, 13wells; Fujifilm, Tokyo, Japan). Precision Plus Protein Dual Color Standard (Bio-Rad, Hercules, USA) was used as a protein-loading marker. The proteins were transferred to an Immobilon-P PVDF membrane (0.2 μm, Merck KGaA, Darmstadt, Germany) by semidry blotting (Bio-Rad, Hercules, USA). The membranes were incubated in Blocking One (Nakalai tesque, Kyoto, Japan) and then in the solution containing anti-YFP antibody (anti-GFP antibody, JL-8, mouse monoclonal, Takara Bio, Shiga, Japan), anti-AOD antibody (rabbit polyclonal; Sakai *et al.*, 1996), anti-DAS antibody (rabbit polyclonal; Sakai *et al.*, 1996) or anti-β-actin (mAbcam 8224, mouse monoclonal, Abcam, Cambridge, UK) at dilutions recommended in the protocol with TBS-T buffer (50 mM Tris-HCl, 138 mM NaCl, 2.7 mM KCl, 0.05% Tween 20, pH 7.5). The membranes were washed 3 times with TBS-T buffer and incubated with anti-mouse-HRP (No. 330, goat polyclonal, Merck Millipore, Darmstadt, Germany) or anti-rabbit-HRP (#7074, goat polyclonal, Abcam, Cambridge, UK) at a 1:5,000 dilution for 1 h. Finally, bound secondary antibodies were detected using Western Lightning (Perkin-Elmer Life Science, Waltham, MA) and the signals were detected using Lummino-Graph II (ATTO, Tokyo, Japan).

Quantification of formaldehyde concentration

To determine formaldehyde concentration, cultured media were harvested at the same indicated time points as cell growth measurement. Then, they were centrifuged (6,000 g, 2 min, 4°C). 100 μL of each supernatant (diluted appropriately) was mixed with the same amount of Nash reagent (1.95 M ammonium acetate, 0.3% acetate, 0.2% acetylacetone) and incubated for 30 min at 30°C. Subsequently, the absorbance at 420 nm of each sample was measured using the microplate spectrophotometer (Tecan, Sunrise Rainbow Thermo RC-R, F039300RTRCR, Männedorf, Switzerland). A calibration curve was generated from a standard specimen of formaldehyde solution (0-0.20 mM, 37% solution; Nacalai tesque, Kyoto, Japan).

Fluorescence microscopy observation

Yeast cells were grown in YPD and SD as described above and shifted from SD to SM medium containing 0.5 % methanol at 28°C for 5 h. The cells were treated with 70% ethanol for 30 min and subsequently incubated in DAPI solution (50 µg/L, Nakalai tesque, Kyoto, Japan) for 20 min. Observations were carried out with an IX81 fluorescence microscope (Olympus, Tokyo, Japan). Fluorescent images were captured with a charged coupled device (CCD) camera (SenSys; PhotoMetrics, Tucson, AZ) at the fixed exposure time of 200 msec in DIC field, 1000 msec in YFP field and 50 msec in DAPI field using MetaMorph software (Universal Imaging, West Chester, PA).

Southern-blot analysis

The DNA probe for confirmation of transformation and plasmid copy number was designed in *URA3* gene. A 669 bp DNA fragment was prepared by PCR from genomic DNA using primer pair Southern-URA3-Fw/ Southern-URA3-Rv. The purified DNA fragment was denatured by boiling for 5 min and then incubated on ice for 5 min. 10 mg/L of the fragment was labeled with alkaline phosphatase (Amersham Gene Images AlkPhos Direct Labelling and Detection System, GE Healthcare, IL, USA).

Approximately 3 µg of yeast genomic DNA was digested with HindIII and electrophoresed on a 1.0% agarose gel. The gel was exposed to a basic aqueous solution (500 mM NaOH and 1.0 M NaCl) for 40 min, and then in a solution (0.5 M Tris-HCl,1.5 M NaCl, pH 7.0) for 1 h. Fractionated DNA was blotted on a positively charged nylon transfer membrane (Amersham Hybond-N$^+$, 0.45 µm, GE Healthcare, IL, USA) by suction of 20x SSC transfer buffer (3M NaCl, 300 mM sodium citrate, pH 7.0). The membrane was washed with 6x SSC buffer for 5 min and fixed by baking at 80 °C for 2 h. Subsequently, hybridization of the membrane and labeled DNA probe was performed at 55 °C. The membrane was washed twice and detected by CDP-Star detection reagent (GE Healthcare, IL, USA). The signal was analyzed with a Light-Capture System (ATTO, Tokyo, Japan).

Acid phosphatase (APase) activity assay

Yeast cells were grown in YPD and SD containing 0.5% yeast extract, and then transferred to SM medium containing 0.7% methanol for 8 h at a cell density OD610 of 1.0. Cells were harvested, washed twice with 50 mM acetate buffer (pH 4.0) and suspended in 200 µL of 50 mM acetate buffer (pH 4.0) with the appropriate dilution of the cells. Acid phosphatase activity was assayed based on the method described in the previous study (Torriani, 1960). Cells were mixed with 800 µL of 1.72 mM p-Nitrophenyl phosphate disodium solution (Wako, Fujifilm, Osaka, Japan) and they were enzymatically reacted at 37°C for 10 min. The reaction was stopped by the addition of 1 mL of 10% trichloroacetic acid (final concentration: 5% v/v, Fujifilm, Osaka, Japan). The sample was well mixed with 1 mL of saturated

sodium carbonate solution (Wako, Fujifilm, Osaka, Japan). Cell density (Optical density 610 nm) and absorbance 420 nm were measured using a spectrophotometer. A calibration curve was created from the standard specimen of p-Nitrophenol (pNP, 0-5 mM, Nacalai chemicals, Kyoto, Japan).

The specific APase activity of a cell suspension was calculated according to the reported method (Toh-e *et al.*, 1973). One unit of the enzyme was defined as the amount of enzyme which liberated 1 nmol of p-nitrophenol per min.

$$\text{Specific APase activity [U]} = \frac{\text{Generated pNP [nmol]}}{\text{OD610} \cdot 10 \text{ [min]}} \cdot \frac{3000 \text{ [µL]}}{200 \text{ [µL]}}$$

Statistical analysis

All data were obtained from three independent biological replicates and presented as mean ± S.E. Student's t-test was performed to determine the differences among grouped data. Statistical significance was assessed at $p < 0.05$. For comparison between some groups, a parametric one-way analysis of variance (one-way ANOVA) based on Turkey-Kramer test was performed.

Results

2.1 Constitutive or excessive expression of *CbMPP1* causes a deficiency of growth delay

To investigate the physiological significance of methanol inducibility of *CbMPP1*, the strains expressing *CbMPP1* constitutively or excessively were constructed (Figure 2-1A). *TDH3* encodes glyceraldehyde-3-phosphate dehydrogenase (GAPDH), which involves in glycolysis and gluconeogenesis, and *TDH3* promoter (P$_{TDH3}$) is constitutively activated regardless of carbon sources. The control strain M1 possesses a copy of plasmid for expressing *CbMPP1*-YFP under the control of P$_{MPP1}$. Strain T1 possesses a copy of plasmid for expressing *CbMPP1*-YFP under the control of P$_{TDH3}$ and strain T3 has three copies of that plasmid (constitutive expression strains). The *Cbmpp1Δ* strain was used as a transformation host of strains M1, T1 and T3. Strain M2 has a copy of P$_{MPP1}$-*CbMPP1*-YFP (over-expression strain) in addition to the native *CbMPP1* gene. The number of *CbMPP1* gene copies in these strains was confirmed by quantitative PCR against the genomic DNA (Figure 2-1B).
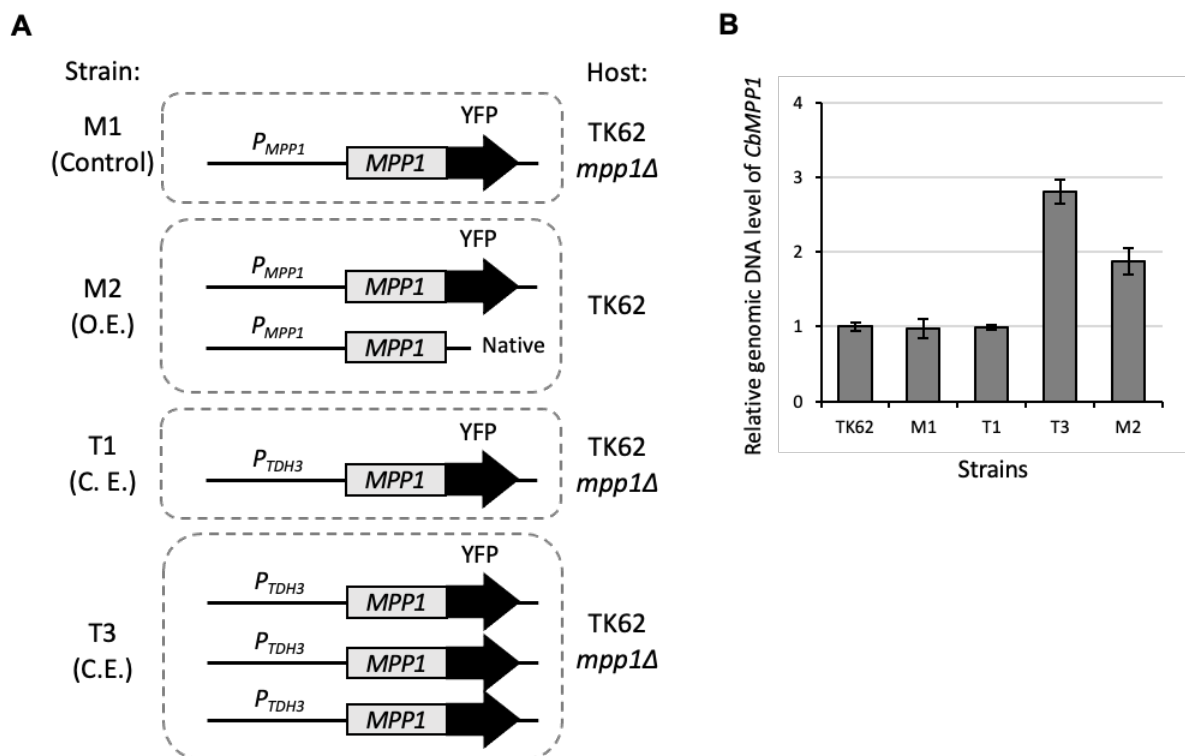
Figure 2-1. Construction of *C. boidinii* strains constitutively or excessively expressing *CbMPP1*.
(A) The strains used in this experiment. Control strain M1 possesses a copy of plasmid for expressing *CbMPP1*-YFP. Strain T1 possesses a copy of *CbMPP1*-YFP under the control of *TDH3* promoter and strain T3 possesses three copies of MPP1-YFP under the control of *TDH3* promoter. Strain M2 has two copies of P$_{MPP1}$-*CbMPP1*. C.E.; constitutive expression, O.E.; over-expression. (B) Genomic copy number of *CbMPP1*. The chromosomal DNA was extracted after the culture in YPD media for 24 h. 200 ng of the genomic DNA was used to quantitative PCR. Error bars represent standard error values from three independent experiments.

Cell growth of strains M1, T1, T3 and M2 on SM, SD and SE media was compared (Figures 2-2A and 2-2B). Strain T1 did not grow at all and strain T3 showed a remarkable growth delay under methanol culture condition compared to M1 (Figure 2-2A). Strain M2 also exhibited a growth delay on methanol culture (Figure 2-2B). There was no difference in the growth of all strains on glucose and ethanol media (Figures 2-2A and 2-2B). These results suggested that constitutive or excessive expression of *CbMPP1* leads to the growth delay.

Formaldehyde concentration in the supernatant of SM media at the same time point of the growth measurement was quantified in these strains (Figures 2-2C and 2-2D). In strain M1, rapid accumulation of formaldehyde was observed at 23 h and it immediately disappeared during growth on methanol. In strain T1, accumulation of formaldehyde was not observed, while 0.1-0.2 mM formaldehyde was accumulated in strain T3 for a long period and the consumption of formaldehyde stagnated (Figure 2-2C). Moreover, the accumulation of formaldehyde in strain M2 was abnormally induced (~ 0.9 mM) compared to strain M1. Therefore, it was estimated that the expression level of *CbMPP1* was too low in strain T1 to generate formaldehyde and grow on methanol media. And these results indicate that constitutive expression of *CbMPP1* leads to a long-period accumulation of formaldehyde in strain T3 and excessive expression of *CbMPP1* causes a surplus accumulation of formaldehyde in strain M2. Such formaldehyde accumulation is thought to be toxic to the cells and delay the growth on methanol.
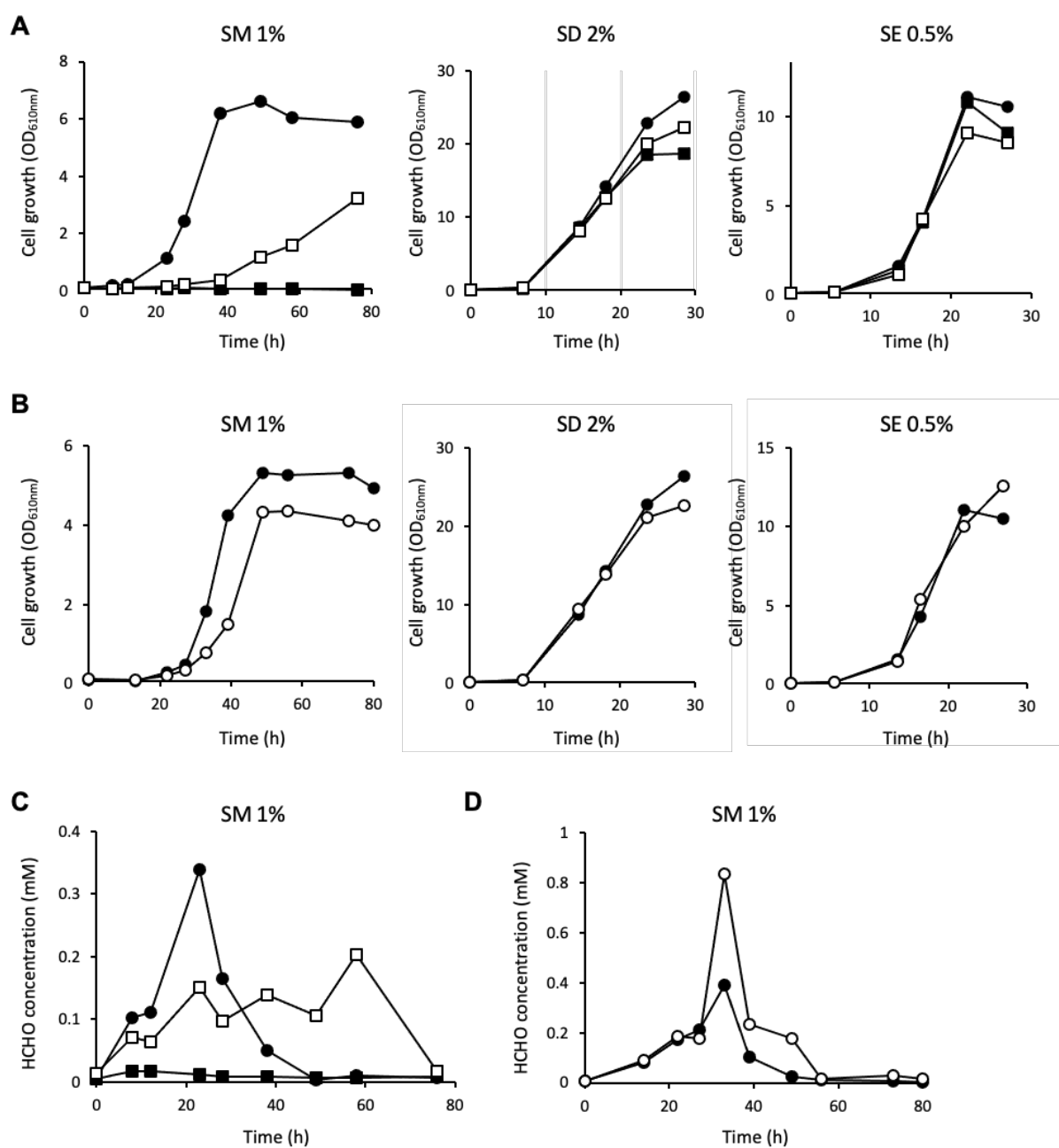
Figure 2-2. The effects of *CbMPP1* constitutive or excessive expression on cell growth and formaldehyde accumulation.

(A) Cell growth of strains M1 (filled circles), T1 (filled squares) and T3 (open squares) on YNB media containing 1% methanol, 2% glucose or 0.5% ethanol. (B) Cell growth of strains M1 (filled circles) and M2 (open circles) on YNB media containing 1% methanol, 2% glucose or 0.5% ethanol. (C and D) Formaldehyde concentration in the supernatant of SM media at the same time point of the methanol growth measurement using strains M1 (filled circles), T1 (filled squares), T3 (open squares) and M2 (open circles). Cells were pre-cultured in YPD media for 24 h and cultured in SD media for 12 h at 28°C. Subsequently, the cells were shifted to YNB media containing 1% methanol, 2% glucose or 0.5% ethanol.

55

2.2 Constitutive or excessive expression of *CbMPP1* also affects the transcript level and CRMI of methanol-induced genes

The effect of *CbMPP1* constitutive or excessive expression on the transcript levels was analyzed using strains M1, T1, T3 and M2. As shown in Figure 2-3A, the transcript levels of *CbMPP1* in strains T1 and T3 were induced even in glucose-culture condition, while they were lower than the control strain in methanol culture condition. The *CbMPP1* transcript level in strain T3 was higher than that in strain T1 at all of the time points. These results confirmed the constitutive expression of *CbMPP1* in strains T1 and T3 in glucose- and methanol-culture conditions and multiple cassettes of *CbMPP1* expression plasmid in strain T3. The transcript levels of *AOD1*, *DAS1* and *FLD1* in strains T1 and T3 decreased under methanol culture condition compared to strain M1 (Figure 2-3A). It is considered that *CbMPP1* expressed under P_{TDH3} was not enough to proper methanol induction of methanol-induced genes and constitutive expression of *CbMPP1* leads to the decrease of methanol-induced gene expression.

The transcript level of *CbMPP1* in strain M2 in methanol-culture condition increased compared to strain M1 (Figure 2-3A), which confirms excessive expression of *CbMPP1*. In contrast, *AOD1*, *DAS1* and *FLD1* transcript levels in strain M2 were lower than those in strain M1 on methanol medium (Figure 2-3A). This result indicates that excessive expression of *CbMPP1* causes a defect in the expression of methanol-induced genes.

Next, I focused on the relationship between the regulation of *CbMPP1* expression and CRMI. Transcript levels of *CbMPP1*, *AOD1*, *DAS1* and *FLD1* in strains M1, M2, T1 and T3 were measured, and their dependency on methanol concentration was evaluated. In strain M1, the transcript levels of *CbMPP1*, *AOD1* and *DAS1* increased in the presence of 0.01-0.1% methanol but decreased in the presence of more than 0.1% methanol (Fig. 2-3B). It was confirmed that the expressions of *CbMPP1*, *AOD1* and *DAS1* are regulated depending on methanol concentration also in *C. boidinii*. Although the transcript level of *FLD1* increased in the presence of 0.01-0.1% methanol, it was not repressed under 1% methanol culture condition. Consistently, the transcript levels of *CbMPP1* in all methanol concentrations were lower in strains M2, T1 and T3 than that in strain M1 (Fig. 2-3B). Furthermore, transcriptional activation and repression in a methanol concentration-dependent manner were not observed in *CbMPP1* expression of strains M2, T1 and T3 (Fig. 2-3B). The transcript level of *AOD1* and *DAS1* also decreased in strains M2, T1 and T3 compared to strain M1 (Fig. 2-3B). The CRMI of *DAS1* was lost in strains M2 and T3 (Fig. 2-3B). These results suggest that CRMI of *CbMPP1* under the control of P_{MPP1} is important in keeping sufficient induction and proper regulation of methanol-induced gene expression. In addition, constitutive or excessive expression of *CbMPP1* leads to impede the CRMI. The expression of *CbMPP1* is tightly and accurately regulated for maintaining the proper methanol metabolism and cell growth on methanol.
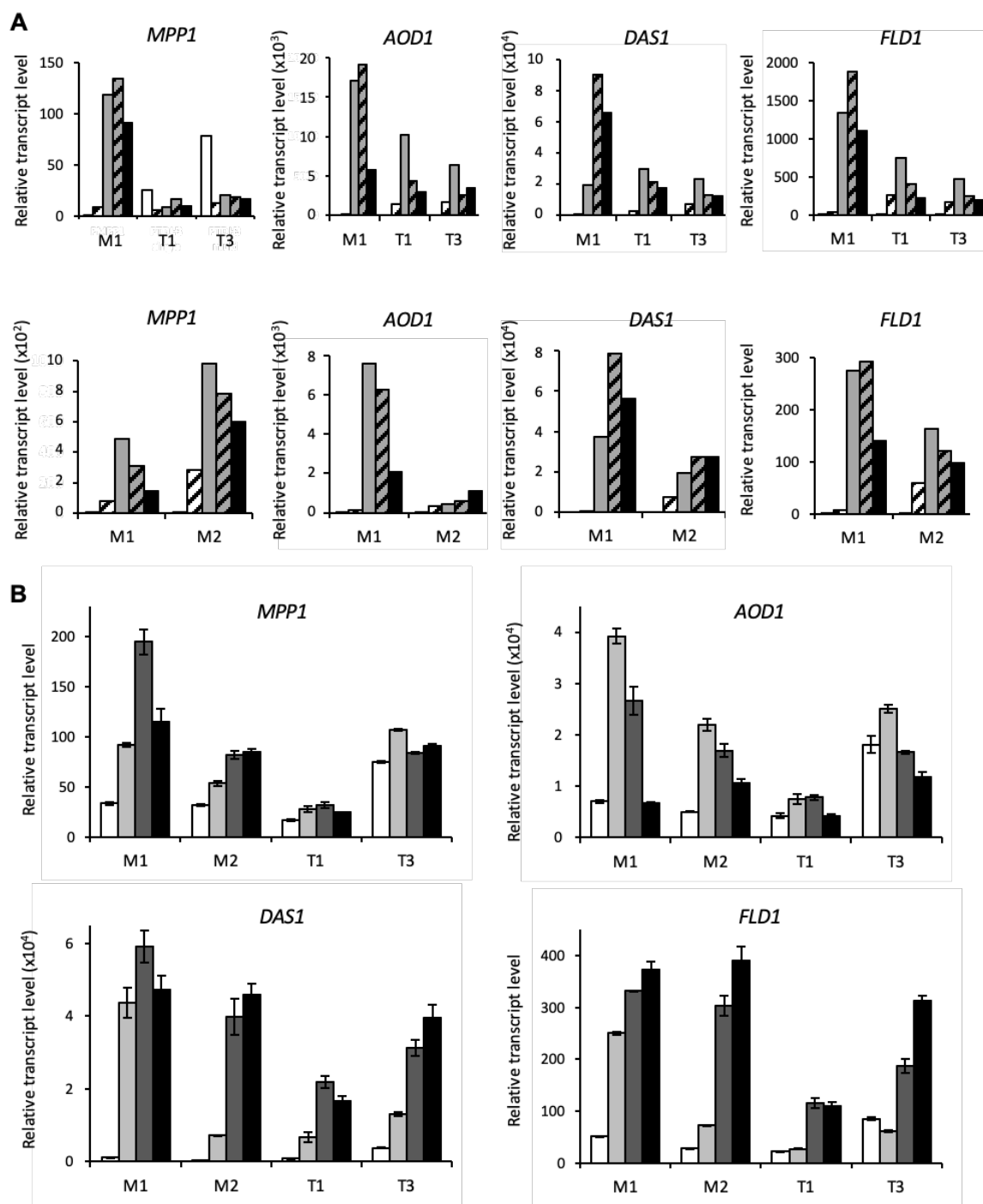
Figure 2-3. Transcript levels of methanol-induced genes in constitutively or excessively expressing strains during methanol culture.

(A) Temporal changes of *CbMPP1*, *AOX1*, *DAS1* and *FLD1* transcript levels in strains M1 (control), T1, T3 and M2. Total mRNA was prepared from cells of each strain cultured in 0.7% methanol medium for 0 h (white bars), 1h (white bars with diagonal line), 2h (grey bars), 3h (grey bars with diagonal line) and 4h (black bars). The transcript levels were normalized using *ACT1* gene as the standard. Relative transcript levels compared to that of the 0 h sample of strain M1 are indicated. (B) Transcript levels of *CbMPP1*, *AOX1*, *DAS1* and *FLD1* depending on methanol concentration in strains M1, T1, T3 and M2. Total mRNA was prepared from cells of each strain cultured in 0% (white bars), 0.01% (light grey bars), 0.1% (dark grey bars) and 1% (black bars) methanol medium for 2h. The transcript levels were normalized using *ACT1* gene as the standard. Relative transcript levels compared to that of the glucose cultured sample of strain M1 are indicated. Error bars represent standard error values from three independent experiments.

2.3 The protein level of CbMpp1 was not kept in proper quantity in strains T1, T3 and M2

The protein levels of CbMpp1-YFP, AOD and DAS in strains M1, T1, T3 and M2 were analyzed by immunoblot. In strain M1, CbMpp1-YFP protein was observed after 2 h and 5 h from the medium shift to methanol (Figure 2-4). On the other hand, the CbMpp1-YFP protein in strains T1 and T3 was observed under glucose culture condition (0 h) and decreased during growth on methanol (Figure 2-4), which is consistent with the result of the transcript level analysis (Figure 2-3A). The protein level of AOD and DAS decreased in strains T1 and T3 compared to strain M1 (Figure 2-4). Contrary to my expectation, the protein level of strain M2 during growth on methanol was entirely different from that of strain M1 (Figure 2-4). CbMpp1-YFP was highly induced in strain M2 at 0 h and degraded after 2 h from the medium shift, while the protein in strain M1 increased after 2 h from the medium shift. Although AOD and DAS were slightly detected at 0 h in strain M1, there is no band signal at 0 h in strain M2. CbMpp1-YFP level in strain M2 during growth on methanol seemed to be barely lower than that in strain M1. These results indicate that the difference of promoter or copy number of *CbMPP1* between strains T1, T3, M2 and M1 affected the abundance of AOD and DAS. Moreover, CbMpp1 protein produced during growth on glucose seemed to be rapidly degraded by the medium shift to methanol. Therefore, *CbMPP1* expression under P$_{MPP1}$ is necessary to keep the proper amount of CbMpp1 and methanol-induced proteins in the cells.
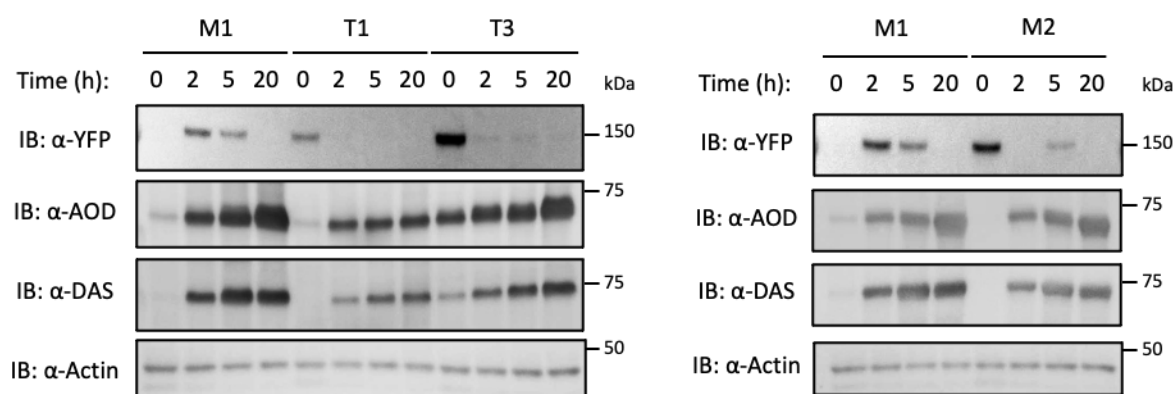

Figure 2-4. The protein levels of CbMpp1-YFP, AOD and DAS in strains M1, T1, T3 and M2 during methanol culture.
Immunoblot analysis of CbMpp1-YFP (α-YFP), AOD (α-AOD) and DAS (α-DAS) protein levels in strains M1 (control), T1, T3 and M2. Actin was blotted as a loading control (α-Actin). Cells were shifted from glucose medium (SD) to 0.5% methanol medium (SM) for 20 h and collected at the indicated time points. The samples were loaded on 7.5% acrylamide SDS-PAGE gel (SuperSep Ace). Molecular weights of the protein size marker are indicated.

2.4 Subcellular localization of CbMpp1 was not influenced in strains T1, T3 and M2

It has been reported that CbMpp1 localizes to the nucleus under methanol culture condition (Zhai, 2012). Subcellular localization of CbMpp1-YFP in strains M1, T1, T3 and M2 was observed by fluorescent microscopy. CbMpp1-YFP was not observed in strain M1 on glucose medium, while it was localized to the nucleus during methanol culture (Figure 2-5). CbMpp1-YFP in strains T1, T3 and M2 localized to the nucleus regardless of the carbon sources (Figure 2-5). As also shown in Figure 2-4, CbMpp1-YFP protein level was not kept properly under methanol culture condition. These results suggest that CbMpp1-YFP localizes to the nucleus regardless of the carbon sources and it was not affected by the expression timing and level.
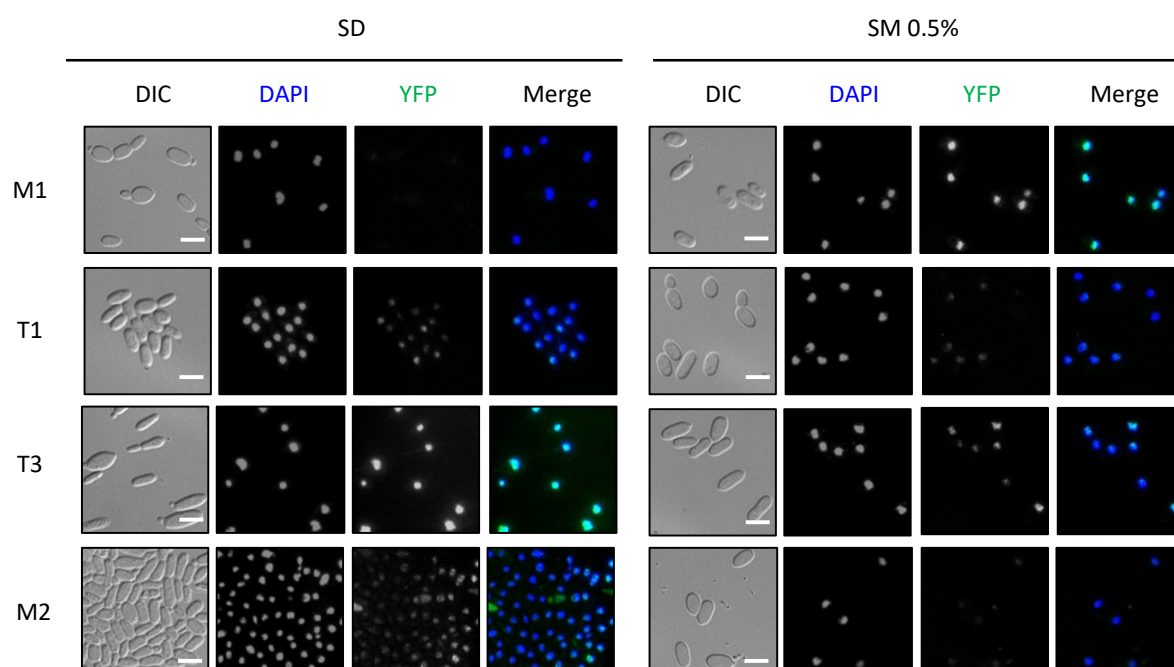
Figure 2-5. Localization of CbMpp1-YFP in strains M1, T1, T3 and M2.

Fluorescence microscopy of CbMpp1-YFP in strains M1 (control), T1, T3 and M2. Cells were shifted from SD to SM medium containing 0.5% methanol at 28℃ for 5h. Subsequently, they were treated with 70% ethanol for 30 min and stained with 50 μg/L DAPI for 20 min. DAPI was used to stain the cell nucleus. DIC, differential interference contrast. The scale bars correspond to 5.0 μm.

2.5 Identification of UASs in the *CbMPP1* promoter by promoter deletion analysis

To identify the DNA regions for P_{MPP1} activation (upstream activating sequences; UASs) during methanol induction, the truncated P_{MPP1} activity was measured by acid phosphatase assay (APase assay) using the reporter gene *ScPHO5*. I planned four types of P_{MPP1} truncation in this experiment: (i) deletion from 3' to 5' (ii) deletion from 5' to 3' (iii) partial deletion of putative UAS for confirmation of the necessity (iv) addition of putative UAS to P_{ACT1} for confirmation of the sufficiency (Figure 2-6A). The assay was performed using the strains TK62 (wild-type) and *Cbtrm2Δ* as hosts to investigate whether the function of UAS is dependent on CbTrm2 or not. According to the previous study (Zhai, 2012), it has been found that the *CbMPP1* promoter activity is entirely lost in *Cbtrm1Δ* and *Cbhap3Δ* strains but remained in *Cbtrm2Δ* strain about 25% of wild-type strain. Therefore, *Cbtrm2Δ* strain can be used for *CbMPP1* promoter deletion analysis to evaluate the decrease of APase activity. Single copy insertion of each plasmid in all the strains for acid phosphatase assay was confirmed by southern-blot analysis (Figures 2-6B and 2-6C).
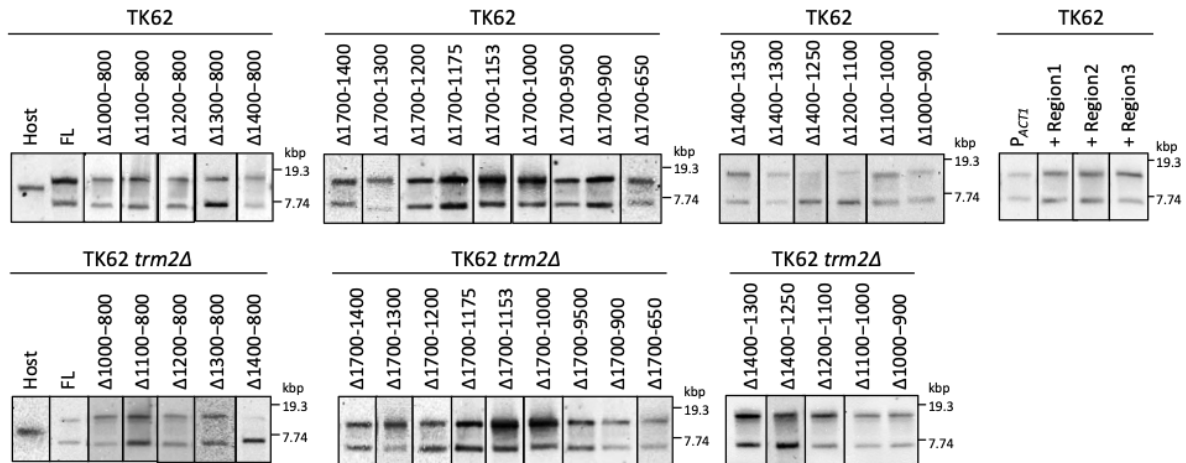
A

-1700 P_{MPP1} ScPHO5   -1   Control
[5']   [3']

(i) Deletion from 3' to 5'   -800

(ii) Deletion from 5' to 3'

(iii) Partial deletion of UAS   UAS

(iv) Addition of UAS to P_{ACT1} P_{MPP1}-UAS P_{ACT1}

B

Host strain
HindIII   ura3   HindIII
kbp
19.3
7.74
... Genomic DNA of *C. boidinii*
Probe
9.33 kbp

Single-copy strain
HindIII   ura3 P_{MPP1} ScPHO5   HindIII   URA3   HindIII
kbp
19.3
7.74
10.7 kbp   7.15 kbp

Multi-copy strain
HindIII   ura3 P_{MPP1} ScPHO5   HindIII   URA3 P_{MPP1} ScPHO5   HindIII   URA3   HindIII
kbp
19.3
7.74
10.7 kbp   8.56 kbp   7.15 kbp

Figure 2-6. Scheme and preparation of acid phosphatase assay for truncated *CbMPP1* promoter activity measurement.

(A) Four ways of *CbMPP1* promoter (P$_{MPP1}$) truncation: (i) deletion from 3' to 5' (ii) deletion from 5' to 3' (iii) partially deletion of putative UAS for confirmation of the necessity (iv) addition of putative UAS to P$_{ACT1}$ for confirmation of the sufficiency. In (ii) method, the promoter deletion was started from -800 bp because the DNA region from -1 to -800 is thought to be necessary for the interaction with general transcription factor and RNA polymerase. Based on the results of (i) and (ii), the putative UAS was deleted in (iii), or added to P$_{ACT1}$ (iv). (B) The diagram shows the structure of *URA3* locus in genomic DNA of *C. boidinii* host strain (TK62), single-copy inserted strain and multi-copy inserted strains for southern-blot analysis. The theoretical fragment size from genomic DNA by HindIII digestion was indicated. The labelled DNA probe was designed in *URA3* region and prepared for southern-blot analysis. The plasmid pMPU1 was introduced in TK62 or TK62 *Cbtrm2Δ* strain, resulting in single-copy inserted or muti-copy inserted strain. A single band signal was detected from the host strain as a result of southern blot. Two band signals were detected from single-copy strain, and three band signals from multi-copy strain. (C) Southern-blot analysis of the strains used in the acid phosphatase assay for confirming single-copy insertion of the plasmid. Cells were cultured in YPD media for 24 h and genomic DNA was extracted.

Based on approach (i), APase assay of P$_{MPP1}$ truncated from 3' to 5' was performed in wild-type and *Cbtrm2Δ* strains (Figure 2-7A). From the results of deletion analyses in wild-type strains, the APase activity was decreased between PHO-FL and PHOΔ1000-800, PHOΔ1100-800 and PHOΔ1200-800, PHOΔ1200-800 and PHOΔ1300-800. These results imply that the regions from -1000 to -800, from -1200 to -1100 and from -1300 to -1200 are crucial for *CbMPP1* promoter activity. Moreover, the APase activities in *Cbtrm2Δ* strains were decreased between PHO-FL and PHOΔ1000-800, PHOΔ1200-800 and PHOΔ1300-800, which suggests that the function of the promoter regions from -1000 to -800 and from -1300 to -1200 were independent on CbTrm2 while that from -1200 to -1100 was dependent on CbTrm2.

In the same way, the results of the strains harboring partial *CbMPP1* promoter deleted from 5' to 3' {approach (ii)} indicated that the region from -1400 to -1300 (independent on CbTrm2), from -1175 to -1153 (dependent on CbTrm2) and from -950 to -900 (independent on CbTrm2) were important for P$_{MPP1}$ activity (Figure 2-7B).
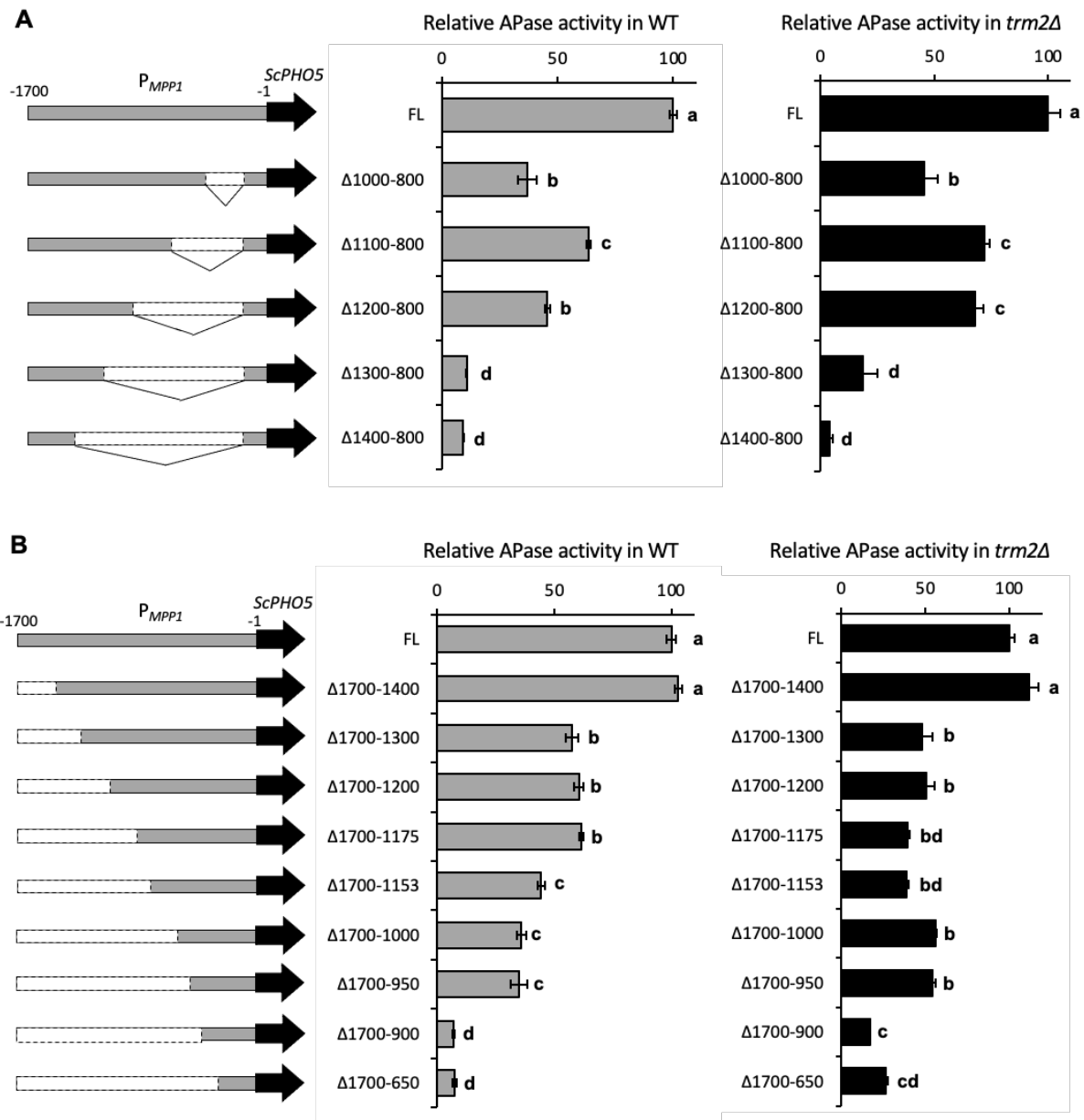
Figure 2-7. APase assay of 3' to 5' and 5' to 3'truncated *CbMPP1* promoter.

The activity of truncated *CbMPP1* promoter (P*MPP1*) deleted from 3' to 5' (A) and from 5' to 3' (B) in wild-type strain (grey bars) and *Cbtrm2Δ* strain (black bars). Cells were pre-cultured in SD media and shifted to SM media (0.7% methanol) at 28°C for 8h. Relative activity levels compared to that in control strain possessing full-length (FL) of *CbMPP1* promoter are indicated. Error bars represent standard error values from three independent experiments. The groups indicated with different symbol means significant difference (e.g., between **a** and **b**, $p < 0.05$) by the statistical analysis (One-way ANOVA).

Judging from the results of APase analysis with approaches (i) and (ii), partial deletion of putative UAS regions was performed for confirmation of its necessity in *CbMPP1* promoter. The APase activity was decreased between PHO-FL and PHOΔ1400-1300, PHOΔ1400-1250 and PHOΔ1000-900 in wild-type strain (Figure 2-8 left panel). This result suggests that the DNA region from -1350 to -1250 and -1000 to -900 are important to *CbMPP1* activity. Moreover, the activity of *CbMPP1* promoters lacking these regions was also decreased in *Cbtrm2Δ* strain compared to that of FL promoter, which indicates that these promoter regions are independent on CbTrm2 (Figure 2-8 right panel).
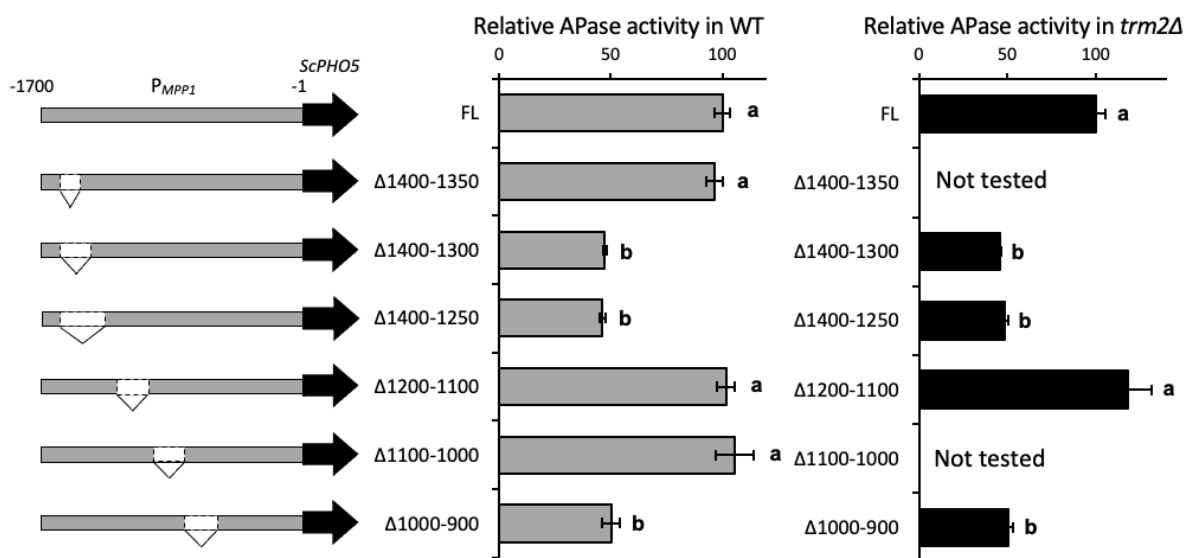
Figure 2-8. APase assay of partially truncated *CbMPP1* promoter.

The activity of partially truncated *CbMPP1* promoter in wild-type strain (grey bars) and *Cbtrm2Δ* strain (black bars). Cells were pre-cultured in SD media and shifted to SM media (0.7% methanol) at 28°C for 8h. Relative activity levels compared to that in control strain possessing full-length (FL) of *CbMPP1* promoter are indicated. Error bars represent standard error values from three independent experiments. The groups indicated with different symbol means significant difference (e.g., between **a** and **b**, $p < 0.05$) by the statistical analysis (One-way ANOVA).

The *CbMPP1* promoter regions from -1350 to -1250, from -1200 to -1100 and from -1000 to -900 were defined as putative UAS region1, retion2 and region3, respectively. To investigate their sufficiency for its promoter activity, region1, region2 and region3 were fused to P_{ACT1}. The APase activities of $P_{(CbMPP1\text{-}Region1)}$-$P_{ACT1}$ and $P_{(CbMPP1\text{-}Region3)}$-$P_{ACT1}$ were significantly increased by methanol culture (Figure 2-9). On the other hand, the activity of $P_{(CbMPP1\text{-}Region2)}$-$P_{ACT1}$ was not significantly increased (Figure 2-9). These results indicate that region1 and region3 were sufficient as UASs (UAS1 and UAS2, respectively) for *CbMPP1* promoter activity.
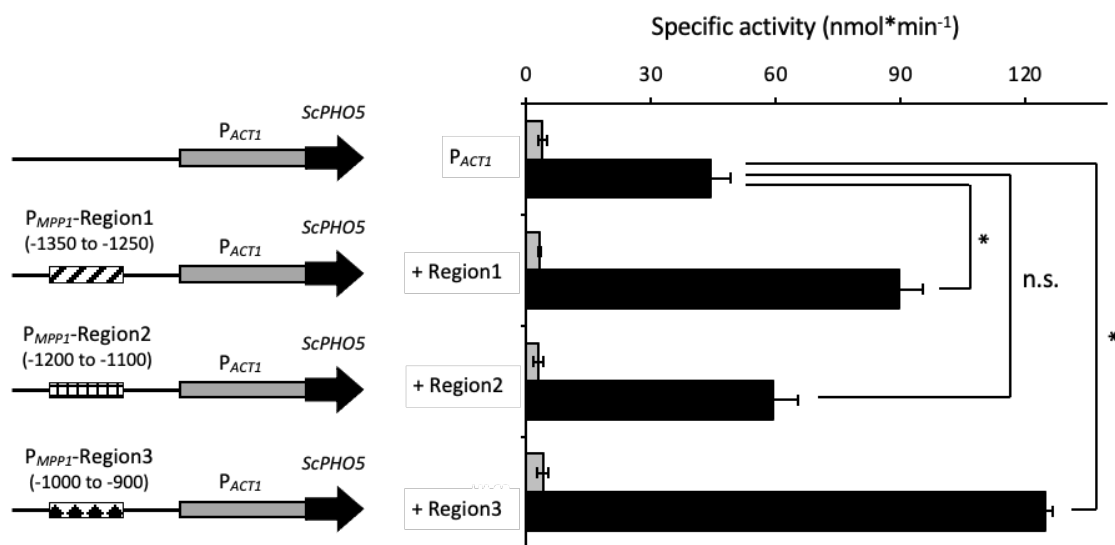
Figure 2-9. APase assay for promoter activity measurement of P_{ACT1} connected with partial P_{MPP1}.

Acid phosphatase (APase) assay of *ACT1* promoter (P_{ACT1}) attached with putative regions of upstream activating sequence in P_{MPP1}. Cells were pre-cultured in SD media, and then shifted to SD media (2% glucose, grey bars) or SM media (0.7% methanol, black bars) at 28°C for 8h. Error bars represent standard error values from three independent experiments. *: $p < 0.05$, n.s.: not significant. Region 1, Region2 and Region3 means the *CbMPP1* promoter region from -1350 to -1250, from -1200 to -1100 and from -1000 to -900, respectively.

Discussion

In this study, I focused on the regulation of *CbMPP1* and the physiological significance of its methanol-inducibility under methanol-culture conditions. The results of constitutive or excessive expression of *CbMPP1* revealed that lower or higher protein level of CbMpp1 in the cells leads to the growth delay in methanol medium (Figure 2-2) probably because of insufficient methanol consumption or abnormal formaldehyde accumulation. CRMI of *CbMPP1* gene and CbMpp1 protein level was not appropriately kept in *CbMPP1*-constitutive or excessive expression strains (Figures 2-3 and 2-4). CbMpp1-YFP localized to the nucleus regardless of the carbon sources and it was not influenced by the expression timing and level of *CbMPP1* (Figure 2-5).

CbMpp1 plays an important role in the regulation of expression levels of multiple methanol-inducible genes (Figure 2-10). The expression of *CbMPP1* (a homolog of *KpMIT1*) is induced under the control of CRMI by transcription factors CbTrm2 (a homolog of *KpMXR1*), CbTrm1 and CbHap complex. It is considered that the protein level of CbMpp1 is controlled depending on methanol concentration and this regulation contributes to CRMI of methanol-induced gene expression. The balance of metabolic flux (generation and consumption of formaldehyde) during growth on methanol requires a proper amount of the enzymes, such as AOD, DAS and FLD, which is dependent on *CbMPP1* expression level (Figures 0A and 2-10).

The development of peroxisomes in strains M1, T1, T3 and M2 needs to be elucidated. The relationship between peroxisomal biosynthesis and transcription factors for methanol metabolism has been studied (Lin-Cereghino *et al.*, 2006; Wang *et al.*, 2016b). The decreased transcript levels of methanol-induced genes resulted in abnormal or small peroxisomes produced in the cells lacking peroxisomal matrix proteins such as AOD, DAS and FLD (Sasano *et al.*, 2008).

From P*MPP1* deletion analysis, the P*MPP1* region from -1350 to -1250 and from -1000 to -900 were identified as UAS1 and UAS2 (Figures 2-8, 2-9 and 2-10). These UASs were independent on CbTrm2, implying that some transcription factors except CbMpp1 interact with UAS1 or UAS2. The direct interaction of UASs with transcription factors should be investigated in the future. In addition, the activity of P*MPP1* is remarkably decreased in *Cbtrm2Δ* strain (Zhai, 2012), so there is a possibility that *CbMPP1* promoter has other UAS which is dependent on CbTrm2. The promoter activity of PHOΔ1700-1000 strain was lower than that of PHOΔ1700-1200 strain (Figure 2-7B left panel), while there is no significant difference in the promoter activity between PHOΔ2Δ1700-1200 and PHOΔ2Δ1700-1000 (Figure 2-7B right panel). Therefore, the promoter region from -1200 to -1000 may be a UAS dependent on CbTrm2. Moreover, the cooperative effects of UASs need to be verified because the activity of partially deleted promoters in PHOΔ1400-1250 and PHOΔ1000-900 strains did not entirely lose.
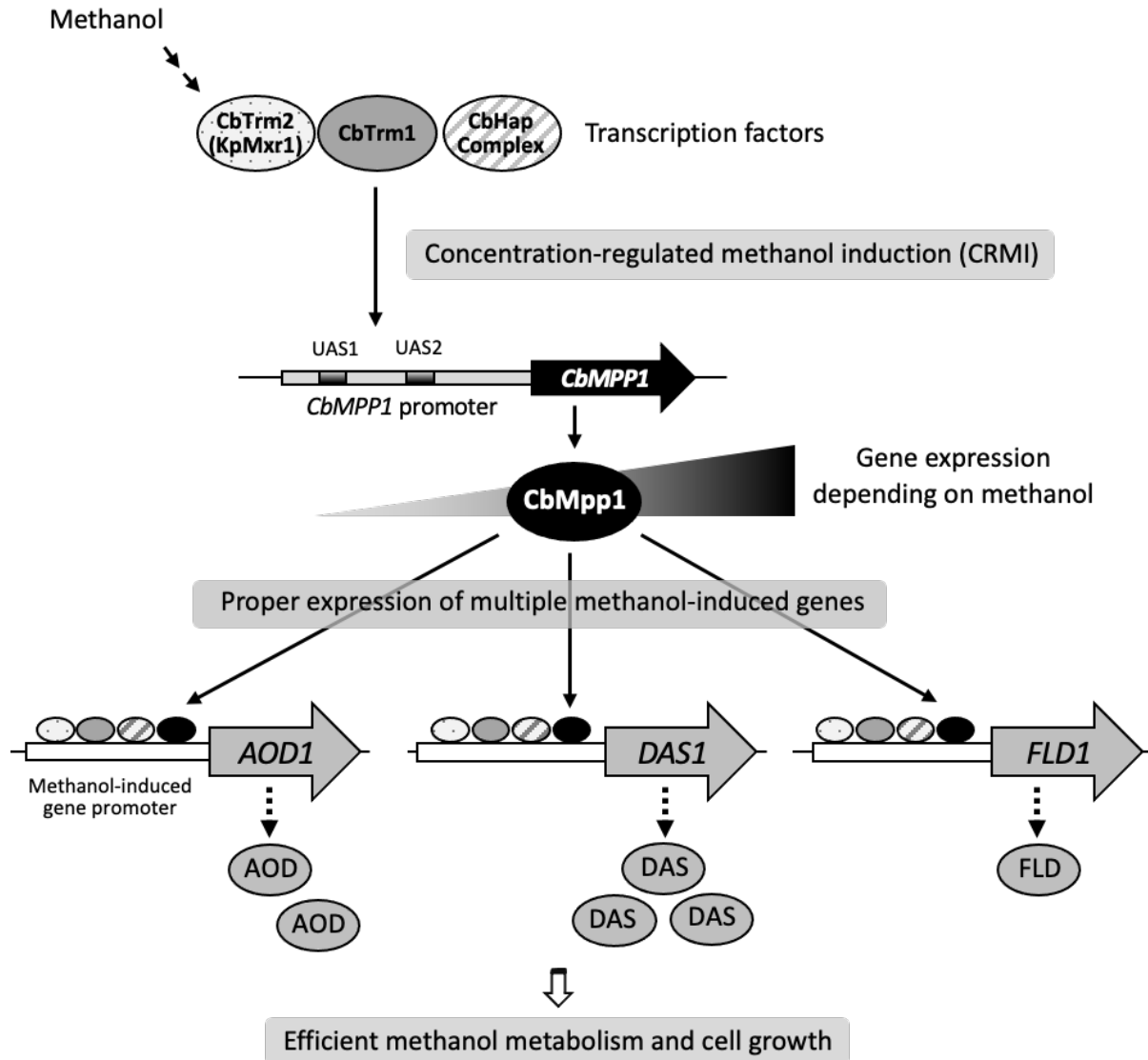
Figure 2-10. Regulation model of *CbMPP1* expression and its role in proper expression of multiple methanol-induced genes.

When the cells are shifted from glucose to methanol media, the expression of *CbMPP1* (a homolog of *KpMIT1*) is induced under the control of CRMI by transcription factors CbTrm2 (a homolog of *KpMXR1*), CbTrm1 and CbHap complex. The protein level of CbMpp1 is under the control of CRMI and this regulation contributes to proper expression of multiple methanol-induced genes (*AOD1, DAS1, FLD1, etc.*), efficient methanol metabolism and cell growth. CRMI of *CbMPP1* is maintained by the transcription factors via the interaction with UAS1 (region1) and UAS2 (region3) of *CbMPP1* promoter.

Chapter III

Methanol represses pexophagy through MAP kinase cascade and its downstream phosphatases in *Komagataella phaffii*

Introduction

Although the molecular mechanism and machinery of autophagy in the methylotrophic yeasts have been well understood, physiological roles of methanol-induced peroxisomal degradation (pexophagy) in yeasts and fungi have been less studied except for plant pathogenicity (Asakura *et al.*, 2009; Oku *et al.*, 2014; Oku *et al.*, 2016). It has been previously reported in this laboratory that the methylotrophic yeasts *C. boidinii* and *K. phaffii* proliferated slowly on plant leaves, undergoing 3 to 4 cell divisions in 7-10 days by adapting to the methanol concentration in the environment (Kawaguchi *et al.*, 2011). Not only induction of peroxisomes and methanol-utilizing enzymes but also Atg30-dependent pexophagy were necessary for methylotrophic yeast cells to proliferate on plant leaves indicating the essentiality of peroxisome homeostasis and its regulation for cellular survival on plant leaves. In *K. phaffii*, phosphorylation of KpAtg30 by the kinase KpHrr25 is required for the interaction with KpAtg11 and it serves as a cue for pexophagy induction (Zientara-Rytter *et al.*, 2018).

As described in chapter I, it has also been reported that the cell-surface protein KpWsc1, a homolog of ScWsc1 in *S. cerevisiae,* was responsible for sensing the concentration of environmental methanol and regulation of methanol-inducible gene expression, i.e., peroxisome synthesis and methanol-metabolizing enzymes, in *K. phaffii* (Ohsawa *et al.*, 2017). ScWsc1 is a GPI-anchored plasma membrane protein sensing the perturbation of cell wall integrity (CWI) (Dupres *et al.*, 2009; Lodder *et al.*, 1999) that initiates a phosphorylation cascade (MAPK cascade) leading to the activation of a mitogen-activated kinase ScMpk1 (MAPK) to activate cell wall-related gene expressions, such as those related to glucan synthesis (Irie *et al.*, 1993; Lee *et al.*, 1993; Levin, 2011; Rodicio *et al.*, 2010). The previous study with *K. phaffii* showed that knock-out of *KpWSC1* led to unbalanced methanol metabolism, resulting in formaldehyde accumulation and retardation of cell growth (Ohsawa *et al.*, 2017). Moreover, it has been demonstrated that *Kpwsc1Δ* strain exhibited an earlier onset of pexophagy (Ohsawa, 2017). KpWsc1 and its downstream factor KpRom2 were involved not only in the high-temperature stress response in *K. phaffii* which was similar to the CWI pathway in *S. cerevisiae* (Philip *et al.*, 2001) but also in methanol-induced gene expression (Ohsawa *et al.*, 2017). ScMpk1 relays the CWI signaling cascade by phosphorylation of the transcription factors ScRlm1, ScSwi4, and ScSwi6, which were required for gene expression involved in cell wall synthesis (Levin, 2011; Watanabe *et al.*, 1995). The phosphatases ScMsg5 and

ScPtp2 are transcriptionally induced in several conditions that activate the CWI pathway (García *et al.*, 2004; Hahn *et al.*, 2002; Marín *et al.*, 2009; Mattison *et al.*, 1999) in an ScSlt2-dependent manner and have a function as a negative-feedback loop toward ScSlt2 (García *et al.*, 2016). It is estimated that *K. phaffii* has a similar signaling pathway based on the CWI pathway in *S. cerevisiae*, but the detailed molecular mechanism of methanol signal transduction for pexophagy regulation needs to be elucidated.

In this chapter, I examined how the environmental methanol concentration affects and regulates pexophagy. In addition, I explored the downstream phosphatases of KpRlm1 involving in phosphoregulation of KpAtg30 and pexophagy regulation. The results indicate that the presence of methanol, which was sensed by KpWsc1, activates its downstream MAPK and suppresses pexophagy. Cellular sensing of methanol concentrations has been shown to play a critical role in maintaining organellar homeostasis during methanol culture.

Materials & Methods

Strains, media and culture conditions

The yeast strains used in this study are listed in Table 3-1. *K. phaffii* cells were grown at 28°C on YPD (1% yeast extract, 2% peptone, 2% glucose) or YNB medium (0.67% yeast nitrogen base without amino acids, pH 6.0). 2% (w/v) glucose (synthetic dextrose medium; SD medium) or several concentrations of methanol (SM medium) were used as carbon sources in YNB medium. SD medium without amino acids and ammonium sulfate was used for induction of nitrogen starvation. All the components other than the carbon sources used in these media were purchased from Difco Becton Dickinson (Franklin Lakes, NJ). The growth of the yeast was monitored by the optical density (OD) at 610 nm. For the culture with Beppu flasks, 15 mL of SM medium (0.5% methanol) was poured into each compartment which was separated by 0.22 μm PVDF membrane (Dupapore φ47 mm, Merck KGaA, Darmstadt, Germany).

    K. phaffii strain GS115 or PPY12 was used as the host of transformants. Gene disruption was performed by homologous recombination with the Blasticidin-S resistance gene (Bsd^R) or Zeocin resistance gene (Zeo^R) as a selective marker. The transformation protocol of *K. phaffii* was based on the improved lithium acetate method (Cregg *et al.*, 1985; Wu *et al.*, 2004).

    E. coli HST08 Premium (Takara Bio, Otsu, Japan) was used as a host strain for plasmid DNA preparation. *E. coli* cells were grown in LB medium (1% tryptone, 0.5% yeast extract, 0.5% NaCl) at 37°C.

Table 3-1. *K. phaffii* strains used in this study.

Designation	Genotype	Reference
PPY12	*arg4, his4*	Sakai *et al.* (1998)
GS115	*his4*	Cregg *et al.* (1985)
PPY-PEX11	PPY12, *arg4::(P$_{KpPEX11}$-KpPEX11-YFP, ARG4), his4::HIS4*	Ohsawa *et al.* (2021)
Kpwsc1Δ	PPY-PEX11, *Kpwsc1Δ*::Zeo^R	Ohsawa *et al.* (2017)
Kpwsc1ΔKpatg30Δ	PPY-PEX11, *Kpwsc1Δ*::Zeo^R, *Kpatg30Δ*::Bsd^R	This study
Kprlm1Δ	PPY-PEX11, *Kprlm1Δ*::Zeo^R	Ohsawa *et al.* (2021)
PPY-ATG30	PPY12, *Kpatg11Δ*::Bsd^R, *his4::(P$_{KpATG30}$-KpATG30-HA, HIS4)*	Ohsawa *et al.* (2021)
Kpmsg5Δ	PPY-ATG30, *Kpmsg5Δ*::Zeo^R *arg4::ARG4*	Ohsawa *et al.* (2021)
Kpptp2AΔ	PPY-ATG30, *Kpptp2AΔ*::Zeo^R,*arg4::ARG4*	Ohsawa *et al.* (2021)
Kpmsg5ΔKpptp2AΔ	PPY-ATG30, *Kpptp2AΔ*::Zeo^R, *arg4::(Kpmsg5Δ, ARG4)*	Ohsawa *et al.* (2021)

Table 3-2. Plasmids used in this study.

Designation	Description	Reference
pIB1	*KpHIS4*	Sears *et al.* (1998)
pNT204	*KpARG4*	Tamura *et al.* (2010)
pOH100	*Kpwsc1Δ*::Zeo^R	Ohsawa *et al.* (2017)
pOH104	*Kpatg30Δ*::Bsd^R	Ohsawa *et al.* (2021)
pOH103	*Kprlm1Δ*::Zeo^R	Ohsawa *et al.* (2021)
pIS100	*Kpatg11Δ*::Bsd^R	Ohsawa *et al.* (2021)
pOH107	*Kpmsg5Δ*:: Zeo^R	Ohsawa *et al.* (2021)
pOH108	*Kpptp2AΔ*::Zeo^R	Ohsawa *et al.* (2021)
pOH109	*Kpmsg5Δ*::*ScARG4*	Ohsawa *et al.* (2021)
pSY302	P$_{KpPEX11}$-*KpPEX11*-EYFP, *ARG4*	Ohsawa *et al.* (2021)
pRN001	P$_{KpATG30}$-*KpAtg30*-3xHA, pIB1	Ohsawa *et al.* (2021)

Plasmid construction

The plasmids used in this study are shown in Table 3-2.

Immunoblot analysis

Yeast cells were grown in YPD and SD as described above, and the cells were shifted to SM medium at 28°C for 30 min to 2 h. The cells equivalent to about 2 OD$_{610}$ units (for immunoblot analysis) were cultured and collected for protein extraction. Protein samples were prepared and the experiment was performed as described in chapter I. 10 µL of the supernatant was electrophoresed on a 10% or 12% SDS-PAGE gel. The membranes were incubated in Blocking One (Nakalai tesque, Kyoto, Japan) and then in anti-YFP antibody (Living Colors A.v. Monoclonal Antibody JL-8, Takara Bio, Otsu, Japan), anti-HA (mouse monoclonal HA.C5, Abcam, Cambridge, UK) or anti-beta actin (mouse monoclonal ab8224, Abcam, Cambridge, UK) at dilutions recommended in the protocol with TBS-T buffer. The membranes were washed 3 times with TBS-T buffer and incubated with anti-mouse-HRP (Merck Millipore, Darmstadt, Germany) at a 1:5,000 dilution for 1 h.

GC-MS analysis for methanol quantification

Aliquots of the culture medium were subjected to gas chromatography (GC) analysis. After removing yeast cells by centrifugation, 2 µL of the culture medium was injected into a Porapak Q (Agilent Technologies, Santa Clara, CA, USA) column. The injector temperature was 180°C. The detection temperature was held at 180°C for 4 min.

RNA isolation and quantitative reverse transcription-PCR (qRT-PCR)

A single colony was inoculated in YPD medium and grown overnight at 28°C. Yeast cells were transferred into SD medium and cultivated to early exponential phase. Then, the cells were shifted to SM medium. Cells equivalent to 5 OD_{610} units were harvested at the indicated time points by centrifugation at 10,000 g for 1 min at 4°C. Total RNA was extracted from the cells as described in chapter I. Primers for *KpMSG5, KpPTP2A, KpPTP2B, AOX1, DAS1,* and *GAP* are shown in Table 3-3. Transcript levels of all genes were normalized using *GAP* as a control.

Statistical analysis

All data were obtained from three independent biological replicates and presented as mean ± S.E. Student's t-test was performed to determine the differences among grouped data. Statistical significance was assessed at $p < 0.05$.

Table 3-3. Oligonucleotide primers used in this study.

Designation	DNA Sequence
RT-MSG5-Fw	5'-ACCGATCCCGGAATACCAAG-3'
RT-MSG5-Rv	5'-TCCAGTTCTGTGGCGGACTT-3'
RT-PTP2A-Fw	5'-TGGCTTCTCCTGGATGTGGT-3'
RT-PTP2A-Rv	5'-GGTCTTTGGCACTTGCTGCT-3'
RT-PTP2B-Fw	5'-GCAAACTTCGGATGGCAAAG-3'
RT-PTP2B-Rv	5'-AGGGACGATCAACCAGCGTA-3'
RT-AOX1-Fw	5'-TTTCGAAGGTCCAATCAAGG-3'
RT-AOX1-Rv	5'-GTTCAGCACCGTGAGCAGTA-3'
RT-DAS1-Fw	5'-GGTGACGAGTTAGTAAAGAAC-3'
RT-DAS1-Rv	5'-CCTCTAACACGAGAAAGGAAC-3'
RT-GAP-Fw	5'-CCACCGGTGTTTTCACCACT-3'
RT-GAP-Rv	5'-CACCGACAACGAACATTGGA-3'

Results

3.1 Pexophagy during the growth on methanol is negatively regulated by KpWsc1 and KpRlm1 in *K. phaffii*

To compare pexophagy between two different strains of *K. phaffii* in response to the methanol concentration, I used *Beppu* flasks in which the two compartments of the flask are separated by a membrane that allows media components, including methanol, to pass through and be maintained at the same level, but does not allow yeast cells to mix (Fig. 3-1A). The cell growth on methanol in *Kpwsc1Δ* strain exhibited a decreased growth yield compared to wild-type strain (Fig. 3-1B). *Kprlm1Δ* strain also showed a slight growth delay during methanol culture (Fig. 3-1B). Owing to the effect of a *Beppu* flask, methanol concentration in the media was kept at the same level during the culture in each strain (Fig. 3-1C). From these results, it is confirmed that CWI-like pathway in *K. phaffii* including KpWsc1 and KpRlm1 are important to the growth on methanol media.

Then, I investigated the pexophagy of *Kpwsc1Δ* and *Kprlm1Δ* strains. Pexophagy was monitored by cleavage of the YFP-fused peroxisomal membrane protein KpPex11 (KpPex11-YFP), yielding a YFP fragment resistant to vacuolar proteases. In *Kpwsc1Δ* strain, higher ratios of the cleaved YFP band to the full-length Pex11-YFP were observed as early as 12 h of cultivation (Fig. 3-1D upper panel) when more than 0.25% methanol was still present in the medium (Fig. 3-1C left panel). In other words, the *Kpwsc1Δ* strain showed an earlier onset of pexophagy than the wild-type strain despite remaining methanol. I also found that cleavage of YFP from Pex11-YFP at 12 h was slightly enhanced in *Kprlm1Δ* strain (Fig. 3-1D lower panel) when methanol remained in the media (Fig. 3-1C right panel). These results suggested that KpWsc1 and KpRlm1 involve in suppressing the degradation of methanol-induced peroxisomes in the presence of more than 0.15% methanol.
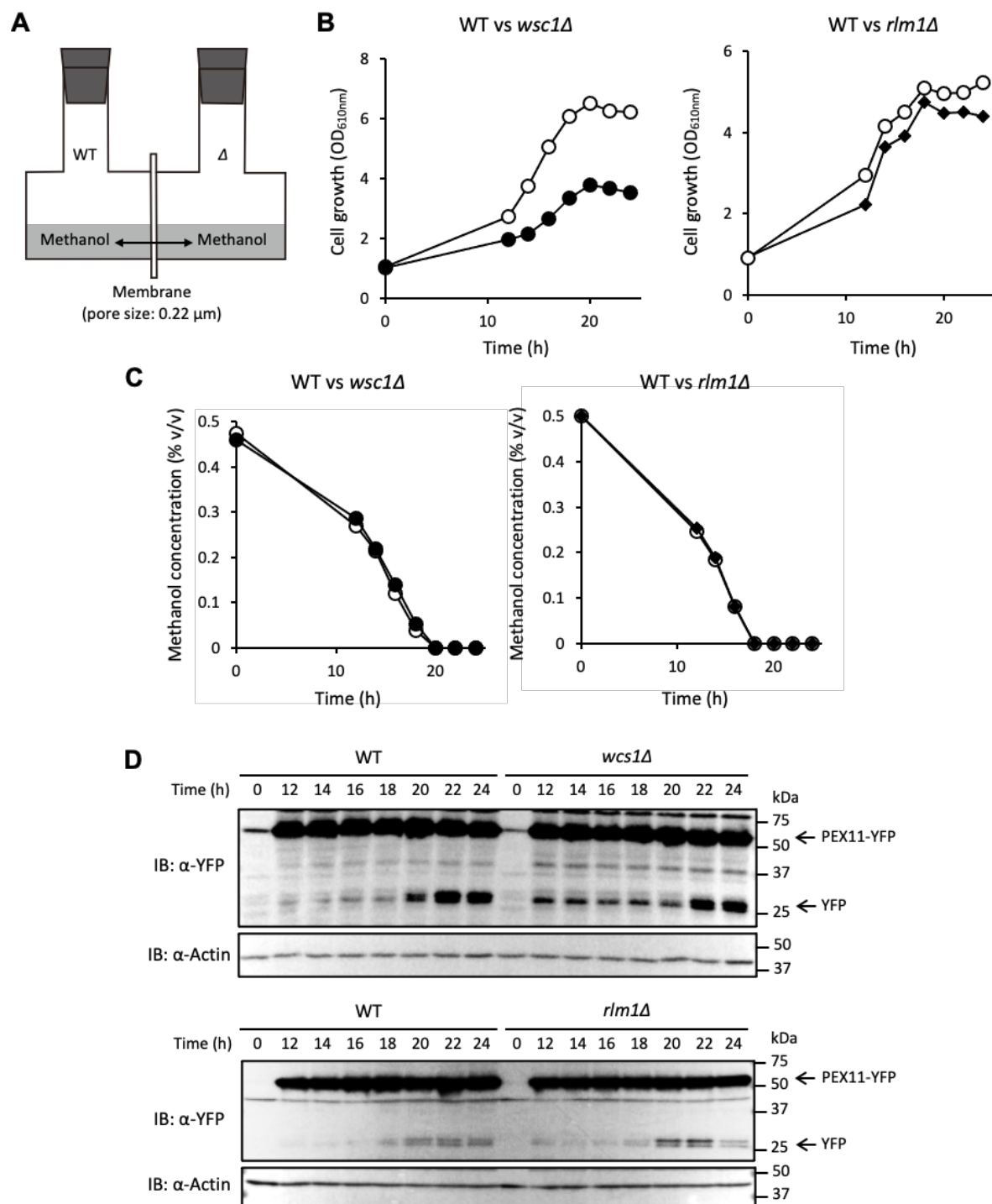
Figure 3-1. Cell growth, methanol consumption and pexophagy in *Kpwsc1Δ* and *Kprlm1Δ* strains during methanol culture using Beppu flasks.

(A) Illustration of a Beppu flasks separated by 0.22 μm PVDF membrane. (B) Cell growth (OD$_{610\,nm}$) of *Kpwsc1Δ* strain (closed circles) and *Kprlm1Δ* strain (closed diamonds) comparing with wild-type strain (WT, open circles) in two chambers of the Beppu flasks. Cells were cultured in YNB-glucose media and shifted to YNB-methanol (0.5%) media at 28℃. (C) Methanol consumption kinetics of wild-type (open circles), *Kpwsc1Δ* (closed circles) and *Kprlm1Δ* (closed diamonds) strains. The supernatant of methanol-cultured media was harvested at the same time point of cell growth analysis and its methanol concentration was measured by GC-MS. (D) Immunoblot analysis of KpPex11-YFP (α-YFP) expressed in *Kpwsc1Δ* and *Kprlm1Δ* strains comparing with that in wild-type (WT) strain. Anti-β-actin antibody was used for detection of actin as a loading control (α-Actin). Cells of these strains were harvested at the same time point of cell growth analysis (B) and used for immuno-blot assay. Molecular weights of the protein size marker were indicated.

3.2 Identification of a putative phosphatase suppressing phosphorylation of KpAtg30

In *S. cerevisiae*, ScMpk1 relays the CWI signaling cascade by phosphorylation of the transcription factors ScRlm1, ScSwi4, and ScSwi6, which were required for gene expression involved in cell wall synthesis (Levin, 2011; Watanabe *et al.*, 1995). The previous study has demonstrated that KpMpk1 suppresses phosphorylation of KpAtg30 via the transcriptional control under KpRlm1, but not KpSwi4 (Ohsawa, 2017).

Based on the reports about the CWI pathway in *S. cerevisiae* (Sanz *et al.*, 2018), I explored phosphatases for phosphoregulation of KpAtg30 under the control of KpRlm1. *KpMSG5* (a paralogue of *ScMSG5*, XM_002492799.1), *KpPTP2A* (a paralogue of *ScPTP2*, PAS_chr2-1_0203, XP_ 002491091.1) and *KpPTP2B* (a paralogue of *ScPTP2*, PAS_chr1-3_0061, XM_002489352.1) were identified by Protein BLAST. The transcript level of *KpMSG5* and *KpPTP2A* was increased by the treatment of Congo Red which induces a cell surface stress, while that of *KpPTP2B* was not influenced (Figure 3-2A). Therefore, it was estimated that KpMsg5 and KpPtp2A lie on the downstream of the CWI-like signaling pathway about cell surface stress including KpWsc1. The transcript level of *KpMSG5* and *KpPTP2A* decreased in *Kprlm1Δ* strain, but that of *AOX1* and *DAS1* did not change in *Kprlm1Δ* strain during methanol culture (Figure 3-2B). These results suggest that KpRlm1 regulates the expression of *KpMSG5* and *KpPTP2A* but did not affect the expression of methanol-induced genes.

Next, I investigated whether these phosphatases were involved in the suppression of KpAtg30 phosphorylation by immunoblot analysis. In the following experiments, I used the *Kpatg11Δ* strain as the background strain to prevent the degradation of KpAtg30-3xHA and detect clear phosphorylated bands of KpAtg30-3xHA. The *Kpatg11Δ, Kpatg11ΔKpmsg5Δ, Kpatg11ΔKpptp2AΔ, Kpatg11ΔKpmsg5Δ Kpptp2AΔ* strains were compared in their cell growth, methanol consumption and phosphorylation levels. There is no significant difference in cell growth and methanol consumption among *Kpatg11Δ, Kpatg11ΔKpmsg5Δ* and *Kpatg11ΔKpptp2AΔ* strains (Figures 3-2C and 3-2D). *Kpatg11ΔKpmsg5Δ Kpptp2AΔ* strain showed a slight delay of growth and methanol consumption (Figures 3-2C and 3-2D).

In the periodically sampled lysate of the *Kpatg11Δ* strain, the phosphorylation level of KpAtg30-3xHA was found to increase gradually with cultivation time, giving multiple bands of less mobility than the non-phosphorylated form (Figure 3-2E). In *Kpatg11ΔKpmsg5Δ* and *Kpatg11ΔKpptp2AΔ* strain, phosphorylation of KpAtg30-3xHA was enhanced after 17 h culture on methanol where methanol was still present in the medium (Figure 3-2D). In addition, *Kpatg11ΔKpmsg5ΔKpptp2aΔ* strain exhibited higher phosphorylation levels than that observed in other strains (Figure 3-2E), although methanol remained in higher concentration with this triple disruption strain than other strains (Figure 3-2D). This result indicated that KpPtp2A and KpMsg5 phosphatases function the downstream of KpRlm1 and suppress KpAtg30 phosphorylation during methanol culture in *K. phaffii*.
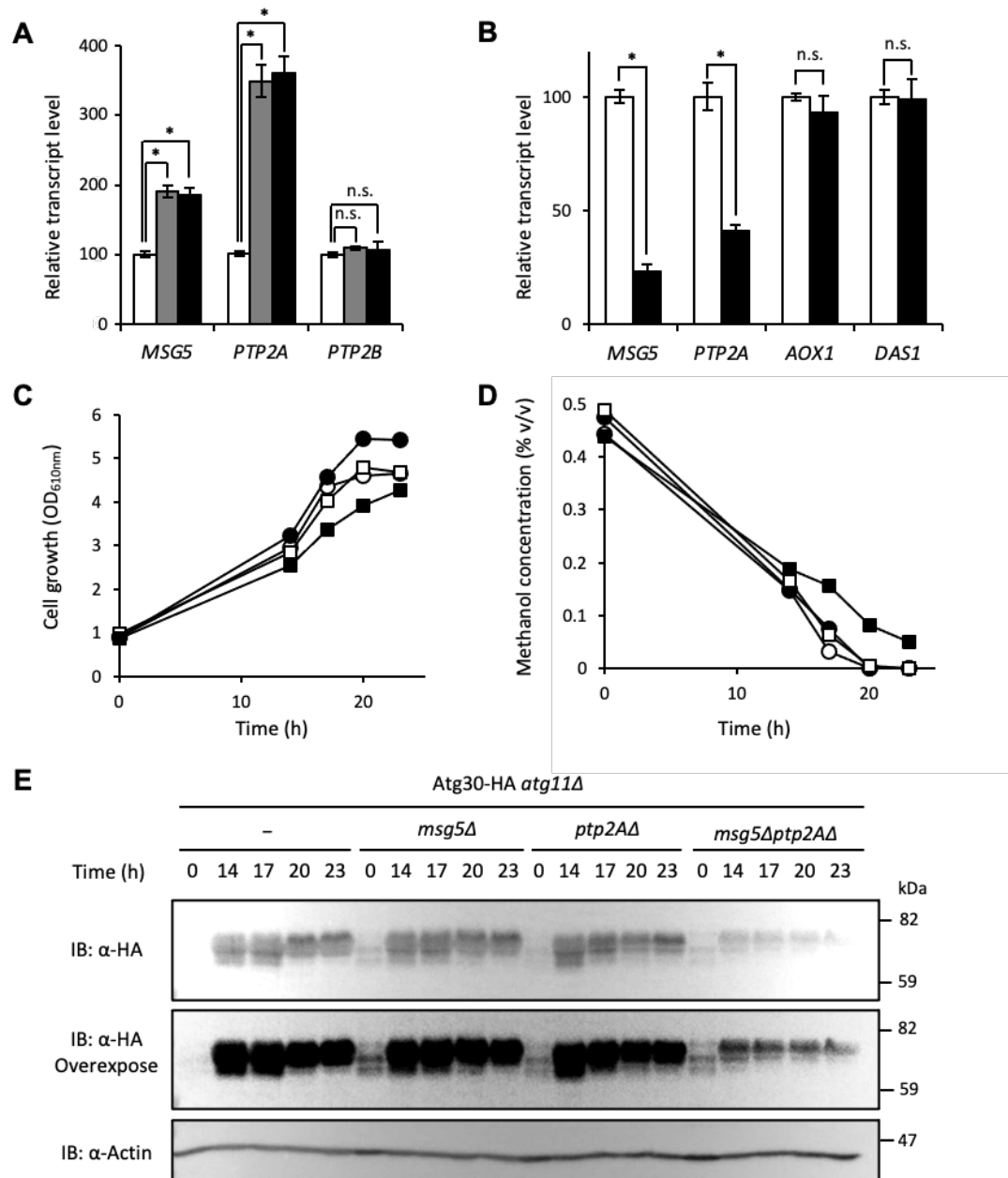
Figure 3-2. Phosphatases KpMsg5 and KpPtp2A repress pexophagy under the control of KpRlm1.
(A) Transcript levels of *KpMSG5*, *KpPTP2A* and *KpPTP2B* under the cell surface stress. Total mRNA was prepared from *K. phaffii* cells cultured on YNB-glucose medium and treated with 0 mg/L (white bars), 30 mg/L (grey bars) or 60 mg/L (black bars) of Congo Red for 2 h. The transcript levels were normalized using *GAP* gene as the standard. Relative transcript levels compared to that of the untreated sample are indicated. Error bars represent standard error values from three independent experiments. *: $p < 0.05$, n.s.: not significant. (B) Transcript levels of *KpMSG5*, *KpPTP2A*, *AOX1* and *DAS1* in wild-type (white bars) or *Kprlm1Δ* (black bars) strain. Total mRNA was prepared from the cells cultured on YNB-methanol medium for 16 h. The transcript levels were normalized using *GAP* gene as the standard. Relative transcript levels compared to that of wild-type strain are indicated. Error bars represent standard error values from three independent experiments. *: $p < 0.05$, n.s.: not significant. (C-D) Cell growth on 0.5% methanol medium (C) and methanol concentration in the medium (D) using *Kpatg11Δ* (open circles), *Kpatg11ΔKpmsg5Δ* (closed circles), *Kpatg11ΔKpptp2AΔ* (open squares) and *Kpatg11ΔKpmsg5Δ Kpptp2AΔ* (closed squares) strains. I Immunoblot analysis of KpAtg30-3xHA (α-HA) expressed in *Kpatg11Δ*, *Kpatg11ΔKpmsg5Δ*, *Kpatg11ΔKpptp2AΔ* and *Kpatg11ΔKpmsg5Δ Kpptp2AΔ* strains for detecting KpAtg30 phosphorylation levels during methanol culture. The image with higher exposure time (overexpose) was also indicated. Anti-β-actin antibody was used for detection of actin as a loading control (α-Actin). Cells of these strains were harvested at the same time point of cell growth analysis (C) and used for immunoblot analysis. Molecular weights of the protein size marker were indicated.

Discussion

KpWsc1 has been found to initiate dual signaling pathways: one leading to the expression of methanol-inducible genes and peroxisome biogenesis, and the other dictating the high-temperature stress response via the *S. cerevisiae* CWI-like pathway (This thesis, Figure 3-3) (Ohsawa *et al.*, 2017). These two pathways were clearly distinguished via the tyrosine 53 residue of KpWsc1 (Ohsawa *et al.*, 2021). KpWsc1 determines the synthesis or degradation of peroxisomes depending on the environmental methanol concentration. KpWsc1-downstream molecules, KpRom2, KpMpk1 and the transcription factor KpRlm1 also regulate the phosphorylation level of KpAtg30. Based on analogy with the *S. cerevisiae* CWI pathway, *K. phaffii* homologs of ScRho1, ScPkc1, and the MAP kinase cascade including ScMpk1 are speculated to be involved in the suppression of pexophagy.

I revealed that the KpWsc1-MAPK pathway including KpRlm1, KpMsg5 and KpPtp2A negatively regulates pexophagy in *K. phaffii*, and defined this pathway as pexophagy repression pathway (Figure 3-3). This pathway is activated by the depletion of methanol during methanol culture and initiates pexophagy. Observation of yeast pexophagy has been followed after a medium shift from peroxisome-proliferating medium (methanol or oleate medium) to glucose or ethanol medium in which peroxisomes are not required for metabolism, or to nitrogen starvation conditions. Since such drastic changes of the medium components and pH could simultaneously trigger multiple input signals to the cells, their complexity has made the analyses of signaling pathways and their effects difficult. In this study, I focused on a single environmental stimulation (i.e., methanol concentration) when I analyzed the intracellular signaling pathway. Higher methanol concentrations (0.15-2.0%) were found to suppress pexophagy. Surprisingly, the single sensor molecule KpWsc1 received and transmitted the input signal about methanol concentration, and then regulated methanol-induced gene expression, peroxisome synthesis and pexophagy. These results provide a perspective for molecular mechanism and switching of multiple signal transduction in response to environmental input.

The more detailed mechanism of pexophagy repression pathway needs to be elucidated. It is possible that some other proteins also contribute to pexophagy regulation in cooperation with KpMsg5 and KpPtp2A. KpSwi4, which was also considered to lie under KpRlm1, was not involved in the repression of pexophagy (Ohsawa *et al.*, 2021). Also, KpAtg30 is phosphorylated by the kinase KpHrr25 (Zientara-Rytter *et al.*, 2018). Although I demonstrated that the phosphatases KpMsg5 and KpPtp2A were involved in the phosphoregulation of KpAtg30, it is unknown whether its phosphorylation is direct or not. This should be revealed in the future study.
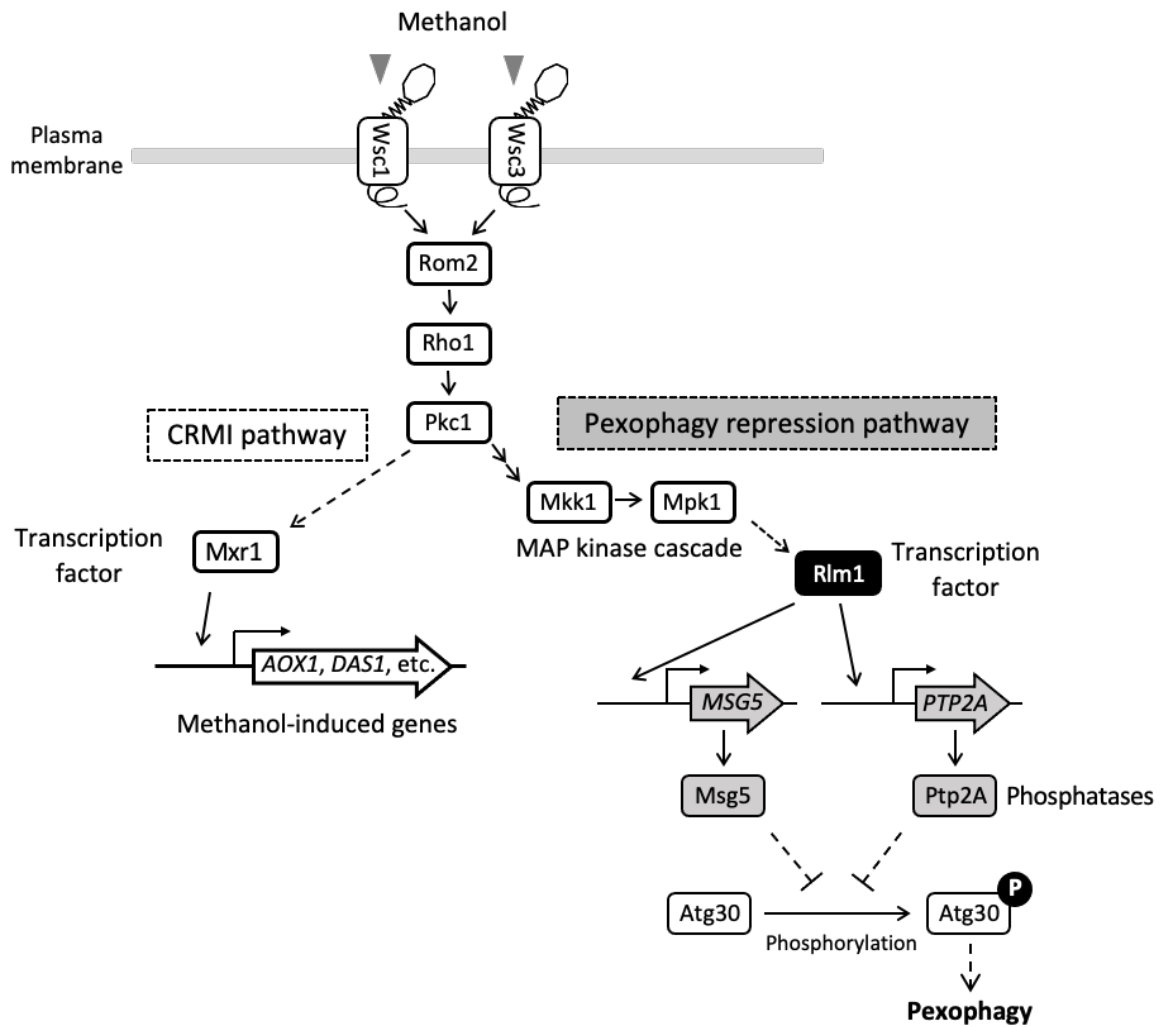
Figure 3-3. Pexophagy repression pathway from KpWsc1 to phosphatases KpMsg5/ KpPtp2A in *K. phaffii*.

K. phaffii cells sense methanol concentrations in the range of 10^{-4} – 2.0 % (Takeya *et al.*, 2018) via sensing machinery including KpWsc1 and KpWsc3. KpWsc family proteins transmit the signal to KpRom2, KpRho1 and KpPkc1. This signal divides into two pathways; CRMI pathway controlling methanol-induced genes (chapter I) and pexophagy repression pathway. Transcription factor KpRlm1 and KpRlm1-dependent phosphatases KpMsg5/ KpPtp2A regulate the phosphorylation level of KpAtg30 and control pexophagy.

Conclusion

This study aims to unravel the regulatory mechanism of CRMI in methylotrophic yeasts.

In chapter I, I elucidate the phosphoregulation of KpMxr1 and its function for CRMI of methanol-induced genes in *K. phaffii*. The results of immunoblot with anti-phosphor amino acid residues, LC-MS/MS analysis and phos-tag SDS-PAGE showed novel phosphorylation residues and the phosphorylation state of KpMxr1 was dependent on the carbon source or methanol concentration in the media. The methanol signaling from KpWsc proteins to KpMxr1 via KpPkc1 is identified and defined as the CRMI pathway.

In chapter II, I describe the physiological significance of the methanol-inducibility of *CbMPP1*. Constitutive or excessive expression of *CbMPP1* resulted in the growth delay and abnormal formaldehyde accumulation in methanol medium and improper CRMI of methanol-induced genes (*AOD1, DAS1, FLD1, etc.*), suggesting that the expression of *CbMPP1* is induced under the control of CRMI and this is crucial in keeping appropriate methanol-induced gene expression and cell growth on methanol. Moreover, I identified the UASs in *CbMPP1* promoter by promoter deletion analysis.

In chapter III, I explore phosphatases under the control of KpRlm1 and revealed that the KpWsc1-MAPK pathway including KpRlm1, KpMsg5 and KpPtp2A negatively regulates KpAtg30 phosphorylation and pexophagy in *K. phaffii*, and defined as pexophagy repression pathway.

These insights will contribute to improving the system of heterologous protein production in methylotrophic yeasts. Methanol is an inducer of methanol-induced gene promoters and a carbon source for cell growth. Therefore, it has been difficult to maintain optimal protein production and constant methanol metabolism in industrial culture conditions. If the intracellular signaling and gene expression can be arbitrarily controlled independent on the substrate concentration, the efficiency of heterologous protein production would be made higher. In addition, this is the first report on CRMI in methylotrophic yeasts. The signal from methanol is thought to be not transmitted by two types of mediators (activated or inactivated) but by the mediators continuously varying corresponding to substrate concentration. Thus, these discoveries of "analog (continuous)" signal transduction will help us to understand the mechanism of the concentration-regulated gene expression system.

References

Asakura, M., Ninomiya, S., Sugimoto, M., Oku, M., Yamashita, S.I., Okuno, T., *et al.* (2009) Atg26-mediated pexophagy is required for host invasion by the plant pathogenic fungus *Colletotrichum orbiculare*. *Plant Cell* **21**: 1291–1304.

Cregg, J.M., Barringer, K.J., Hessler, A.Y., and Madden, K.R. (1985) *Pichia pastoris* as a host system for transformations. *Mol Cell Biol* **5**: 3376–3385.

Cregg, J.M., Lin-Cereghino, J., Shi, J., and Higgins, D.R. (2000) Recombinant protein expression in *Pichia pastoris*. *Mol Biotechnol* **16**: 23–52.

De, S., Mattanovich, D., Ferrer, P., and Gasser, B. (2021) Established tools and emerging trends for the production of recombinant proteins and metabolites in *Pichia pastoris*. *Essays Biochem* **65**: 293–307.

Dupres, V., Alsteens, D., Wilk, S., Hansen, B., Heinisch, J.J., and Dufrene, Y.F. (2009) The yeast Wsc1 cell surface sensor behaves like a nanospring *in vivo*. *Nat Chem Biol* **5**: 857–862.

García, R., Bermejo, C., Grau, C., Pérez, R., Rodríguez-Peña, J.M., Francois, J., *et al.* (2004) The global transcriptional response to transient cell wall damage in *Saccharomyces cerevisiae* and its regulation by the cell integrity signaling pathway. *J Biol Chem* **279**: 15183–15195.

García, R., Sanz, A.B., Rodríguez-Peña, J.M., Nombela, C., and Arroyo, J. (2016) Rlm1 mediates positive autoregulatory transcriptional feedback that is essential for Slt2-dependent gene expression. *J Cell Sci* **129**: 1649–1660.

Gellissen, G. (2000) Heterologous protein production in methylotrophic yeasts. *Appl Microbiol Biotechnol* **54**: 741–750.

Gupta, A., Rao, K.K., Sahu, U., and Rangarajan, P.N. (2021) Characterization of the transactivation and nuclear localization functions of *Pichia pastoris* zinc finger transcription factor Mxr1p. *J Biol Chem* **297**: 101247.

Hahn, J.S. and Thiele, D.J. (2002) Regulation of the *Saccharomyces cerevisiae* Slt2 kinase pathway by the stress-inducible Sdp1 dual specificity phosphatase. *J Biol Chem* **277**: 21278–21284.

Hartner, F.S. and Glieder, A. (2006) Regulation of methanol utilisation pathway genes in yeasts. *Microb Cell Fact* **5**: 1–21.

Irie, K., Takase, M., Lee, K.S., Levin, D.E., Araki, H., Matsumoto, K., and Oshima, Y. (1993) *MKK1* and *MKK2*, which encode *Saccharomyces cerevisiae* mitogen-activated protein kinase-kinase homologs, function in the pathway mediated by protein kinase C. *Mol Cell Biol* **13**: 3076–3083.

Kalender, Ö. and Çalık, P. (2020) Transcriptional regulatory proteins in central carbon metabolism of *Pichia pastoris* and *Saccharomyces cerevisiae*. *Appl Microbiol Biotechnol* **104**: 7273–7311.

Kawaguchi, K., Yurimoto, H., Oku, M., and Sakai, Y. (2011) Yeast methylotrophy and autophagy in a methanol-oscillating environment on growing *Arabidopsis thaliana* leaves. *PLoS One* **6**: e25257.

Kumar, N.V. and Rangarajan, P.N. (2012) The zinc finger proteins Mxr1p and repressor of phosphoenolpyruvate carboxykinase (ROP) have the same DNA binding specificity but regulate methanol metabolism antagonistically in *Pichia pastoris*. *J Biol Chem* **287**: 34465–34473.

Leão-Helder, A.N., Krikken, A.M., van der Klei, I.J., Kiel, J.A.K.W., and Veenhuis, M. (2003) Transcriptional down-regulation of peroxisome numbers affects selective peroxisome degradation in *Hansenula polymorpha*. *J Biol Chem* **278**: 40749–40756.

Lee, B., Yurimoto, H., Sakai, Y., and Kato, N. (2002) Physiological role of the glutathione-dependent formaldehyde dehydrogenase in the methylotrophic yeast *Candida boidinii*. *Microbiology* **148**: 2697–2704.

Lee, K.S., Irie, K., Gotoh, Y., Watanabe, Y., Araki, H., Nishida, E., *et al.* (1993) A yeast mitogen-activated protein kinase homolog (Mpk1p) mediates signalling by protein kinase C. *Mol Cell Biol* **13**: 3067–3075.

Levin, D.E. (2005) Cell wall integrity signaling in *Saccharomyces cerevisiae*. *Microbiol Mol Biol Rev* **69**: 262–291.

Levin, D.E. (2011) Regulation of cell wall biogenesis in *Saccharomyces cerevisiae*: the cell wall integrity signaling pathway. *Genetics* **189**: 1145–1175.

Lin-Cereghino, G.P., Godfrey, L., la Cruz, B.J. de, Johnson, S., Khuongsathiene, S., Tolstorukov, I., *et al.* (2006) Mxr1p, a key regulator of the methanol utilization pathway and peroxisomal genes in *Pichia pastoris*. *Mol Cell Biol* **26**: 883–897.

Lodder, A.L., Lee, T.K., and Ballester, R. (1999) Characterization of the Wsc1 protein, a putative receptor in the stress response of *Saccharomyces cerevisiae*. *Genetics* **152**: 1487–1499.

Madaule, P., Axel, R., and Myers, A.M. (1987) Characterization of two members of the *rho* gene family from the yeast *Saccharomyces cerevisiae*. *Proc Natl Acad Sci USA* **84**: 779–783.

Marín, M.J., Flández, M., Bermejo, C., Arroyo, J., Martín, H., and Molina, M. (2009) Different modulation of the outputs of yeast MAPK-mediated pathways by distinct stimuli and isoforms of the dual-specificity phosphatase Msg5. *Mol Genet Genomics* **281**: 345–359.

Mattison, C.P., Spencer, S.S., Kresge, K.A., Lee, J., and Ota, I.M. (1999) Differential regulation of the cell wall integrity mitogen-activated protein kinase pathway in budding yeast by the protein tyrosine phosphatases Ptp2 and Ptp3. *Mol Cell Biol* **19**: 7651–7660.

Nakatogawa, H. and Mochida, K. (2015) Reticulophagy and nucleophagy: New findings and unsolved issues. *Autophagy* **11**: 2377–2378.

Nonaka, H., Tanaka, K., Hirano, H., Fujiwara, T., Kohno, H., Umikawa, M., *et al.* (1995) A

downstream target of *RHO1* small GTP-binding protein is *PKC1*, a homolog of protein kinase C, which leads to activation of the MAP kinase cascade in *Saccharomyces cerevisiae*. *EMBO J* **14**: 5931–5938.

Oda, S., Yurimoto, H., Nitta, N., and Sakai, Y. (2016) Unique C-terminal region of Hap3 is required for methanol-regulated gene expression in the methylotrophic yeast *Candida boidinii*. *Microbiology* **162**: 898–907.

Oda, S., Yurimoto, H., Nitta, N., Sasano, Y., and Sakai, Y. (2015) Molecular characterization of Hap complex components responsible for methanol-inducible gene expression in the methylotrophic yeast *Candida boidinii*. *Eukaryot Cell* **14**: 278–285.

Ogata, K., Nishikawa, H., and Ohsugi, M. (1969) A yeast capable of utilizing methanol. *Agric Biol Chem* **33**: 1519–1520.

Ohsawa, S. (2017) *Doctoral thesis (Kyoto Univ.)*

Ohsawa, S., Inoue, K., Isoda, T., Oku, M., Yurimoto, H., and Sakai, Y. (2021) The methanol sensor Wsc1 and MAPK Mpk1 suppress degradation of methanol-induced peroxisomes in methylotrophic yeast. *J Cell Sci* **134**.

Ohsawa, S., Nishida, S., Oku, M., Sakai, Y., and Yurimoto, H. (2018) Ethanol represses the expression of methanol-inducible genes via acetyl-CoA synthesis in the yeast *Komagataella phaffii*. *Sci Rep* **8**: 18051.

Ohsawa, S., Yurimoto, H., and Sakai, Y. (2017) Novel function of Wsc proteins as a methanol-sensing machinery in the yeast *Pichia pastoris*. *Mol Microbiol* **104**: 349–363.

Oku, M. and Sakai, Y. (2016) Pexophagy in yeasts. *Biochim Biophys Acta - Mol Cell Res* **1863**: 992–998.

Oku, M., Takano, Y., and Sakai, Y. (2014) The emerging role of autophagy in peroxisome dynamics and lipid metabolism of phyllosphere microorganisms. *Front Plant Sci* **5**: 1–4.

Ozimek, P., Veenhuis, M., and van der Klei, I.J. (2005) Alcohol oxidase: A complex peroxisomal, oligomeric flavoprotein. *FEMS Yeast Res* **5**: 975–983.

Parua, P.K., Ryan, P.M., Trang, K., and Young, E.T. (2012) *Pichia pastoris* 14-3-3 regulates transcriptional activity of the methanol inducible transcription factor Mxr1 by direct interaction. *Mol Microbiol* **85**: 282–298.

Philip, B. and Levin, D.E. (2001) Wsc1 and Mid2 are cell surface sensors for cell wall integrity signaling that act through Rom2, a guanine nucleotide exchange factor for Rho1. *Mol Cell Biol* **21**: 271–280.

Ratnakumar, S., Kacherovsky, N., Arms, E., and Young, E.T. (2009) Snf1 controls the activity of Adr1 through dephosphorylation of Ser230. *Genetics* **182**: 735–745.

Reggiori, F. and Klionsky, D.J. (2013) Autophagic processes in yeast: Mechanism, machinery and regulation. *Genetics* **194**: 341–361.

Rodicio, R. and Heinisch, J.J. (2010) Together we are strong--cell wall integrity sensors in yeasts. *Yeast* **27**: 531–540.

Sahu, U., Krishna Rao, K., and Rangarajan, P.N. (2014) Trm1p, a Zn(II)$_2$Cys$_6$-type transcription factor, is essential for the transcriptional activation of genes of methanol utilization pathway, in *Pichia pastoris*. *Biochem Biophys Res Commun* **451**: 158–164.

Sahu, U. and Rangarajan, P.N. (2016a) Methanol expression regulator 1 (Mxr1p) is essential for the utilization of amino acids as the sole source of carbon by the methylotrophic yeast, *Pichia pastoris*. *J Biol Chem* **291**: 20588–20601.

Sahu, U. and Rangarajan, P.N. (2016b) Regulation of acetate metabolism and acetyl Co-A synthetase 1 *(ACS1)* expression by methanol expression regulator 1 (Mxr1p) in the methylotrophic yeast *Pichia pastoris*. *J Biol Chem* **291**: 3648–3657.

Sakai, Y., Kazarimoto, T., and Tani, Y. (1991) Transformation system for an asporogenous methylotrophic yeast, *Candida boidinii*: Cloning of the orotidine-5'-phosphate decarboxylase gene (*URA3*), isolation of uracil auxotrophic mutants, and use of the mutants for integrative transformation. *J Bacteriol* **173**: 7458–7463.

Sakai, Y., Koller, A., Rangell, L.K., Keller, G. a, and Subramani, S. (1998) Peroxisome degradation by microautophagy in *Pichia pastoris* : identification of specific steps and morphological intermediates. *J Cell Biol* **141**: 625–636.

Sakai, Y., Murdanoto, A.P., Konishi, T., Iwamatsu, A., and Kato, N. (1997) Regulation of the formate dehydrogenase gene, *FDH1*, in the methylotrophic yeast *Candida boidinii* and growth characteristics of an *FDH1*-disrupted strain on methanol, methylamine, and choline. *Annu Rev Popul Law* **179**: 4480–4485.

Sakai, Y., Oku, M., van der Klei, I.J., and Kiel, J.A.K.W. (2006) Pexophagy: Autophagic degradation of peroxisomes. *Biochim Biophys Acta - Mol Cell Res* **1763**: 1767–1775.

Sakai, Y., Saiganji, A., Yurimoto, H., Takabe, K., Saiki, H., and Kato, N. (1996) The absence of Pmp47, a putative yeast peroxisomal transporter, causes a defect in transport and folding of a specific matrix enzyme. *J Cell Biol* **134**: 37–51.

Sanz, A.B., García, R., Rodríguez-Peña, J.M., and Arroyo, J. (2018) The CWI pathway: Regulation of the transcriptional adaptive response to cell wall stress in yeast. *J Fungi* **4**: 1–12.

Sasano, Y., Yurimoto, H., Kuriyama, M., and Sakai, Y. (2010) Trm2p-dependent derepression is essential for methanol-specific gene activation in the methylotrophic yeast *Candida boidinii*. *FEMS Yeast Res* **10**: 535–544.

Sasano, Y., Yurimoto, H., Yanaka, M., and Sakai, Y. (2008) Trm1p, a Zn(II)$_2$Cys$_6$-type transcription factor, is a master regulator of methanol-specific gene activation in the methylotrophic yeast *Candida boidinii*. *Eukaryot Cell* **7**: 527–536.

Sears, I.B., O'Connor, J., Rossanese, O.W., and Glick, B.S. (1998) A versatile set of vectors for constitutive and regulated gene expression in *Pichia pastoris*. *Yeast* **14**: 783–790.

Shen, W., Kong, C., Xue, Y., Liu, Y., Cai, M., Zhang, Y., *et al.* (2016) Kinase screening in *Pichia pastoris* identified promising targets involved in cell growth and alcohol oxidase 1 promoter (PAOX1) regulation. *PLoS One* **11**: e0167766.

Shi, L., Wang, X., Wang, J., Zhang, P., Qi, F., Cai, M., *et al.* (2018) Transcriptome analysis of *Δmig1Δmig2* mutant reveals their roles in methanol catabolism, peroxisome biogenesis and autophagy in methylotrophic yeast *Pichia pastoris*. *Genes and Genomics* **40**: 399–412.

Suzuki, K., Kirisako, T., Kamada, Y., Mizushima, N., Noda, T., and Ohsumi, Y. (2001) The pre-autophagosomal structure organized by concerted functions of *APG* genes is essential for autophagosome formation. *EMBO J* **20**: 5971–5981.

Suzuki, K. and Ohsumi, Y. (2007) Molecular machinery of autophagosome formation in yeast, *Saccharomyces cerevisiae*. *FEBS Lett* **581**: 2156–2161.

Takeya, T., Yurimoto, H., and Sakai, Y. (2018) A *Pichia pastoris* single-cell biosensor for detection of enzymatically produced methanol. *Appl Microbiol Biotechnol* .

Tamura, N., Oku, M., and Sakai, Y. (2010) Atg8 regulates vacuolar membrane dynamics in a lipidation-independent manner in *Pichia pastoris*. *J Cell Sci* **123**: 4107–4116.

Toh-e, A., Yoshinami, U., Kakimoto, S., and Oshima, Y. (1973) Isolation and characterization of acid phosphatase mutants in *Saccharomyces cerevisiae*. *J Bacteriol* **113**: 727–738.

Torriani, A. (1960) Influence of inorganic phosphate in the formation of phosphatases by *Escherichia coli*. *Biochim Biophys Acta* **38**: 460–469.

van der Klei, I.J., Yurimoto, H., Sakai, Y., and Veenhuis, M. (2006) The significance of peroxisomes in methanol metabolism in methylotrophic yeast. *Biochim Biophys Acta* **1763**: 1453–1462.

Wang, X., Cai, M., Shi, L., Wang, Q., Zhu, J., Wang, J., *et al.* (2016a) PpNrg1 is a transcriptional repressor for glucose and glycerol repression of *AOX1* promoter in methylotrophic yeast *Pichia pastoris*. *Biotechnol Lett* **38**: 291–298.

Wang, X., Wang, Q., Wang, J., Bai, P., Shi, L., Shen, W., *et al.* (2016b) Mit1 transcription factor mediates methanol signaling and regulates the alcohol oxidase 1 (*AOX1*) promoter in *Pichia pastoris*. *J Biol Chem* **291**: 6245–6261.

Watanabe, Y., Irie, K., and Matsumoto, K. (1995) Yeast *RLM1* encodes a serum response factor-like protein that may function downstream of the Mpk1 (Slt2) mitogen-activated protein kinase

pathway. *Mol Cell Biol* **15**: 5740–5749.

Wen, X. and Klionsky, D.J. (2016) An overview of macroautophagy in yeast. *J Mol Biol* **428**: 1681–1699.

Wu, S. and Letchworth, G.J. (2004) High efficiency transformation by electroporation of *Pichia pastoris* pretreated with lithium acetate and dithiothreitol. *Biotechniques* **36**: 152–154.

Yashar, B., Irie, K., Printen, J.A., Stevenson, B.J., Sprague, G.F., Matsumoto, K., and Errede, B. (1995) Yeast MEK-dependent signal transduction: response thresholds and parameters affecting fidelity. *Mol Cell Biol* **15**: 6545–6553.

Young, E.T., Dombek, K.M., Tachibana, C., and Ideker, T. (2003) Multiple pathways are co-regulated by the protein kinase Snf1 and the transcription factors Adr1 and Cat8. *J Biol Chem* **278**: 26146–26158.

Yurimoto, H. (2009) Molecular basis of methanol-inducible gene expression and its application in the methylotrophic yeast *Candida boidinii*. *Biosci Biotechnol Biochem* **73**: 793–800.

Yurimoto, H., Kato, N., and Sakai, Y. (2005) Assimilation, dissimilation, and detoxification of formaldehyde, a central metabolic intermediate of methylotrophic metabolism. *Chem Rec* **5**: 367–375.

Yurimoto, H., Komeda, T., Lim, C.R., Nakagawa, T., Kondo, K., Kato, N., and Sakai, Y. (2000) Regulation and evaluation of five methanol-inducible promoters in the methylotrophic yeast *Candida boidinii*. *Biochim Biophys Acta - Gene Struct Expr* **1493**: 56–63.

Yurimoto, H., Lee, B., Yano, T., Sakai, Y., and Kato, N. (2003) Physiological role of *S*-formylglutathione hydrolase in C1 metabolism of the methylotrophic yeast *Candida boidinii*. *Microbiology* **149**: 1971–1979.

Yurimoto, H., Oku, M., and Sakai, Y. (2011) Yeast methylotrophy: Metabolism, gene regulation and peroxisome homeostasis. *Int J Microbiol* 1–8.

Yurimoto, H. and Sakai, Y. (2019) Methylotrophic yeasts: Current understanding of their C1-metabolism and its regulation by sensing methanol for survival on plant leaves. *Curr Issues Mol Biol* **33**: 197–209.

Zhai, X. (2012) *Doctral thesis (Kyoto Univ.)*

Zhai, Z., Yurimoto, H., and Sakai, Y. (2012) Molecular characterization of *Candida boidinii MIG1* and its role in the regulation of methanol-inducible gene expression. *Yeast* **29**: 293–301.

Zientara-Rytter, K., Ozeki, K., Nazarko, T.Y., and Subramani, S. (2018) Pex3 and Atg37 compete to regulate the interaction between the pexophagy receptor, Atg30, and the Hrr25 kinase. *Autophagy* **14**: 368–384.

Acknowledgements

Publications

1. **<u>Inoue, K.</u>**, Ohsawa, S., Yurimoto, H., and Sakai, Y. (2022)
   "Phosphoregulation of the transcription factor Mxr1 plays a crucial role in the concentration-regulated methanol induction in *Komagataella phaffii*"
   Mol Microbiol, **118**:683–697.

2. **<u>Inoue, K.</u>**, Iwase, S., Yurimoto, H., and Sakai, Y.
   "Role of the transcription factor Mpp1 in the concentration-regulated methanol induction in *Candida boidinii*"
   Manuscript in preparation.

3. Ohsawa, S.*, **<u>Inoue, K.*</u>**, Yurimoto, H., and Sakai Y. (2021)
   "Methanol sensor Wsc1 and MAP kinase suppress degradation of methanol-induced peroxisomes in methylotrophic yeast"
   J Cell Sci, **134**,
   *These authors contributed equally to this work as the first co-author.